Aus der Universitätsklinik für Nieren- und Hochdruckkrankheiten, Diabetologie und Endokrinologie der Medizinischen Fakultät der

Otto-von-Guericke-Universität Magdeburg

“Game-based assessment of peripheral neuropathy in patients with diabetes by combining sensor-equipped insoles with video games and machine learning algorithms”

D i s s e r t a t i o n

zur Erlangung des Doktorgrades

Dr. rer. medic.

(doctor rerum medicarum)

an der Medizinischen Fakultät der Otto-von-Guericke-Universität Magdeburg

vorgelegt von Antao Ming

aus Shandong, V.R. China

Magdeburg 2022

Bibliographic description

Antao, Ming:

Game-based assessment of peripheral neuropathy in patients with diabetes by combining sensor-equipped insoles with video games and machine learning algorithms. ─ 2022 - 127 Pages, 28 Figures, 3 Tables, 6 Supplementary Appendix.

Abstract:

Diagnosis of diabetic peripheral neuropathy (DPN) is essential to prevent complications, such as the diabetic foot syndrome. Diagnosis mostly relys on a time-consuming clinical examination by standardized procedures (pinprick test, vibration perception, Tip Therm, reflexes, muscle function). Furthermore, investigator-related bias confounds findings.

To explore the potentials of a video game-based approach to diagnose polyneuropathy, a gaming platform (“Gamidiagnostics”) was set up. Participants utilized pressure sensor-equipped insoles as control units and played four games that were specifically designed to test for reaction time, sensation, skillfulness, endurance, balance, and muscle strength. A pilot study with 71 healthy volunteers and 112 patients diagnosed with DPN by clinical examination (neuropathy deficit score, NDS) evaluated the feasibility of this approach. Unbiased training of prediction algorithms with data sets identified 15 independent variables with discriminatory functions that indicated DPN. In age-matched cohorts, the support vector machines achieved a training accuracy of 87.8% (AUC-ROC 0.91) and an adjusted accuracy of 85.2% on a held-out testing data set (sensitivity 92.6%, specificity 77.8%). Distinct variables were identified for each nerve fiber deficit and allowed correct classification with adjusted accuracies of 88.1%, 91.9%, and 95.3% for Achilles tendon reflex, Aδ-/C-fiber, and Aβ-fiber impairment, respectively.

Thus, a video game-based approach with smart footwear sensors was able to diagnose advanced peripheral nerve malfunction with high accuracy. This was set up in an examiner-independent manner and may be established as telemedical device.

Keywords

Diabetes; peripheral sensorimotor neuropathy; sensor-equipped insoles; video games; artificial intelligence; support vector machine; machine learning; telemedicine

Contents

Abbreviations

AC	Apple-Catch
ACC	Accuracy
AI	Artificial intelligence
ANN	Artificial neural network
AUC-ROC	Area under curve receiver operating characteristics
BF	Balloon-Flying
BMI	Body mass index
CCM	Corneal confocal microscopy
CF	Candidate feature
CON	Control
CP	Cross-Pressure
DM	Diabetes mellitus
DNS	Diabetic neuropathy symptom score
DPN	Diabetic peripheral neuropathy
DT	Decision trees
ECU	Electronic control unit
EEG	Electroencephalography
FN	False negative
FP	False positive
FPR	False positive rate
GB	Gigabyte
HD	High dynamic
HDL-c	High-density lipoprotein cholesterol
IDF	International diabetes federation
III	three
IJ	Island-Jump
IMU	Inertial measuring unit
IV	four
JSON	Java script object notation
KIN	Microsoft-Kinect®
LR	Logistic regression
ML	Machine learning
MLP	Multi-layer perceptron
MMSE	Mini-mental state examination
MNSI-q	Michigan neuropathy screening instrument-questionnaire
MTK	Metatarsal
MVC	Model-View-Controller
NCT	Nerve conduction testing
NCV	Nerve conduction velocity
NDS	Neuropathy disability score
NSS	Neuropathy symptom score
NYHA	New York Heart Association
OAO	One against one

PCA	Principal components analysis
PNP	Polyneuropathy
POCD	Point-of-care device
RBF	Radial basis function
SD	Standard deviation
SEN	Sensitivity
SMT	Step-mat-training
SPE	Specificity
SVM	Support vector machine
SVM-Linear	Support vector machine with a linear basis Kernel function
SVM-Poly	Support vector machine with a polynomial basis Kernel function
SVM-Radial	Support vector machine with a radial basis Kernel function
TC	Task combination
TN	True negative
TP	True positive
TPR	True positive rate
UI	User interface

1. Introduction

1.1. Peripheral neuropathy

Peripheral nerves refer to 43 pairs of motor and sensory nerves that branch out from the central nervous system (CNS) and connect the rest of the body (1). The nerves are responsible for maintaining body homeostasis, mediating sensation, movement and coordination (2). Peripheral neuropathy (PN) is a medical term to describe damage to nerves within the peripheral nervous system, which includes nerve cells, fibers (axons), and coverings (myelin sheath) (3). PN varies in its distribution pattern and several classification schemes exist. The most common classification categorizes into distal symmetric polyneuropathy (DSPN), mononeuropathy, and mononeuropathy multiplex, according to the location of affected nerves.

1.1.1. Causes and prevalence

The most common distribution pattern of the DSPN is a diffuse, length-dependent process with diverse underlying causes, such as diabetes, excessive and chronic alcohol use, vitamin B12 deficiency, chemotherapy, chronic kidney disease, paraproteinemia or thyroid disease (4). Register studies and surveys reported an approximate prevalence rate of 2.4% that increases with age to around 7% (5). For 49% of patients the polyneuropathy is asymptomatic and undiagnosed (6). Table 1 provides an overview on reported prevalence rates of peripheral polyneuropathy and its subtypes from epidemiological studies.

Table 1. Prevalence of peripheral neuropathy and its subtypes. *T1DM: Type 1 diabetes mellitus; T2DM: Type 2 diabetes mellitus; DSPN: Distal symmetric polyneuropathy; DPN: Diabetic peripheral neuropathy. *Incidence rate.*

Study	Country	Population (n)	Prevalence
Peripheral neuropathy (PN)			
(7)	Italy	14,540	2.7% (7% by age ≥ 55 years)
(8)	India	14,010	2.4%
(9)	USA	2,514 (age ≥ 40 years)	9%
Distal symmetric polyneuropathy (DSPN, polyneuropathy)			
(10)	Netherlands	age ≥ 18 years	77.0/100,000 person-years*
(6)	Netherlands	1,310 participants (mean age 70 years, 55% female)	5.5%, 6.7% (male), 4.5% (female), 31% (DPN among DSPN)
(11)	Germany	983 (age ≥ 50 years)	53.8% (No Diabetes), 43.8% (T1DM), and 55.6% (T2DM)
	UK	19,897 controls	0.12%
Diabetic peripheral neuropathy (DPN)			
(12)	Germany	1004 patients with diabetes	40.3%, 29.1% (T1DM), and 42.2% (T2DM)
(13)	USA	Total population	3.9% (12,522,483 cases)
	Germany		4.7% (3,904,730 cases)
	Italy		2.7% (1,636,426 cases)
	Japan		0.002% (2,332 cases)
(14)	Germany	45,633 newly diagnosed T2DM patients	5.7% (5.5-5.9%)
	UK	14,205 newly diagnosed T2DM patients	2.4% (1.9-2.9%)

1.1.2. Symptoms and clinical presentations of peripheral neuropathy

Regarding the clinical appearance of peripheral polyneuropathy lack of sensation may prevail, resulting in absence of information (numbness, loss of sensation, balance impairment). On the other hand patients may complain about an excess of sensation with discomfort feelings (such as prickling, tingling, burning, pain). These absent or plus symptoms relate to sensory nerve malfunctions that most often occur in a symmetric pattern. In addition motor weakness (muscle weakness and atrophy) may develop. These symptoms typically begin in the toes and later on ascend insidiously up the legs in a stocking distribution. Symptoms may spread throughout the body, reaching hands and knees (15). Over time, the ankle and Achilles reflexes may be impacted with aggravation of disease (16). Autonomic symptoms may include sweating, circulatory abnormalities and postural hypotension (17). Disturbed proprioception and abnormal sensorimotor function result in impaired balance coordination and mobility with increased risk of falls and fractures (18).

1.1.3. Diabetic peripheral neuropathy (DPN)

DPN is defined as a subtype of PN with no other identifiable cause than diabetes (19). According to the International Diabetes Federation (IDF), more than 435 million people worldwide are diagnosed with diabetes, and this number is expected to rise to 693 million in 2045 (20). Correspondingly, the burden of diabetes-associated comorbidities and sequela of hyperglycemia will increase, e.g., every second afflicted individual (both diabetes type 1 and 2) will eventually develop polyneuropathy (21).

DPN has a significant impact on the mobility of patients. As a consequence a disturbed gait and movement coordination ensues, the likelihood of falls increases, the share of patients with diabetic foot syndrome rises, and a frail mental health is often seen (22). Besides impaired or lack of sensation, DPN may also cause plus symptoms, such as discomfort and pain. Complications such as tissue damage, infections, and ultimately minor and major foot ulcerations are seen in 19 – 34% of individuals with diabetes during their lifetime, especially with delayed diagnosis of DPN and/or inadequate implementation of preventive measures (23). Notably, every fifth moderate-to-severe diabetes-related infection will prompt lower extremity amputation (23, 24). On the other hand, four out of five amputations may be prevented by adequate podiatry care (25). All these aspects urge for a timely DPN diagnosis, interventions for primary and secondary prevention of foot damage, and possibly interventions to combat nerve damage itself. Due to the nature of the disease, timely diagnosis and repeated monitoring of individuals at risk are mandatory, given the insidious onset of DPN with diverse presentations. Up to 50% of affected individuals remain asymptomatic (26), while the remainder develop numbness, tingling, pain, or weakness (27). Symptoms commonly originate

distally (i.e., the tips of the toes) and spread proximally with a symmetric distribution. Peripheral nerves encompass Aδ- and C-fibers (small, spinothalamic; temperature sensation, nociception; assessed by pinprick), as well as Aβ-fibers (large, back nervous system; assessed by vibration and monofilament) (28, 29). In addition, the reflex status may be altered, most commonly an impaired Achilles tendon reflex status is observed (30).

1.2. Diagnostic strategies and challenges of PN

Early detection of peripheral neuropathy is a key measure to open the window for preventive action, e.g. to maintain tissue integrity of the feet with walking aids, protection by specialized shoes for sustained physical health and mental quality of life (31). Effective handling of diabetes mellitus and normalization of blood glucose levels may prevent or retard further damage to the nerves (32). Because only 10% to 15% of diabetic polyneuropathy (DPN) patients are symptomatic, a large proportion of patients are unaware of their disease and do not seek aid, although they are at highest risk for foot ulcer formation (31). Consequently, there is consensus that detection of earliest signs should be performed, which mostly occur at the distal limbs, particularly the feet, to improve patient care (16).

The diagnosis of PN should consider multiple symptoms and clinical signs. Initially, paying attention to family and personal medical history and inquiring about toxin exposure and medications should be proceeded to exclude causes other than diabetes, such as neurotoxins and heavy metal poisoning, alcohol abuse, vitamin B12 deficiency, renal disease, chronic inflammatory demyelinating polyradiculoneuropathy, inherited neuropathies, and vasculitis (17). Dyck et al. pointed out that up to 10% of PN in patients with diabetes was not due to diabetes (33). The physical examination includes performing sensory tests (different modalities like light touch, vibration, temperature, pain sensation, and proprioception), evaluating the patients' mental status, reflexes, cranial nerves, and motor system (i.e. gait). Researchers have developed composite scoring systems (using symptoms, clinical signs, or both) to quantify general neuropathic deficits better and enhance diagnostic accuracy (Table 2).

Table 2. Clinical scoring systems for PN screening. *NSS, neuropathy symptom score; MNSI, Michigan Neuropathy Screening Instrument; NDS, neuropathy disability score*

Scoring System	Items	Thresholds
NSS (33)	Muscle weakness (8 points) Sensory disturbances (5 points) Autonomic symptoms (4 points)	Presence of a symptom if ≥ 1 point
MNSI (34)	A 15-item self-administered questionnaire: pain, temperature sensation, tingling, numbness, sensory symptoms, cramps and muscle weakness, foot ulcers or cracks, and amputation	Abnormal, if ≥ 3/15 response
NDS (35)	Vibration sensation (128-Hz tuning fork) Temperature sensation Pin-prick Ankle reflex	Abnormal, if ≥ 6/10 points

A sensorineural impairment assessment (Quantitative Sensory Testing: QST) is based on clinical sensory nerve tests. Clinical sensory nerve tests generate specific physical vibratory, pressure, noxious, or thermal stimuli using specialized equipment, such as 128-Hz tuning fork, 10-g Semmes-Weinstein monofilament, Pin-prick, or Tip Therm (AXON GmbH, Düsseldorf, Germany). QST was developed to detect the thresholds of thermal perception (cold or warm), vibration perception, pressure pain, and sudomotor function (36).

The nerve conduction testing (NCT) and nerve biopsy are considered gold standards for PN diagnosis (37). The NCT is a reliable and rather objective diagnostic tool that relies on an evoked stimulus, which is independent from the subjective response, to calculate the nerve conduction velocity in excitated nerves. Impaired NCT are encountered with segmentally demyelinated axons (38, 39). A nerve biopsy is a valid method to evaluate abnormalities in small nerve fiber density and integrity, however is rarely applied in clinical practice or routine screening programs due to its invasiveness (40).

In summary, multiple approaches are available to detect polyneuropathy. However, physicians are still facing distinct clinical challenges. First of all, the above-mentioned bedside assessments and QST are subjective, examiner dependent, time-consuming, easily influenced by patients' cooperation and confounding factors, and primarily utilized to detect advanced neuropathy (41). The late stage diagnosis of neuropathy by these crude tests usually goes along with irreversible nerve damage (22, 42). Secondly, NCT and skin biopsy are broadly considered as gold standards in clinical research (37). However, they are not applicable in clinical practice because they are invasive, time-consuming, require well-trained examiners and expensive devices as well as specialists for result interpretation (43, 44). Thirdly, most patients are unaware of their disease and severe symptoms have not developed, making the diagnosis difficult. This highlights the urgent demand for an approach to screen PN in asymptomatic patients that is efficient, practical, objective with quantitation of the extent of nerve damage. Such an approach may overcome the limitations of the current state of the art.

1.3. Innovative tools to diagnose PN

Recently, noninvasive point-of-care devices (POCD) have been developed to diagnose DPN (22, 45), which includes the DPN-Check (46, 47), NeuroQuick (48), NeuroPAD (49), Corneal Confocal Microscopy (CCM) (50, 51) and Sudoscan (52, 53). The DPN-Check is a brief version of the nerve conduction testing that may be completed within three minutes (47). It achieves 95% sensitivity and 71% specificity when compared to the findings of the nerve conduction testing (46, 47). Similar to NCT, it only assesses large nerve fiber function and provides no information on small nerve fiber functions. Therefore, other POCDs have been developed to identify small fiber impairments (abnormal pain perception, autonomic and sudomotor

dysfunction), such as the assessment tools NeuroQuick, NeuroPad, Corneal confocal microscopy, and Sudoscan.

NeuroQuick is a simple tool to quantify thermal sensation thresholds that are mediated by thinly myelinated Aδ and unmyelinated C-fibers. A study reported that the NeuroQuick is more sensitive in detecting small fiber dysfunction than bedside tests using a tuning fork in a diabetes cohort (48). However, as a psychophysical test, the test results might be affected by patients' attention and cognition. Moreover, its validity and reproducibility still need to be evaluated in larger cohorts.

The NeuroPad is a 10 minute test that evaluates sweat production of the feet. Validation studies have reported high sensitivity of this test for small fiber neuropathy and high reproducibility (45, 54). However, the sensitivities of NeuroPad for large fiber neuropathy is low and has been reported to range between 50 and 64% in these studies.

Corneal confocal microscopy is a noninvasive technique to identify corneal nerve impairment that is associated with peripheral nerve function (55). However, the devices are expensive and only specialists may perform the examination (16).

The Sudoscan quantifies sudomotor function within three minutes. Sudomotor dysfunction has been proposed as an indicator of small fiber neuropathy. Its sensitivity and specificity to classify DPN are reported to reach 87.5% and 76.2%, respectively (52, 53, 56). Nevertheless, it only assesses the autonomic nerve function and no motor- and sensory nerve status.

Advanced neuroimaging techniques, such as magnetic resonance neurography, diffusion tensor imaging, and nerve ultrasonography may provide additional insights into neuropathology of large and small myelinated fibers (57). However, these examinations need expensive devices and well-trained examiners. Thus, they are not appropriate for routine screening, but rather for experimental setups and study cohorts.

In summary, noninvasive POCDs have acceptable sensitivity rates for detection of fiber damage, however these should be combined to assess both large and small-fiber function. The cost-effectiveness and performance of each device still need to be evaluated in further studies (22).

1.4. Current concepts on game-based tools to diagnose PN

Digital game-based approaches have been developed for disease prevention and promotion of health and are known as "Gamification", "Exergames" and "Serious Games". "Gamification" encompasses typical game elements (leader boards, ranking, points, rewards, team activities, and profile design) to enhance motivation and performance. The terms "Exergames" or "Exergaming" refer to video games that interact with users by tracking body movement or

reaction while performance of exercise. The term “Serious Games” refers to games that are designed to deliver serious content, e.g. to address health problems (58).

“Gamification” has been rapidly grown as a hot topic in industry and academia since 2010. The Gamification market was estimated to reach 2.8 billion US dollars in 2016 (59). Most Gamification applications target behaviors associated with physical activity and weight loss. Most commonly used game elements include goal setting, social influences, and challenges (60). In a randomized clinical trial that assessed 602 overweight and obese adults, gamification interventions with incentives significantly increased physical activity in participants, especially when a competition was set up (adjusted difference, $p<0.001$) (61). “Exergames” typical applications are balance challenging exercises, such as step-mat-training (SMT) and Microsoft-Kinect® (KIN) Exergames. Clinical studies have confirmed the positive impact of these unsupervised exercise programs on reducing fall risk, improving proprioception and reaction time, enhancing executive functions, and preventing depression in seniors diagnosed with diabetes (62, 63). Computerized games for serious purposes are denoted “serious games” and commonly combine Gamification and virtual reality to enhance mental health interventions. Serious games are widely applied to assess and improve attention and memory function in seniors at risk for cognitive impairment (64, 65).

According to a recent literature review, there are no video game-based applications that have been specifically designed for peripheral neuropathy screening. However, studies have shown that “Gamification”- and “Exergames”-based programs have great potential to promote proprioception and shorten reaction times, improve balance and postural stability, reduce the risk of falls and improve mental quality of life.

1.5. Advances in machine learning algorithms development

Machine learning (ML) has been defined by Arthur Samuel in 1959 as a “field of study that gives computers the ability to learn without being explicitly programmed” (66–68). The primary precondition for ML is to “introduce algorithms that ingest input data, apply computer analysis to predict output values within an acceptable range of accuracy, identify patterns and trends within the data and finally learn from previous experience” (69). Advanced computational technologies and the extensive amount of data generated in the medical system have promoted broad applications of ML algorithms within the medical field. ML algorithms have shown many potential benefits in handling electronic laboratory data, medical records and imaging (70).

A research hotspot is the use of machine learning algorithms to develop models that may identify gait features that predict balance disorders, deficits following strokes, or diagnose neurodegenerative diseases. Artificial neural network (ANN) and support vector machine (SVM)

are reported to yield high accuracies in clinical studies (71, 72). Another hot research topic is dedicated to image analyses, e.g., to classify biopsy findings in pathology or magnetic resonance imaging (MRI) with deep learning algorithms to detect carcinomas (73). These applications have revolutionized the way both researchers and physicians address clinical concerns (70). Regarding peripheral neuropathy diagnosis, intelligent classification models have been developed using clinical data (such as glycated hemoglobin, physical activity level, surgery trauma history, diabetes mellitus duration) as predictive features. Logistic regression (LR), decision tree (DT), multi-layer perceptron (MLP), and artificial neural networks (ANNs) have performed acceptable accuracies on large study cohorts (74, 75). Overall, these studies highlight the potential strength of machine learning in medicine, particularly for the topic of this thesis.

1.6. Aims of the work

Detection of peripheral neuropathy in patients with diabetes (DPN) is a clinical challenge with high relevance for prevention of the diabetic foot syndrome. Accurate POCDs that are rapid, noninvasive, with investigator-independent evaluations of small and large fiber neuropathy are highly needed, preferentially for usage in the outpatient setting. Game-based applications combined with sensor-equipped insoles may circumvent drawbacks of traditional clinical examinations, however have to be standardized and meet highest standards. Supervised learning algorithms may aid data interpretation and offer an online prediction tool.

In this thesis I wish to establish a playful nerve function assessment device by combining sensor-equipped insoles with video games and machine learning algorithms. I set up the main hypothesis that “a video game-based “Gamidiagnostics” application is able to provide a meaningful assessment of small and large fiber function in a self-administered, examiner-independent manner and may be suited as a telemedicine application”. The following hypotheses will be tested:

(1) A “Gamidiagnostics” application with video-based playful elements combining sensor-equipped insoles and machine learning algorithms is feasible to screen for peripheral neuropathy in patients with diabetes.
(2) In such an application, critical skills may be tested and quantified, i.e. reaction time, quality of sensation, muscle strength, balance, and endurance.
(3) Furthermore, feature extraction methodology may be applied to determine representative game features and calculate key capabilities that correlate to the clinical ground truth (e.g. for NDS).
(4) Trained classification models may identify relevant game parameters, make predictions on DPN and possibly achieve phenotyping of impaired nerve fibers.

Specifically, the following subgoals will be addressed:

(1) Design and development of a “Gamidiagnostics” application that consists of video games controlled by sensor-equipped insoles, with real-time data acquisition, and automatic transmission to a remote server (denoted IQ-Trial).
(2) Validation of the “Gamidiagnostics” application in a pilot exploratory study by testing and quantifying critical skills of enrolled healthy individuals and patients diagnosed with diabetes and peripheral neuropathy.
(3) Performance of correlative analyses to determine differences between healthy volunteers and patients diagnosed with peripheral diabetic neuropathy according to clinical scores (NDS) and predefined key capabilities (reaction time, sensation, skillfulness, endurance, balance, muscle strength).
(4) Training and optimization of AI models for classification of patients with DPN versus healthy controls. Assessment and prediction of the severity of dysfunction for fiber subtypes Aβ-, Aδ-/C and Achilles tendon reflexes.

2. Materials and Methods

2.1. Sensor-equipped insoles

The study was designed to determine the performance of participants with video games that are coordinated by pressure sensor-equipped insoles as steering tools. Such insoles were not commercially available and were thus designed in cooperation with two firms that are knowledgeable in sensor manufacturing, Thorsis Technologies GmbH, Magdeburg, Germany and IEE S.A., Bissen, Luxembourg. Three prototypes were delivered for testing as control units for video games. Their technical features are summarized in Figure 1.

		Gaming Insole 1	Gaming Insole 2	Gaming Insole 3
Insole sensor mapping Pressure Temperature Inertial measurement unit		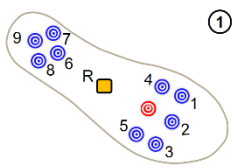	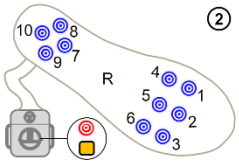	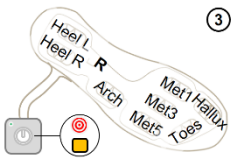
Pressure sensors	Type/Manufacturer	Interlink Electronics FSR™ 402	Interlink Electronics FSR™ 402	IEE high dynamic HD002 FSR
	Number of cells	9	10	8
	Size	Circular with diameter 1cm		Rectangle with area 5.57 cm^2
	Measuring range	0 ~ 15bar		250mbar ~ 7bar
	Accuracy	100mbar		3.4mbar
Temperature sensor		One on the insole and one intergrated in MCU	One intergrated in MCU	One intergrated in MCU
Inertial measurement unit (IMU)	Type/Manufacturer	LIS3DH with 3-axis accelerometer	LIS3DH with 3-axis accelerometer	ICM-20948 with 9-axis gyroscope, accelerometer, compass
	Measuring range	±2G	±2G	±2G ~ ±16G
Data sampling		30Hz	100Hz	25 ~ 500Hz
Communication		Bluetooth 4.1	Bluetooth 4.1	BLE 5.0+
Battery		45mAh, 1h streaming	45mAh, 2h streaming	300mAh, 12h streaming
Charging method		Manually replace the battery	Micro-USB-B charging	USB-C charging
Internal storage		8MB	8GB	Standard 8GB
Electronic Control Unit (ECU)		Integrated	Discrete	Discrete
Data Synchronization (between left & right foot and device)		No	No	Yes
Automatic detection of L/R foot		No	No	Yes
Offline recording		No	No	Yes, up to 10h
Covered shoe size		37 ~ 46 EU	37 ~ 46 EU	28 ~ 47 EU

FSR: Force Sensing Resistor

Figure 1. Overview on technical features of sensor-equipped insoles tested in the study.

The Gaming Insole 1 is an all-in-one plantar pressure-measuring insole system (InterSOLE®, Thorsis Technologies GmbH, Magdeburg, Germany) that embeds an electronic control unit (ECU) and nine circular pressure sensors with diameters of 1cm each, which are integrated into a flat onlay of soft tissue that fits into pantolettes. The sensors are located at the metatarsal 1–5 and calcaneus. According to the manufacturer, the threshold of the pressure sensors is 100 mbar, the measuring frequency equals 30 Hz. The ECU is integrated into the insole together with a temperature sensor and a three-axis accelerometer (LIS3DH). The insole transfers the sensor data to connected devices via Bluetooth (Version 4.1) in real-time. A

rechargeable battery enables the insole to perform continuous recordings without interruptions for about one hour. The insoles were fabricated at standard sizes ranging from EU shoe sizes 37 to 46 (ten sizes).

Gaming Insole 2 is an upgraded version of the aforementioned InterSOLE® (Thorsis Technologies, Magdeburg, Germany), which has a separate ECU (including accelerometer), higher measuring frequency (100 Hz), additional storage capacity (8GB), optimized power consumption and power supply strategy (with ≥ 2 hours streaming duration). The ECU is separate from the insole and connected via a flexible connection. The setup requires the user to strap the ECU to the lower limb or ankle. All other properties of the insole are identical to the first InterSOLE version.

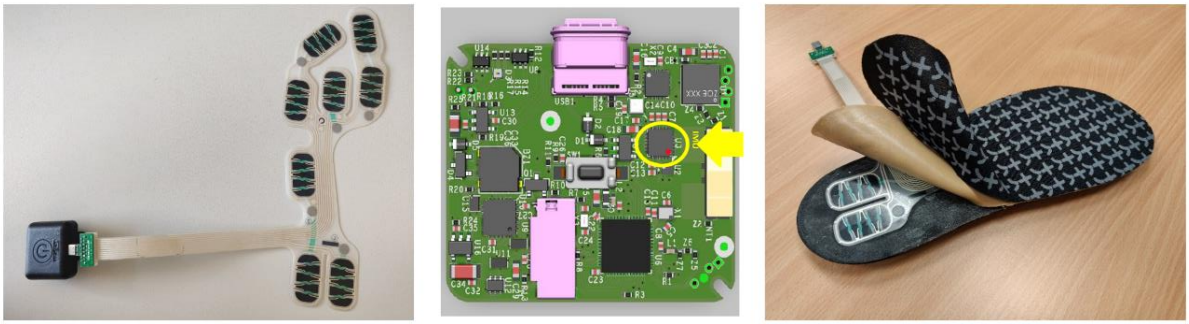

Figure 2. Characteristics of the Gaming Insole 3 (ActiSense System®, IEE S.A., Bissen, Luxembourg). *a) The eight pressure sensors are integrated into a flat laminated flexible foil at distinct locations that correspond to the calcaneus (2 sensors), lateral arch, metatarsal 1, 3, and 5, digitus 1 and 5 of the feet. The sensor areas cover about 5.6 cm^2 each and are seen as dark areas implemented in the foil. b) Printed circuit board of the electronic control unit with a nine-axis inertial measuring unit marked with a yellow circle. c) Gaming sensor placement on top of the more resistant insole beneath a textile cover sheet.*

The Gaming Insole 3 (ActiSense System®, IEE S.A., Bissen, Luxembourg) encompasses an Electronic Control Unit (ECU) and eight pressure sensors (5.6 cm^2 high dynamic HD002 force sensing resistors) that are integrated into flexible foil at locations corresponding to the calcaneus, lateral arch, metatarsal 1, 3, and 5, digitus 1 and 5 of the feet (Figure 2a). The sensors allow for pressure detection with an accuracy of 3.4 mbar in the range of 250 mbar to 7 bar. The ECU consists of a nine degrees of freedom inertial measuring unit (IMU, embedding a 3-axis accelerometer, a 3-axis gyroscope and a 3-axis magnetometer), with a sampling rate of up to 500Hz, data synchronization (between insoles and smart devices), automatic detection of foot side, internal storage of 16 GB and energy supply of up to 10 h (Figure 2b). The sensors are embedded in foil and do not protrude. The foil is placed on top of the ethylene-vinylacetat-30 insole beneath a protective layer of textile covering (Figure 2c). In the “Gamidiagnostics” sessions, sensor data were recorded at 200Hz and transferred in real-time to the App via Bluetooth (5.0) for smooth steering of games.

The aforementioned Gaming Insoles were initially evaluated as steering units for the video games. Six test scenarios were defined to judge insole performances in various use cases, which consist of (1) balanced sitting, maximum pressure on the (2) forefoot or (3) heel while sitting, (4) balance standing, (5) standing only on one foot, and (6) normal walking. The pressure-time profiles of study participants are depicted for the three insoles in Figure 3. All absolute pressure values were normalized to the range of 0 to 1 following the calibration steps that recorded the maximum pressure values achieved for each sensor. No significant differences were observed during the balanced sitting phase with all three types of insoles. However, in the other scenarios, Gaming Insole 1 was outperformed by the other two insoles, given that most of the sensors of Gaming Insole 1 did not respond to applied pressure changes (e.g., only sensor of MTK4 detected pressure variations when the participant applied maximum pressure on the forefoot while seated). Moreover, the pressure profiles recorded with the left and right insole differed markedly while normal walking.

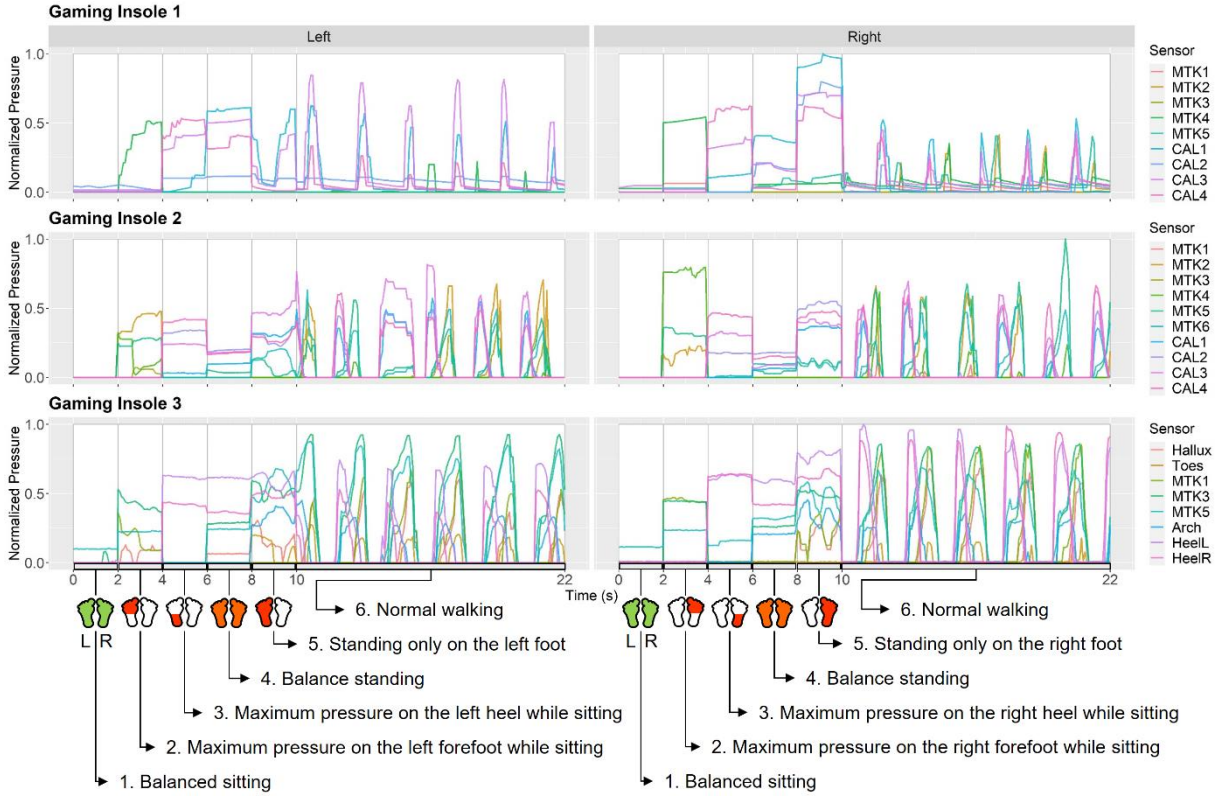

Figure 3. Performance comparison of the three Gaming Insoles with findings during a standardized test protocol. *The pressure-time profiles of a study participants were recorded with different insoles and are visualized for all six tasks, including balanced sitting, maximum pressure on the forefeet while seated, maximum pressure on the heels while seated, balanced standing, standing only on one foot, and walking.*

Gaming Insole 2 revealed noticeable improvement in detecting pressure changes, most of the sensors provided adequate pressure values in the different scenarios, especially when the participant applied maximum pressure on the forefoot or heel while seated. However, with this insole there were still marked differences in the pressure values recorded by the left and right

insole during walking and in the seated position, when the maximum pressure was applied to the heels and forefeet.

In contrast, the Gaming Insole 3 yielded a smoother pressure profile, likely due to the higher transmission frequency of the pressure values. Furthermore, more sensors were activated when maximum pressure was applied to the left and right forefoot in the seated position (test scenario 2). Lastly, the stance phase of walking measured by the insole was longer with Gaming Insole 3 than with the other two insoles. The stance phase is defined as a gait phase that begins when the foot touches the ground and ends when the same foot leaves the ground. The likely reason was a lower sensor detection limit and higher detection frequency of the Gaming Insole 3.

Given these findings Gaming Insole 3 was selected as the control unit for the pilot study on neuropathy detection with video games.

2.2. Game developing architecture

The Android Studio application (the official integrated development environment for Google's Android operating system, Google LLC, U.S.) was chosen to develop an Android-Unity-Plugin. Game developing engine Unity (version 2019.1.8f1, Unity Technologies, U.S.) and Visual Studio 2017 on the Windows platform were utilized to implement the designed video games. Figure 4 summarizes the developing architecture implemented in this work.

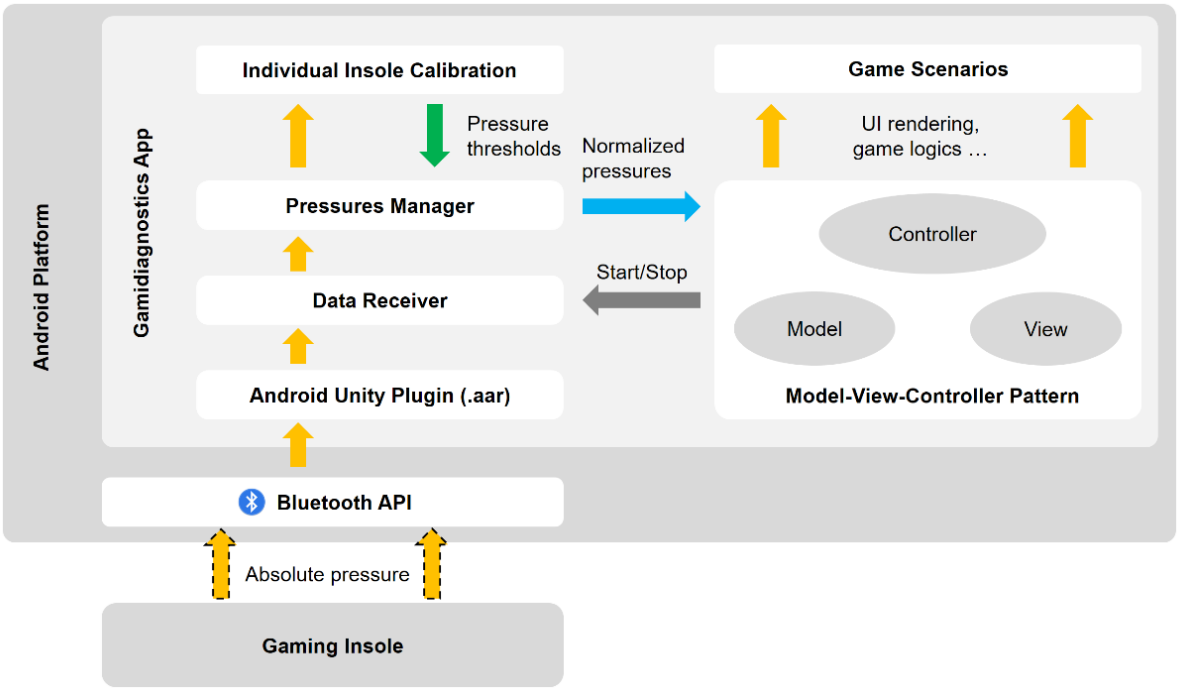

Figure 4. Game environment architecture. *Absolute pressure values detected and quantified by the sensors of the insoles were transferred via Bluetooth to an Android device. The "Gamidiagnostics" App received pressure values through a plugin and the Bluetooth API that controls Bluetooth connections to both insoles. The pressure manager was programmed to normalize pressure values to a range from 0 to 1 (minimum to maximum values),*

depending on pressure results acquired from the calibration steps (see below). In different game scenarios a similar functional pattern named Model-View-Controller (MVC) was implemented. The Model defined the data structure and functions to read, save and transform the data. The View consisted of methods that render the graphics and control the UI elements. The controller connected the model and the views, and performed the game mechanism.

Communications between insoles and Android tablets were established according to the predefined data transfer protocol. An Android-Unity-Plugin was programmed to unify and manage Bluetooth connections to insoles and forward sensor data to the “Gamidiagnostics” App. It normalized absolute pressures to values ranging from 0 to 1 depending on the individual pressure thresholds acquired from insole calibration and transformed pressure changes to corresponding control signals in variant game scenarios. The Model-View-Controller (MVC) Pattern that consisted of three functional parts: Models (Data creating, reading, updating, and deleting), Views (Interface/Detection), and Controllers (Decision/Action) was introduced in four games. The model represents the data portion such as the moving speed of an element, the frequency of collisions between objects, the number of retries in different game levels, and overall game score of a player. The view represents the viewing portion which is linked to the model. The view has direct access to change the property of the UI elements or listened to the events. The controller brings together the model and view by synchronizing state and driving interaction between components in the game.

2.3. Design of video games and setup of “Gamidiagnostics” application

In the following, the usability of the Gaming insoles 3 was tested in video games. The primary quest was to define appropriate exergaming challenges and to design appealing video games with common game elements, such as tasks of limb coordination, anticipation of movements, coordination of bilateral movements, left-right-sidedness. Overall care was taken to simplify the video games in as much that a brief tutorial sufficed to formally instruct and introduce the player into the challenges (overview of “Gamidiagnostics” application in Figure 5). The pressure sensors within the insoles constituted the steering control units. The following requirements were defined for the game design and challenges herein: 1. A low complexity setup allowed a quick entry into all games and an easy understanding of control functions through pressure measuring insoles. 2. Motivational elements encouraged completion of tasks and endurance over 15 minutes. 3. Standardized calibration steps and tutorials before each game allowed initial steering attempts to familiarize with the games. Tutorials were repeated on demand. 4. Standardized data acquisition processed with time stamps link sensor data over the course of games, even in the event of failed efforts (maximum allowance of three failed efforts per game). Comparison of datasets through time frames was maintained. 5. Definition of distinct challenges in each game provided information on movement control of both feet and legs with variables affected by muscle strength, sensation, balance, and coordination. These

variables were tested for each foot separately and both feet in concert. 6. Immediate feedback to the participants on gaming results and overall performance.

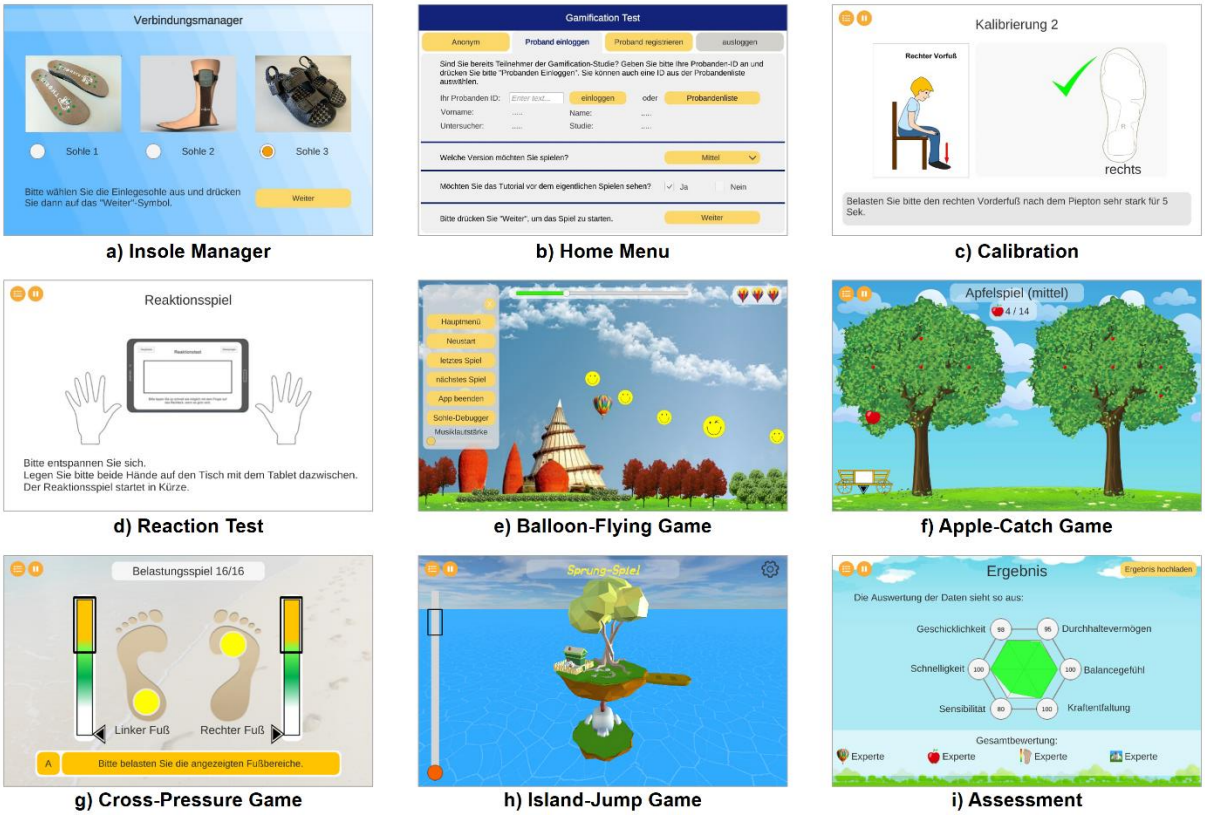

Figure 5. Page-wise set-up and components of the "Gamidiagnostics" application. *Each participant of the Gamidiagnostics sessions performed a parcours of tasks. (a) The "Insole Manager" page was accessed first and a Bluetooth connection of the tablet to both insoles was established. (b) On the "Home Menu" page the participant entered his name and received an ID for pseudonymization. Furthermore the settings of the "Gamidiagnostics" were defined, e.g. with tutorials and middle game length. (c) On the "Calibration" page the participant was asked to perform eight calibration steps. The resulting minimum and maximum pressure values were utilized to normalize all subsequent pressure values to a range from 0 to 1. (d) On the "Reaction Test" page the participant had to respond with an immediate finger movement and touch of the screen when a green colour sign appeared. (e—h) The main part of the Gamidiagnostics application constituted a set of four video games. These were labelled as balloon-flying (BF), apple-catch (AC), cross-pressure (CP) and island jump (IJ) games. Each individual game was introduced by a brief tutorial that explained the challenges and allowed to familiarize the participant with the foot movements that are required to steer the devices. (i) Finally, the "Assessment" page summarized the overall achievements of the participants and visualized these with a spider chart. The subskills were classified into the following subcharacteristics: skillfulness, reaction time, sensation, muscle strength, balance, and endurance.*

The "Gamidiagnostics" application was set up page-wise. The overview on the page composition is provided in Figure 5 and Appendix 11.6. On the first page an insole connection manager handled the Bluetooth connections to abovementioned Gaming Insoles and visualized the sensor positions and values (pressure, temperature, acceleration, and battery status) in real-time (Figure 5a and Figure 6).

On the "Home Menu" page the study personnel logged in to the application and set the game preferences, including middle game length, performance with tutorials, and insole calibration thresholds. All study participants were registered with new Subject-ID (Figure 5b).

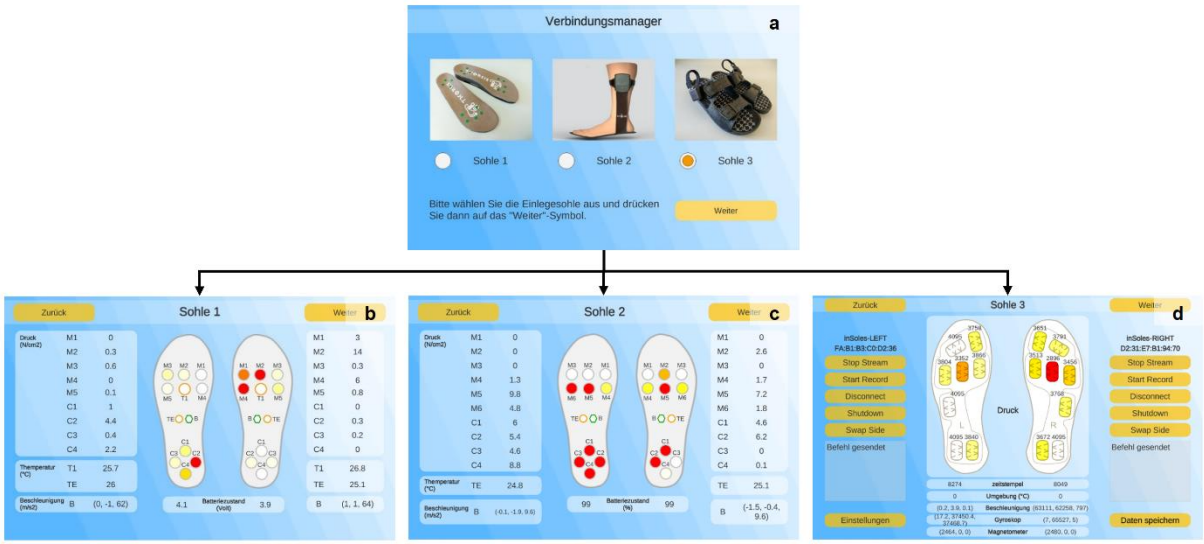

Figure 6. Insole connection manager of the "Gamidiagnostics". *(a) Start page that allowed the study participant to select the insole. (b-d) Sensor views of Gaming Insoles 1, 2, and 3. The battery status of the insoles, and sensors data (pressure, temperature, acceleration, gyroscope, and magnetometer) were visualized.*

To normalize pressure values according to weight and maximum pressure applied by the participants, eight calibration steps were defined. These were visualized on the calibration page and the participants were instructed to perform these before exercising the games (Figure 5c, Figure 14). The recorded minimum and maximum pressure values were the basis for data normalization, which is to define a range from 0 to 1 for each sensor. The steering unit of the insoles was programmed to apply normalized values in the games, which were the transformed values between 0 and 1.

On the next page a "Reaction Test" was set up. Here study participants were instructed to position their hands on both sides of the tablet and be prepared to touch the screen as soon as a green rectangle appears. There were four attempts with different time intervals between signals. All finger reaction times were saved locally on the tablet (Figure 5d).

On the next pages four different video games were implemented, that were denoted according to their key features: Apple-Catch (AC), Balloon-Flying (BF), Cross-Pressure (CP), and Island-Jump (IJ) games (Figure 5e–h).

In the Balloon-Flying (BF) game, the player guides a balloon over a skyline (Figure 5e). The flying height is adjusted by the applied pressure detected at the forefoot of the right or left insole, respectively. The balloon approaches the ground if no pressure is applied. The ideal flying route is paved by 12 smileys that also suit as the games' scoring system. To collect the maximum number of smileys, the player must maneuver the balloon through the skyline and preclude collisions with obstacles, such as clouds, buildings, and trees. In the case of a collision with an obstacle and absent corrective measures in five seconds, a restart is

automatically initiated. The Balloon-Flying parcours consists of twelve distinct tasks, indicating 12 obstacles.

In the Apple-Catch (AC) game, the player is situated in an autumn harvest scenario and tries to catch as many apples as possible with a carriage that is controlled by the plantar pressure application in both forefeet (sensors Met1/3/5) (Figure 5f). The apples grow in size and fall from the tree one by one at equal time intervals. The target pressure has to be adapted for the guidance of the carriage below the apple. Additionally, the player must maintain the appropriate pressure until the apple falls into the carriage; otherwise, the carriage moves out of the ideal area. Following each task, the carriage is automatically reset to the middle line. Eleven distinct parameters per task are defined that are the basis for player performance assessment. The length of the AC game is standardized and encompasses a total of 14 tasks (apples).

In the Cross-Pressure (CP) game, the players are instructed to apply pressure on different foot areas (forefoot or heel) with differing target pressure levels (low or high) (Figure 5g). Low pressure is indicated by green color, high by yellow color. The actual pressure is visualized by black arrows in a pressure bar to the left and right of the virtual feet. To achieve optimal scores, the player must readily adjust the applied pressure on the corresponding plantar foot areas and maintain the correct pressure level for at least 4.5 seconds. A smiley and checkmark confirm accomplishment of the task. If the insole detects no valid action within 25 seconds, the game proceeds to the next task. Sixteen tasks corresponding to 16 combinations of foot areas and ideal pressure levels are designed in the game.

In the Island-Jump (IJ) game, the player steers a virtual bird with jump movements from island to island in an ocean until a final destiny harboring its home is reached (Figure 5h). The player adjusts the jumping distance by modulating the plantar pressure in his forefeet. The jump direction, left or right, is adjusted by the relative pressure distribution below the right and left forefoot. To achieve the optimal score, the player must adjust according to the predefined pressure values and release the pressure at once when this has been reached. If the optimal pressure is not maintained within narrow limits, the bird jumps into the water. It initiates a game restart, and the player faces the same challenge again. There are a total of 16 islands (tasks) with different optimal pressure levels (low, middle, or high) and foot sides (left, right, or both).

Every game was introduced by a prerecorded tutorial, which provided standardized instructions on how to proceed with the games, allowed for some early steps in handling the insoles (examples of pressure application, guidance with insoles). Furthermore motivational elements (scoring system with smileys) were introduced in the games and the possibility to repeat instruction tutorials.

All sensor data together with the pseudonymized data from each participant were transferred to the remote IQ-Trial server for data calculations and interpretation. Moreover, the IQ-Trial server visualized the data and created a result sheet as feedback to the study participants with a spider chart on the participant's game performance, referring to six key capabilities: reaction time, sensation, skillfulness, muscle strength, balance, and endurance (Figure 5i). In addition, the study participants were classified as "beginner", "moderate", "advanced", or "expert" players according to their game performance (i.e. numbers of collected apples in the AC game, acquired smileys in the BF and CP game, and attempts in the IJ game).

2.4. Feature extraction methodologies

Feature extraction was performed to get parameters that representatively reflect players' performance (denoted "representative parameters/features") in the "Gamidiagnostics" session. Game parameters calculated from each game task were considered as primary features. Apart from that, the concept of task combination (TC) was introduced, i.e., a set of game tasks with similar specifications or macro-measurements were combined. Feature extraction of distinct parameters from defined tasks and task combinations (TCs) for the four games was set up.

In the AC game, eleven distinct parameters were defined to represent the player's performance in every task (Figure 7a, b).

1. Reaction time [s]: the time that the player spends to identify the next apple and move the car over ten percent of the target distance (horizontal distance between the initial position of the car and the next apple).
2. Anticipation time [s]: the time that the player takes to bring the car into the catching area through modifying appropriate pressures on his/her feet.
3. Time inside catching area [s]: the time that the car stays in the catching area. The player achieves this by maintaining the appropriate pressure on the insole.
4. Time outside catching area [s]: the time that the car leaves the catching area when the player fails to keep the appropriate pressure on the insole.
5. Frequency outside catching area: the frequency that the car leaves the catching area after initially entering it.
6. Final virtual distance: the distance between the car and the target apple at the end of each task.
7. Apple caught (yes/no): a value that indicates whether the apple is collected or not in the task.
8. Normalized pressure: the sum of the normalized pressures of all frames in the task.
9. Pressure differences between successive frames: the sum of the pressure deviations between frames in a task.
10. Pressure gradients between successive frames: the sum of the pressure gradients between frames in a task.
11. Pressure time integral: the area under the peak pressure-time curve recorded by an insole in a task.

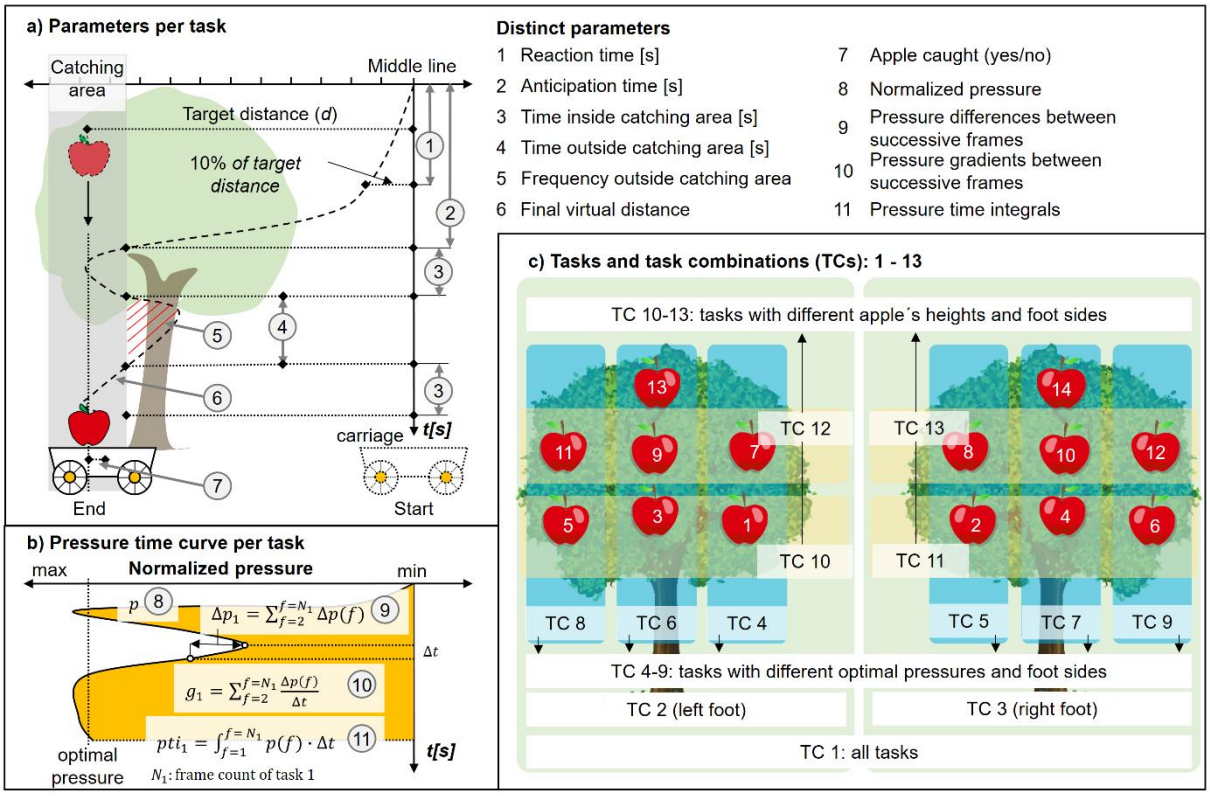

Figure 7. Setup of the Apple-Catch (AC) game and feature extraction. *(a) In order to evaluate the performance in apple collection, eleven distinct parameters were defined per task, constituting the basis for data analyses. (b) Pressure-time curve of each task and calculations of pressure differences, pressure gradients, and pressure-time integration. (c) The Apple-Catch game included fourteen tasks (apples). For feature extraction, tasks and task combinations were furthermore defined (TC 1 through 13) to assess the performance (overall result versus left/right foot, tasks with different ideal pressures, left/right foot, tasks with different apple heights and foot sides).*

In addition, 13 task combinations (TCs) were included to provide a more comprehensive picture of the player's overall performance (Figure 7c). TC1 encompassed all tasks of this game. TC2 covered all tasks that use the left foot for controlling the car movement to catch apples. The corresponding TC3 consisted of all tasks that use the right foot. The player's performance in tasks requiring different feet can thus be tracked. Furthermore, TC4–9 were divided by varying horizontal positions of the apples, and TC10–13 involved game tasks with apples positioned on various heights. The sum, mean, and standard deviation of primary features over game tasks of TCs were treated as secondary features. For example, the "Reaction time [s]" of TC1 was a secondary feature that was computed from the average reaction time of all tasks. Totally, 583 features were extracted from one AC game dataset, which consisted of parameters calculated from 14 game tasks and additional parameters generated from 13 TCs (Figure 11).

In the BF game, eleven distinct task parameters were defined as below (Figure 8a, b).

1. Smiley count (n): the number of smileys that are collected in a task (maximum four)
2. Collision frequency (n): the frequency that the balloon collides with obstacles due to inappropriate pressures detected by the insole in a task.

3. Minimal virtual distance smiley 1/2/3/4: the relative distance between the balloon and the first/second/third/fourth collected smiley at the moment of collision. If the smiley is missed, this variable will be assigned a maximum value.
4. Virtual deviation of ideal flying route: the virtual deviation of the balloon's actual flight route from the ideal positions in each task.
5. Normalized pressure: the sum of the normalized pressures of all frames in the task.
6. Pressure differences between successive frames: the sum of the pressure deviations between frames in a task.
7. Pressure gradients between successive frames: the sum of the pressure gradients between frames in a task.
8. Pressure time integral: the area under the peak pressure-time curve recorded by an insole in a task.

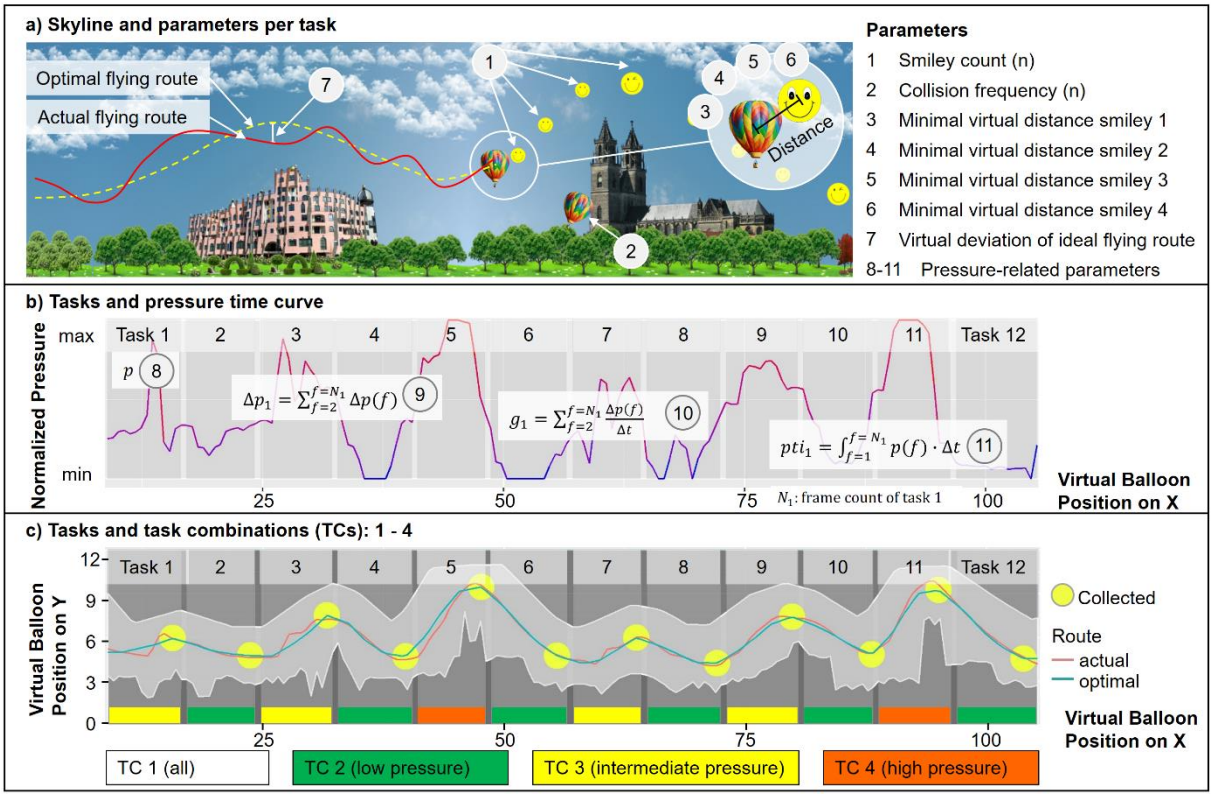

***Figure 8. Setup of the Balloon-Flying (BF) game and feature extraction**. (a) Eleven distinct parameters were extracted following comparison with the predefined optimal flying course of the balloon. These are enlisted and include the overall number of collected smileys (yellow circles), collision frequency, minimum virtual distances balloon to smiley/perfect flight position, and the pressure gradient between consecutive obstacles. (b) The Balloon-Flying parcours consisted of twelve distinct tasks. (c) Definition of tasks and task combinations (TC) corresponding to low, intermediate, and high-pressure applications.*

Additionally, four TCs were introduced in the BF game (Figure 8c). TC1 encompassed all tasks of this game. TC2–4 were divided according to low, intermediate, and high-pressure applications by flying over obstacles of variant heights. Overall, 528 features were extracted from one BF game dataset, which consisted of primary parameters calculated from 12 game tasks and additional parameters generated from four TCs (Figure 11).

In the CP game, eleven distinct parameters per task were defined as below (Figure 9a, b).

1. Anticipation time [s]: the time that the player understands a task and modifies his/her plantar pressures until the optimal pressure zone is reached.
2. Time outside optimal pressure zone [s]: the time that the optimal pressure is not maintained in a task.
3. Relaxation time [s]: the time that the player spends to release the pressure when a task is accomplished.
4. Normalized pressure (left foot): the sum of the normalized pressures of all frames measured by the left insole in the task.
5. Pressure differences between successive frames (left foot): the sum of the pressure deviations between frames measured by the left insole in a task.
6. Pressure gradients between successive frames (left foot): the sum of the pressure gradients between frames measured by the left insole in a task.
7. Pressure time integral (left foot): the area under the peak pressure-time curve recorded by the left insole in a task.
8. Normalized pressure (right foot): the sum of the normalized pressures of all frames measured by the right insole in the task.
9. Pressure differences between successive frames (right foot): the sum of the pressure deviations between frames measured by the right insole in a task.
10. Pressure gradients between successive frames (right foot): the sum of the pressure gradients between frames measured by the right insole in a task.
11. Pressure time integral (right foot): the area under the peak pressure-time curve recorded by the right insole in a task.

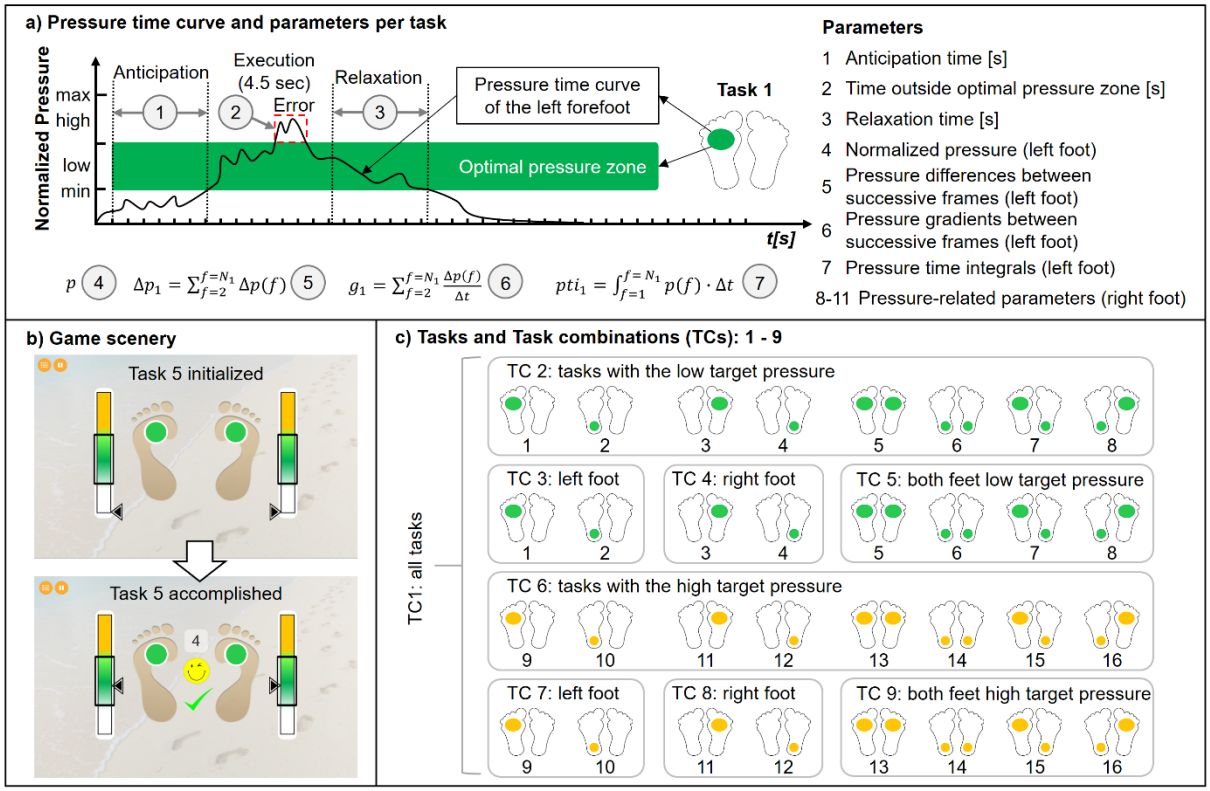

Figure 9. Setup of the Cross-Pressure (CP) game and feature extraction. *(a) Eleven parameters were defined to present the game outcomes per task, which considered time durations of key game events and pressure gradients. (b) Screenshots of an initialized and accomplished game task. (c) The CP game included sixteen tasks corresponding to 16 combinations of foot areas and ideal pressure levels. Nine task combinations were defined for extracting features that addressed players' performance by different pressure levels and foot areas.*

Additionally, nine TCs were considered in the CP game (Figure 9c). TC1 encompassed all tasks of this game. TC2 consisted of tasks with low target pressure. TC3─5 were three subgroups of TC2, divided by the sides of the foot involved (left, right, or both sides). TC6 comprised tasks with high target pressure.TC7─9 represented three subgroups of TC6, similarly classified by the sides of the foot involved (left, right, or both sides). Overall, 473 features were extracted from one CP game dataset, which consisted of primary parameters calculated from 16 game tasks and additional parameters generated from nine TCs (Figure 11).

In the IJ game, eight distinct parameters per task were defined as below (Figure 10a─c).

1. Attempt count (n): the number of attempts to jump over a stage.
2. Deviation from optimal pressure: the absolute deviation between the measured pressure and the ideal pressure (for a perfect jump to the middle of the next stage).
3. Anticipation time [s]: the time that the player spends to modify the proper pressures until 25% of the maximal pressure range is exceeded.
4. Execution time [s]: the duration of the execution period that the player continuously modifies appropriate pressures before the bird jumps to the next stage.
5. Mean pressure of execution phase: the average pressure during the execution period.
6. Pressure differences between successive frames: the sum of the pressure deviations between frames in a task.
7. Pressure gradients between successive frames: the sum of the pressure gradients between frames in a task.
8. Pressure time integral: the area under the peak pressure-time curve in a task.

Additionally, seven TCs were introduced in the IJ game (Figure 10d). TC1 encompassed all tasks of this game. TC2─4 were divided by the direction that the bird jumped. TC5─7 were classified by the different optimal pressures (low, moderate, or high) associated with the distance to the next island (low, medium, or far distant. In total, 296 features were extracted from one IJ game dataset, which consisted of primary parameters calculated from 16 game tasks and additional parameters generated from seven TCs (Figure 11).

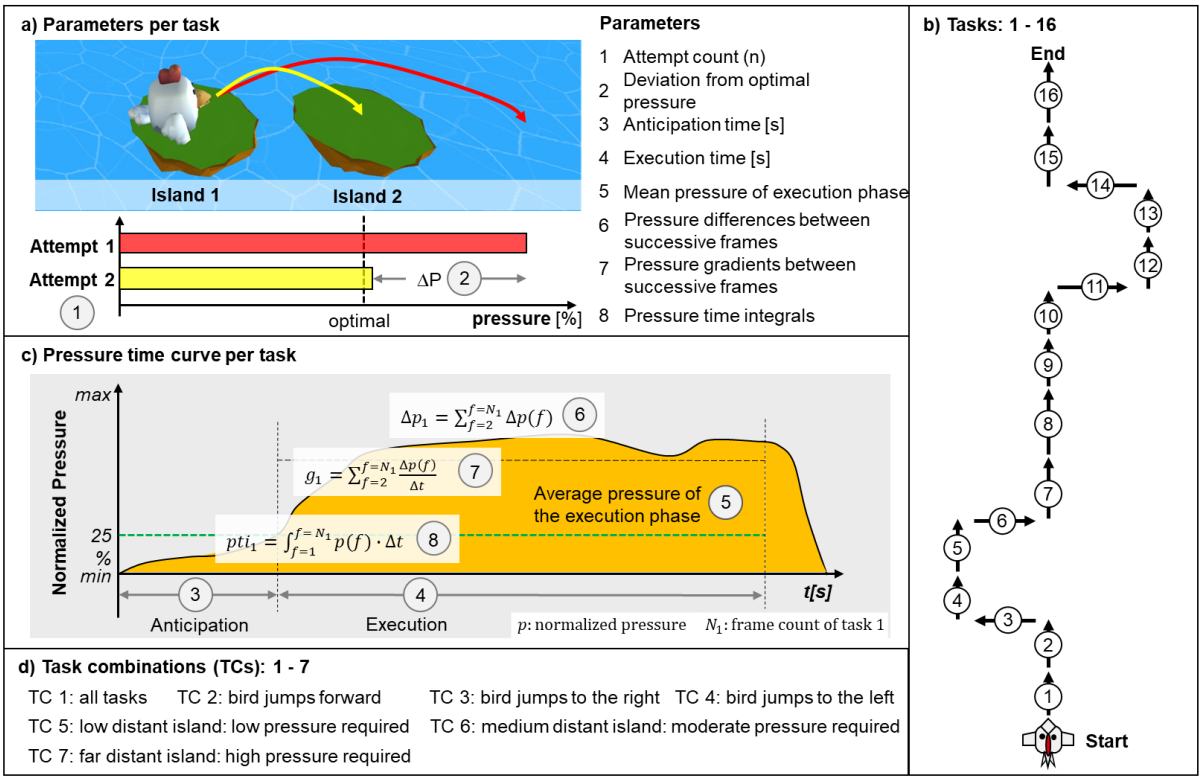

Figure 10. Setup of the Island-Jump (IJ) game and feature extraction. *(a) Eight parameters were defined to indicate the game outcomes per task. (b) The IJ game contained sixteen tasks corresponding to 16 islands that the bird has to jump through until reaching home. (c) Pressure-related parameters include normalized pressure, pressure difference, pressure gradient, and pressure-time integration of the left/right foot. (d) Distribution of task combinations corresponding to low, intermediate, and high-pressure applications on the left, right, or both feet.*

In summary, introducing the concept of TC facilitated the analysis of players' performance in the entirety or among similar tasks and the extraction of the corresponding distinctive parameters. Overall, 1,880 distinctive parameters reflexing players' performance were extracted per dataset (per subject) (Figure 11).

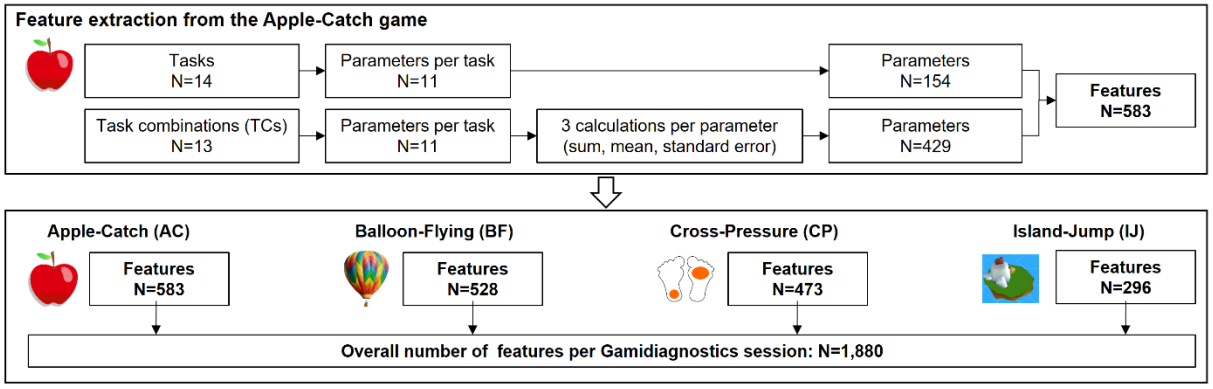

Figure 11. Feature extraction from the "Gamidiagnostics" session. *Distinct parameters defined in each task were initially considered as primary features, such as the reaction time of the first task of the AC game. Task combinations (TC) were additionally included, i.e., a set of game tasks with similar specifications or macro-measurements. The sum, mean, and standard deviation of each predefined game parameter over all TCs were treated as secondary features for analyses. 583 features were extracted for the AC game by adding 429 summarized features of thirteen TCs to the primary task parameters (n=154). Overall, 1,880 features were extracted from four games per session.*

2.5. Hypothesis-driven key capabilities

According to the hypothesis that critical skills are required for successful gaming performance, six hypothesis-driven key capabilities were defined: skillfulness (overall achievements in each game), reaction time (understanding and immediate response to tasks), sensation (fine-tuning of pressure application in subtasks), muscle strength (achievements with high-pressure application), balance (pressure distribution left versus right foot) and endurance (steadiness of pressure application in tasks) (summarized in Figure 12). The “skillfulness” assesses players’ performance comprehensively. It is associated with collected apples (n) in the AC game, acquired smileys (n) in the BF and CP games, and jumping attempts (n) in the IJ game. The “reaction time” is correlated only to the initial phase of each game, i.e., the reaction time [s] and the anticipation time [s] in the AC and CP games. It evaluates the speed that a player recognizes the task requirement and action to modify the proper pressure on his/her feet. The “sensation” addresses perception and execution of low pressures and modulation that are represented as “Final virtual distance” (AC game), “Minimal virtual distance smiley 4” (BF game), “Time outside optimal pressure zone” (CP game), and “Deviation from optimal pressure” (IJ game). The “muscle strength” is related to players’ performance in specific game subtasks that require high-level pressures, such as tasks 5, 6, 11, 12 in the AC game with apples that are located extremely far from the car. This key capability also considers tasks 5 and 11 of the BF game (high obstacles), TC 6 of the CP game (tasks requiring high optimal pressure), and TC 7 of the IJ game (tasks with far distant islands). The “balance” is calculated from calibration steps (Figure 14) that evaluates pressure deviations between the left and right foot while balance standing (step 6) and standing only on a single foot (step 7 and 8). The “endurance” indicates players’ sustainable capacity by maintaining a consistent pressure in specific game scenarios, i.e., waiting for an apple within the catching area in the AC game, an execution phase that requires the optimal pressure for 4.5 seconds in the CP game, and consecutive jumps in the IJ game. The corresponding indicators are “Frequency outside catching area” (AC game), “Time outside optimal pressure zone (sec)” (CP game), and Consecutive jumps without interrupts (IJ game). The six key capabilities have the same range from 0 to 1 and are calculated automatically at the end of the “Gamidiagnostics” session and displayed with a spider chart that delivers feedback on the game performance.

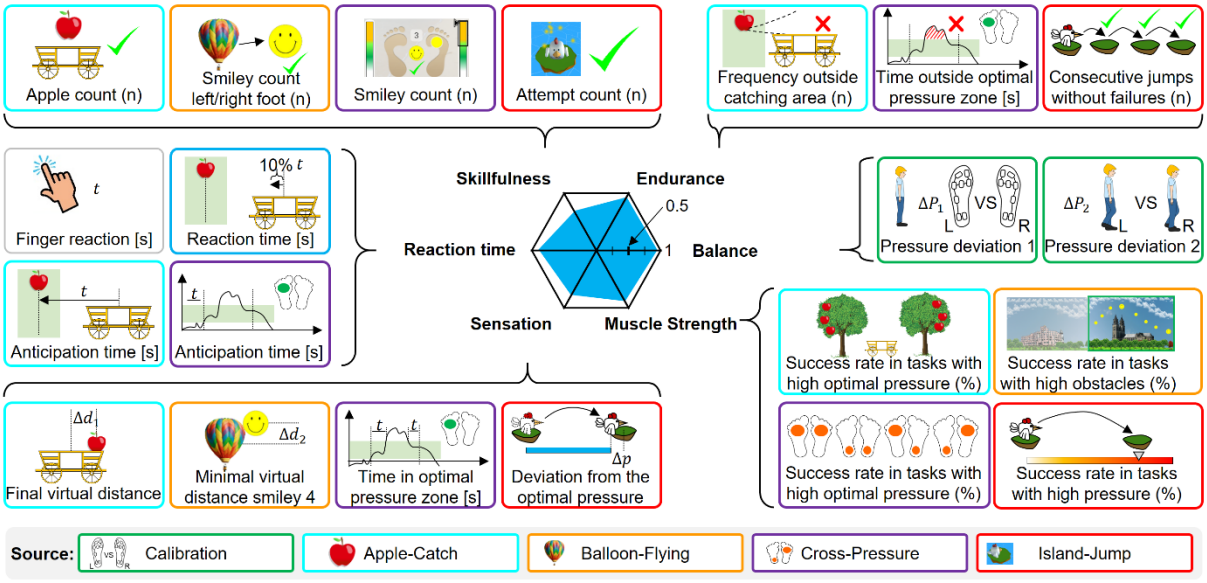

Figure 12. Considerations on key capabilities and scoring of video games (hypothesis-driven). *Six key capabilities for the initial evaluation of the gaming success were defined: skillfulness (overall achievements in each game), reaction time (understanding and immediate response to tasks), sensation (fine-tuning of pressure application in subtasks), muscle strength (achievements with high-pressure application), balance (pressure distribution left versus right foot) and endurance (steadiness of pressure application in tasks). The weighted summation of achievements in each of these was transformed into a score expressed as [%] in a spider diagram for immediate feedback to the players.*

2.6. Study design

2.6.1. Inclusion and exclusion criteria

The pilot study was carried out at the University Clinic for Nephrology and Hypertension, Diabetes and Endocrinology in Magdeburg, Germany, following approval by the local ethical committee (28/17 on 13.04.2017, see Appendix 11.1), with a subcohort from the SmartPreventDiabeticFeet Study (DRKS00013798) (76).

The inclusion criteria of the DPN group were:

1. distal symmetrical polyneuropathy (sensorimotor polyneuropathy);
2. diabetes mellitus type 1 or type 2;
3. absence of manifest neuropathic foot ulceration;
4. NDS $\geqslant$ 2;
5. ability to use a mobile phone.

The inclusion criteria for the control group were:

1. no diagnosis of diabetes mellitus;
2. absent signs of the polyneuropathy of any etiology (according to above examination results and questionnaire survey);
3. a good general state of health;
4. age between 18 and 85 years;
5. ability to use a mobile phone.

The exclusion criteria were:

1. macroangiopathy of the lower extremities;
2. physical deformities (amputations, foot and leg deformities requiring orthopedic shoe fitting);
3. manifest foot ulceration;
4. visual disorders including visual acuity of less than 0.8 (except for corrected myopia and hyperopia);
5. muscular diseases/motor diseases;
6. myocardial infarction <12 weeks;
7. heart failure (NYHA III or IV);
8. age below 18 years;
9. lack of ability to give consent for any reason.

2.6.2. Participants

From 07/2020 to 01/2021 patients diagnosed with diabetes and peripheral neuropathy as well as healthy volunteers were recruited and enrolled following written informed consent (see Appendix 11.2). All received a detailed explanation of the study protocol, test procedure, and data handling policy. A questionnaire about past medical history included diabetes mellitus (time of first diagnosis, type, treatment history, sensory disturbances, complaints, movement restrictions in daily life), autonomic diabetic neuropathy (dizziness, heart rate arrhythmia, urination disorders, sweating function), diabetes-associated comorbidities, daily activities (sports, handedness, dominant foot), recent HbA1c and fasting blood sugar values were recorded (see Appendix 11.3). A physical examination with bedside neurological and sensory nerve testing encompassed pinprick test, vibration perception, Tip Therm, reflexes, muscle function. Subsequently, a Montreal Cognitive Assessment (MoCA) test was performed to determine and quantify the cognitive capabilities of the participants.

2.6.3. Cohorts

Two study cohorts were planned to comprehensively investigate the feasibility of the “Gamidiagnostics” application for the assessment of peripheral nerve functions in patients with diabetes. Cohort 1 consisted of all study participants eligible for the study according to the inclusion and exclusion criteria. Given that diabetic neuropathy predominantly affects the elderly population (>50 years) (77), it was anticipated that patients in the DPN group would generally be older than the control group. Therefore, the second cohort (Cohort 2) encompassed only age-matched elderly participants. The analyses on this cohort minimized the impact of age and investigated mainly the possibility of using the “Gamidiagnostics” application to detect DPN in the elderly population.

2.6.4. Standardization of the test procedure

The “Gamidiagnostics” session was performed with each study participant receiving a size matching pair of shoes harboring Gaming Insole 3 (Figure 13a). The participants were seated on a chair without armrests in front of a table on which an Android tablet (Samsung Galaxy Tab A T580) was positioned that connected to the insole. Sensor data were recorded and transferred in real-time to the study application (“Gamidiagnostics” App) via Bluetooth. The participants initially calibrated the insole through eight standardized steps (Figure 14). The maximum pressure values determined in the calibration steps were utilized to normalize the absolute pressure values within the range of 0 to 1. Subsequently, participants familiarized themselves with the setup of the video games through standardized tutorials that were repeated on demand (see introduction videos and screenshots in Appendix 11.6). Each gaming session consisted of four games: Apple-Catch (AC), Balloon-Flying (BF), Cross-Pressure (CP), and Island-Jump (IJ), which were played sequentially (Figure 13b). Each session lasted about 20 minutes. The acquired insole sensor data and game outcomes were transferred in a complete data package to a remote server for data visualization and analyses (Figure 13c). A spider chart provided feedback on the game performance to participants after the session (key capabilities: reaction time, sensation, skillfulness, muscle strength, balance, and endurance).

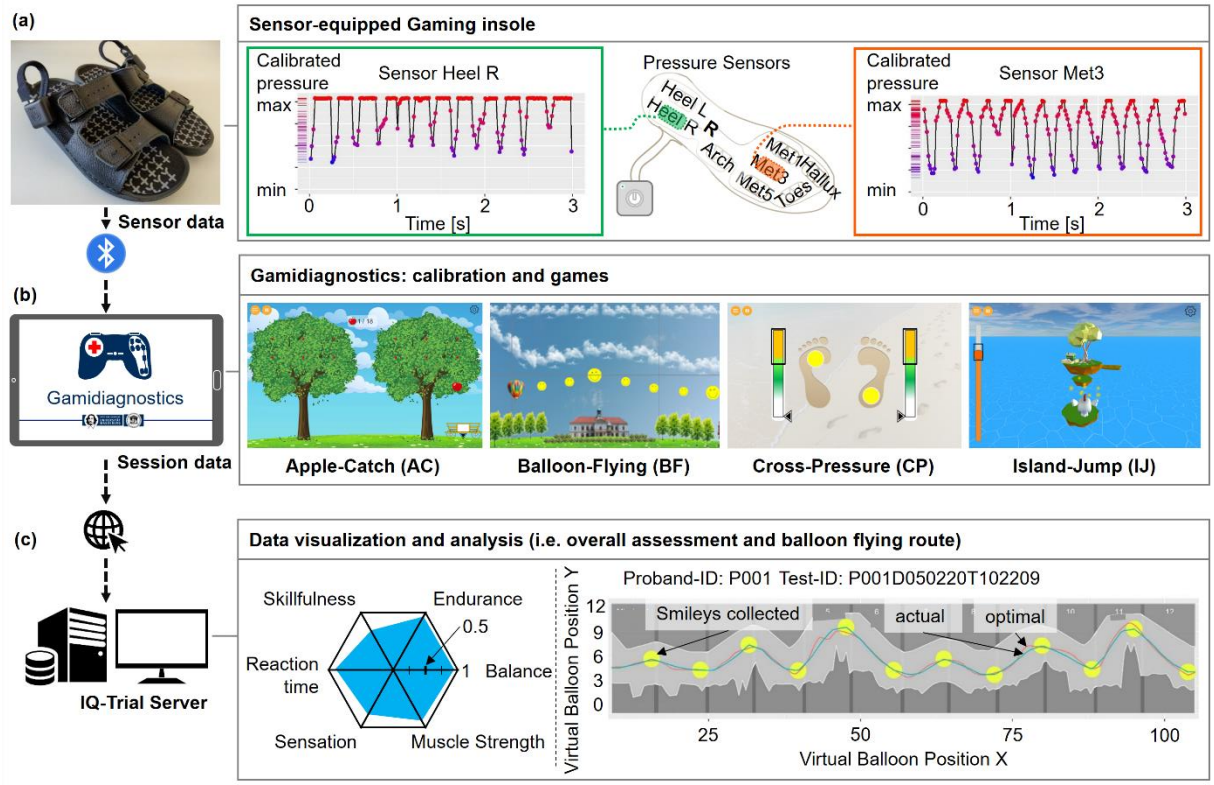

Figure 13. Overview on game setup, data transferal, assessment and visualization. *(a) The sensor-equipped gaming insoles 3 provided eight embedded pressure sensors in distinct areas of the plantar pedis. The top center image depicts the localization of the sensors corresponding to the calcaneus, lateral arch, metatarsal (Met) 1/3/5, digitus 1 and 5 of the forefoot. The complete insole served as a steering unit and was connected to a control unit*

for real-time data transmission via Bluetooth to the "Gamidiagnostics" application, which was run on a tablet. The setup allowed the participants to play games solely by modulating plantar pressure distribution. (b) Each gaming session included a tutorial with calibration steps and four games, i.e., Balloon-Flying (BF), Apple-Catch (AC), Cross-Pressure (CP), and Island-Jump (IJ). (c) Subsequently, the data was uploaded to the IQ-Trial server as a data package. The participants received a brief summary of their performance with a spider chart, scores, levels, and capabilities (beginner, average, advanced, expert). Further data visualization for the physician and data analysis was realized to indicate the performance of participants in the different games in comparison to maximum achievement levels.

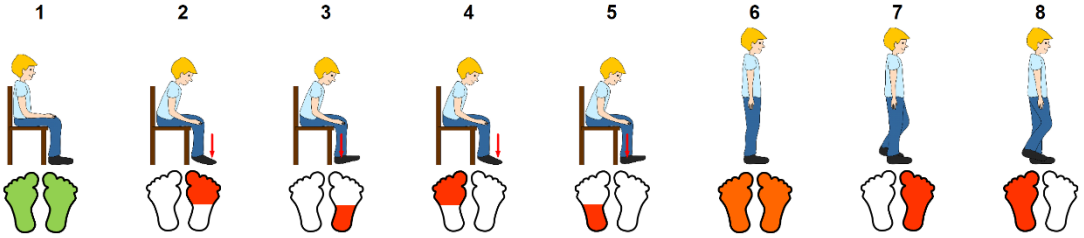

b) Calibration step

1 Balanced sitting (5 sec)
2 Maximum pressure on the right forefoot (5 sec)
3 Maximum pressure on the right heel (5 sec)
4 Maximum pressure on the left forefoot (5 sec)
5 Maximum pressure on the left heel (5 sec)
6 Balance standing (5 sec)
7 Standing on the right foot (5 sec)
8 Standing on the left foot (5 sec)

c) Normalization algorithm

$$p_n = \frac{p_a - p_{min}}{p_{max} - p_{min}}$$

p_n: *normalized pressure*

p_a: *absolute pressure*

p_{min}: *minimal pressure threshold*

p_{max}: *maximal pressure threshold*

Figure 14. Overview of calibration steps. *Eight calibration steps were performed before games. These allowed normalizing pressure values according to weight and maximum pressure applied by the participants. Minimum and maximum pressure were recorded for all positions at forefeet and heels. Furthermore, the participants were instructed to stand up for five seconds and keep balance on each foot alone for 5 seconds. An algorithm was applied to normalize these values that were utilized for the steering unit of the insoles. Minimum-maximum normalization transformed all values to the range of 0 to 1.*

2.7. Data protection and management

An important principle when working with patient data is data protection. At the screening visit, each study participant was assigned a unique ID. The questionnaires on past medical history and physical examinations were archived with this identifier only but not the personal information (name, date of birth and so on).

The encrypted sensor data, insole identification, game setting, calibration thresholds, and game outcomes were also saved with the ID and further transmitted to the study server (Supplementary Figure 1), which was denoted IQ-Trial. It was established during the study to provide physicians and analysts an overview on the study participants' game outcomes, as well as immediate feedback to study participants on their gaming performance by considering six predefined assessments focusing on balance, sensation, muscle strength, reaction time, endurance, and coordination (Supplementary Figure 2–7). Only study personnel and caring physicians were provided with access to the server IQ-Trial. This server is located in the computer centre of the University Hospital of the Otto-von-Guericke University Magdeburg (Figure 15).

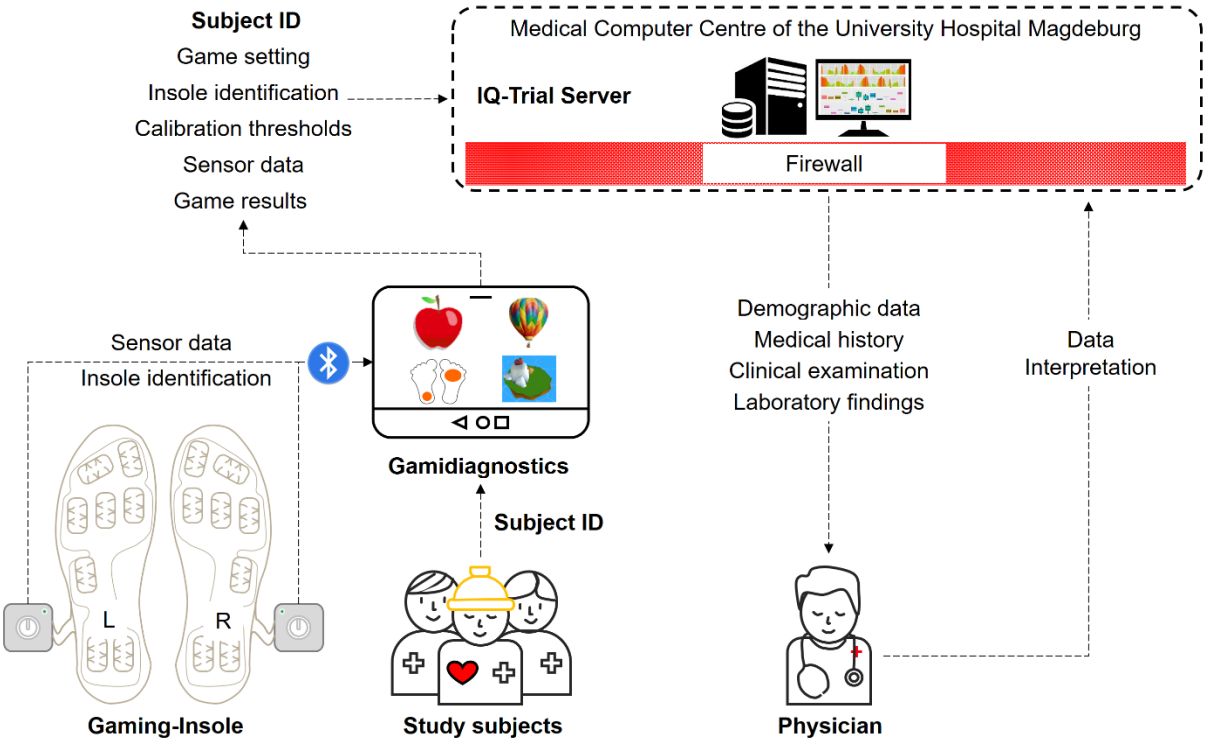

Figure 15. Data management within the "Gamidiagnostics" study. *A unique Subject-ID was assigned to each participant at the enrolment into the study. The study personnel archived screening questionnaires and clinical examination findings according to this identifier only. During the "Gamidiagnostics" session, sensor data and insole information received from the insole were saved with the Subject-ID on an Android tablet and was further transmitted to the IQ-Trial sever together with the encrypted test data, including game setting, calibration thresholds and game results. Only study personnel and caring physicians had access to the study server. Data interpretation was achieved by the physician considering subjects' demographic information as well as medical history and clinical findings.*

The pseudonymization step allowed to trace back the personal data, such as names and date of birth, which was only possible through a list archived separately with the consent form in the Clinic for Nephrology and Hypertension, Diabetes and Endocrinology at the Otto-von-Guericke University Magdeburg. Patients were informed about the setup of data protection, data processing and confidentiality principles. Corresponding declarations of consent were signed.

2.8. Statistical analysis and AI modeling

2.8.1. Statistical tests

Descriptive statistics are presented in proportions and frequencies for categorical variables, while mean values and standard deviations (SD) are provided for continuous variables. A correlation greater than 0.75 was considered a "strong" or "very good" correlation between two variables, according to recommendations from the literature (78, 79). This threshold was utilized for correlation tests that filtered out redundant game parameters with high inter-correlations. The remaining parameters were compared between healthy controls and patients diagnosed with diabetes and peripheral neuropathy. Chi-square tests were performed on categorical variables. The Shapiro-Wilk normality test was utilized to determine the normal

distribution of continuous variables. For normally distributed variables, the group differences were computed with t-tests. Otherwise, Mann-Whitney U tests were performed on variables. In addition, the Kruskal-Wallis H test was utilized for comparing more than two independent samples. Two-sided P values below 0.05 were considered statistically significant. Pairwise tests were performed automatically among multiple groups with the correction of the p values using Holm–Bonferroni method (80).

2.8.2. Support Vector Machine (SVM)

As a popular supervised machine learning algorithm, SVM is applicable both in classification and regression cases. When facing classification problems, the SVM algorithm initially places each observation as a point in n-dimensional space (n=count of features). The position of the observation on a dimensional coordinate corresponds to the value of the feature. The aim of classification is to determine the hyper-plane, which distinguishes the two classes best. In some cases, it is unable to determine a line or hyperplane as desired. The SVM introduces a kernel function to project the data into a higher dimensional space to find a hyperplane that can better differentiate the classes. Frequently used kernel functions are polynomial (SVM-Poly), linear (SVM-Linear), nonlinear (SVM-Nonlinear), radial basis functions (SVM-Radial), etc. The conversion from original space to a high-dimensional space may result in extreme high dimensionality, even endless dimensions, leading to computational complexity and a staggering amount of computation. However, in SVM, the kernel function is introduced so that the operations are still performed in the lower dimensional space, which avoids the time consumption of complex operations in the higher dimensional space (81, 82).

The metric that explicitly evaluates the hyperplane is called margin, and it quantifies the distance between data points of both classes. The classification performance can be improved by maximizing the margin distance. The data points near the hyperplane are support vectors that affect the hyperplane's position and orientation. Therefore, maximizing margin distance using support vectors is critical for building an SVM. The hinge loss is introduced to help maximize the margin, which can be calculated using the loss function (2.1). If the prediction and reference have the same sign, the cost is equal to zero. Otherwise, the loss value is computed (83).

$$c\big(x, y, f(x)\big) = \begin{cases} 0, & if\ y * f(x) \geq 1 \\ 1 - y * f(x), & else \end{cases} \qquad 2.1$$

Another ingenious feature of SVM is the introduction of a slotting variable (also called penalty variables) to deal with possible noise in the sample data, which allows the data points to deviate from the hyperplane to a certain extent. The addition of the slotting variable allows the

SVM to consider the overall distribution of the sample data rather than just pursuing the optimization of local outcomes.

In general, SVM has the following advantages.

1. Handing small samples. Compared with other classification algorithms for training, SVM requires relatively fewer samples for the same problem complexity. Furthermore, SVMs can efficiently deal with high-dimensional data by introducing kernel functions.

2. Minimization of the structural risk. This risk refers to the cumulative error between the classifier's approximation of the real problem model and the real solution to the problem.

3. Addressing nonlinearity. SVM is excellent at handling linear indistinguishability of sample data, mainly through slotting variables (also called penalty variables) and kernel function techniques, and this part is precisely the essence of SVM.

Clinical studies reported that SVM models perform better on medical classification issues with limited and imbalanced datasets (84, 85). Therefore, this work selected the SVM algorithm with kernel functions (linear, radial, and polynomial) for model training.

2.8.3. Performance evaluation metrics

The most intuitive metric for model evaluation is the confusion matrix that presents the proportion of true positive (TP), true negative (TN), false positive (FP), and false negative (FN) cases. In this work, we purpose to train models for automatic prediction of DPN that determines the DPN group to be the positive class. The control group is considered as the negative class. Corresponding TP, TN, FP, and FN can be described below.

TP: the case in which the model predicted DPN and the actual output was also DPN.

TN: the case in which the model predicted Control and the actual output was also Control.

FP: the case in which the model predicted DPN, but the actual output was Control.

FN: the case in which the model predicted Control, but the actual output was DPN.

In healthcare use cases, FNs result in delayed diagnosis and treatment of patients, leading to severe consequences. FPs cause misdiagnosis, waste of healthcare resources, and the potential for doctor-patient disputes. Figure 16a presents a confusion matrix showing the performance of a DPN classification model. The test dataset consists of 36 observations. Twenty-six of them were diagnosed with diabetic peripheral neuropathy. The other ten cases are healthy controls. The model correctly predicts 25 cases with DPN (TP=25) and 4 cases that do not have DPN (TN=4). One DPN patient is falsely not detected (FN=1), and six healthy controls are predicted to have DPN (FP=6). Following metrics are calculated based on the confusion matrix.

a) Confusion matrix example

Total sample: n=36

Actual \ Predicted	DPN	Control
DPN	25 (TP)	1 (FN)
Control	6 (FP)	4 (TN)

b) Receiver operating characteristic curve (ROC) example

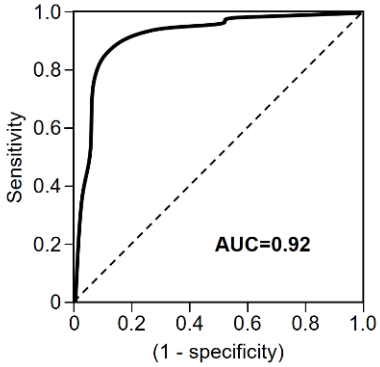

Figure 16. Evaluation metrics for classification models. *DPN: diabetic peripheral neuropathy; AUC: area under the curve.*

Accuracy: the proportion of true predicted cases among the total sample. It is a perfect metric to evaluate classification models with balanced datasets. The accuracy here can be computed to 80.5% with the equation (2.2).

$$Accuracy = \frac{TP + TN}{Total\ Sample} = \frac{25 + 4}{36} = 80.5\% \qquad 2.2$$

Sensitivity (Recall): the proportion of true positive cases among all actual positives. The sensitivity here can be calculated to 96.2% with the equation (2.3).

$$Sensitivity\ (Recall) = \frac{TP}{TP + FN} = \frac{25}{25 + 1} = 96.2\% \qquad 2.3$$

Specificity: the proportion of true negative cases among all actual negatives. The specificity here can be computed to 40.0% with the formula (2.4).

$$Specificity = \frac{TN}{TN + FP} = \frac{4}{6 + 4} = 40.0\% \qquad 2.4$$

Precision: the proportion of true positive cases among all predicted positives. The precision here can be calculated to 80.6%with the equation (2.5).

$$Precision = \frac{TP}{TP + FP} = \frac{25}{25 + 6} = 80.6\% \qquad 2.5$$

In the case of an imbalanced dataset with a skewed class distribution, accuracy is no longer a reliable metric because the major class has a much greater impact on accuracy than the minor class. In the extreme case, the accuracy remains high even through all minor samples are misclassified. Therefore, the F1 score, Cohen's Kappa, and ROC Curves are developed for imbalanced classification problems.

F1 score: the harmonic mean of sensitivity and precision ranging from 0 to 1. In this case, the F1 score can be calculated to 87.7% with the formula (2.6).

$$F_1 = \frac{2}{\frac{1}{Recall} + \frac{1}{Precision}} = \frac{2}{\frac{1}{0.962} + \frac{1}{0.806}} = 87.7\% \qquad 2.6$$

Cohen's kappa: the normalized accuracy by considering the exact class distribution in the dataset. By this binary classification problem, its Cohen's Kappa can be calculated to 0.17 with formula (2.7). The range of Cohen's Kappa is from -1 to 1, but values less or equal to zero suggests that the classifier has the same or worse performance than a random coin toss. The closer the value is to 1, the more superior the performance of the classifier is (86). According to the standard interpretation scheme proposed by Landis and Koch (87), a Cohen's Kappa of 0.81–1 indicates near-perfect segmentation, 0.61–0.80 as substantial 0.41–0.60 as moderate, 0.21–0.40 as fair, and 0–0.20 as slight. In this example, the classes are imbalanced, and DPN is the major class with 72% propriety in the data. Therefore, the accuracy is still around 80%, even though 60% of negative cases are misclassified. Cohen's Kappa 0.17 is a better metric that indicates the classification has reached only a slight agreement.

$$Cohen's\ Kappa = \frac{2 \times (TP \times TN - FN \times FP)}{(TP + FP) \times (FP + TN) + (TP + FN) \times (FN + TN)} = 0.17 \qquad 2.7$$

Alternatively, we could also adjust the accuracy in the case of an unbalanced dataset, which is called adjusted accuracy or balanced accuracy. In this case, the adjusted balance of 68.1% calculated with equation (2.8) is much more reasonable than the accuracy.

$$Adjusted\ Accuracy\ = \frac{Sensitivity + Specificity}{2} = 68.1\% \qquad 2.8$$

The metrics mentioned above only evaluate the performance by calculating positive and negative cases that are judged by one predefined probability threshold, which is normally set as 0.5. However, the percentage of predicted positive and negative samples changes actually with the probability threshold. In order to measure the merit of the classifier with different discriminate thresholds, the Receiver Operating Characteristic (ROC) curve is involved. It is a graph that presents the classification model's true positive rate (TPR, sensitivity) and false positive rate (FPR, 1-specificity) at various probability thresholds on a curve. The nearer the ROC curve is to the top left corner, the better the model performs. The area under the curve is denoted as AUC, and the larger the AUC, the better the overall discrimination of the model. The AUC considers the classifier's ability to identify both positive and negative samples

simultaneously. Thus, it still can be utilized to evaluate the classifier reasonably in the case of an unbalanced dataset (88). Figure 16b demonstrates an example of the ROC curve.

2.8.4. Class definition and model training

AI models were derived to distinguish healthy controls and patients with diabetes and sensory neuropathy in the age-matched cohort (cohort 2) with acquired datasets. The NDS score was utilized to generate class labels for supervised learning. NDS $\geqslant$ 2 and impaired vibration sensation (0-4/8) were considered as existing neuropathy (DPN), and NDS=0 was considered as the absence of neuropathy (Control group). Secondly, in the DPN group, more detailed phenotyping was achieved by analyzing the dysfunction of different fiber types. Briefly, for model 2, severe damage of Aδ-/C-fibers was assumed in patients with reduced/absent pinprick (nociception) or temperature sensation. For model 3, the presence of severe Aβ-fiber polyneuropathy was assumed with impaired vibration sensation (below 3/8) or an abnormal 10g monofilament-test result (reduced/absent). The remaining patients in the DPN group were classified as moderate Aβ-fiber polyneuropathy (impaired vibration sensation: 3-4/8). For model 4, the absence of Achilles tendon reflexes was considered as a positive label in the model training. A negative label was assigned to normal or mildly reduced reflexes.

Regarding to the feature selection, acquired datasets were split into testing and training datasets (ratio 3:7), during which the random sampling occurred in each class and preserved the overall class distribution of the data. The training dataset was imported to the classifier to estimate features' importance based on model-independent metrics, e.g., area under the receiver operating characteristic (AUC-ROC) (89). Figure 17 presents the top ten features for DPN classification ranked by the SVM-Radial classifier. Subsequently, models with different subsets of top-ranked features (i.e., variances of numbers and/or orders of features) were tested. Since the studied dataset was imbalanced, we selected Cohens Kappa (a classification accuracy normalized by the imbalance of the classes in the data) as the performance metric to compare the models trained with different feature combinations. The models with higher Cohens Kappa values were chosen as candidate models.

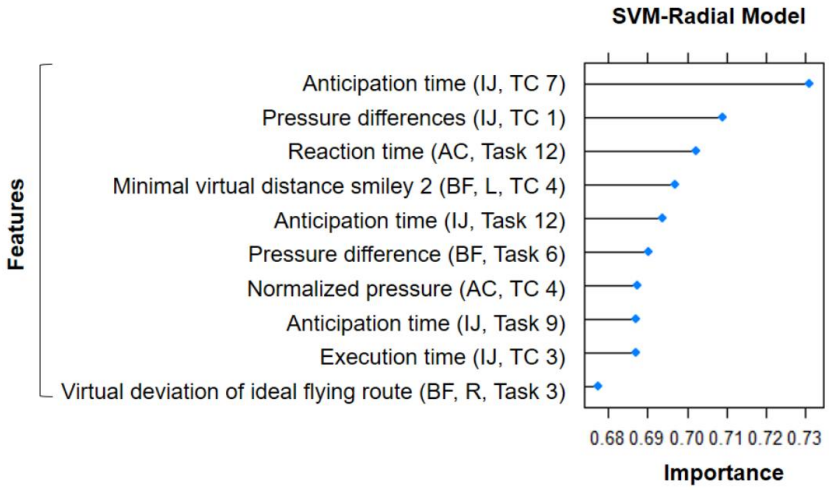

Figure 17. An example of feature ranking using the SVM-Radial model. *SVM: support vector machine; IJ: Island- Jump; BF: Balloon-Flying; AC: Apple-Catch; R: Right; L: Left; TC: task combination.*

Five-fold cross-validation (three repeats) was applied in feature ranking and training to avoid overfitting and to derive a more accurate estimate of the model performance. This statistical method repeatedly divided the training dataset into five subsets with approximately equal sizes three times. Each subset contained the same proportion of labels as the complete dataset. Four out of the five subsets were utilized in the model training, while the remaining subset was used for validation. The average accuracy of cross-validation was considered in the grid search of parameters combination that improves the model performance the most. Ultimately, the obtained candidate models were further applied to the testing dataset to evaluate the models' predictive performance. R programming language (version 4.0.4) and related open-source libraries were utilized for statistical computing and machine learning algorithms (90).

3. Results

3.1. Study participants

Cohort 1 consisted of 71 healthy volunteers and 112 patients with diabetes and peripheral neuropathy (Figure 18). The demographic characteristics of the cohorts are outlined in Table 3. All study participants completed the “Gamidiagnostics” sessions, and data sampled from the first attempt were analyzed only. The gender distribution is skewed towards male patients in the cohort with neuropathy, and control subjects are younger. Therefore cohort 2 was selected from all participants to achieve an age-matching (30 controls and 90 patients with DPN). As expected, the average BMI is higher in patients with diabetes compared to healthy controls. NDS and neuropathy symptom score (NSS) indicated that most of the patients in the DPN group suffered from moderate to severe DPN. In the DPN group, 40% of patients had reduced/absent pinprick or temperature sensation, indicating impairment of Aδ-/C-fiber function. 81% of DPN patients exhibited impaired vibration sensation (0-2/8) or an abnormal 10g-monofilament-test result (reduced/absent). The absence of Achilles tendon reflexes was observed in nearly 50% of patients with diabetes. About 80% of patients were diagnosed with type 2 diabetes mellitus, the remainder with type 1 diabetes except for one. The average time since the first diagnosis of diabetes was ~20 years.

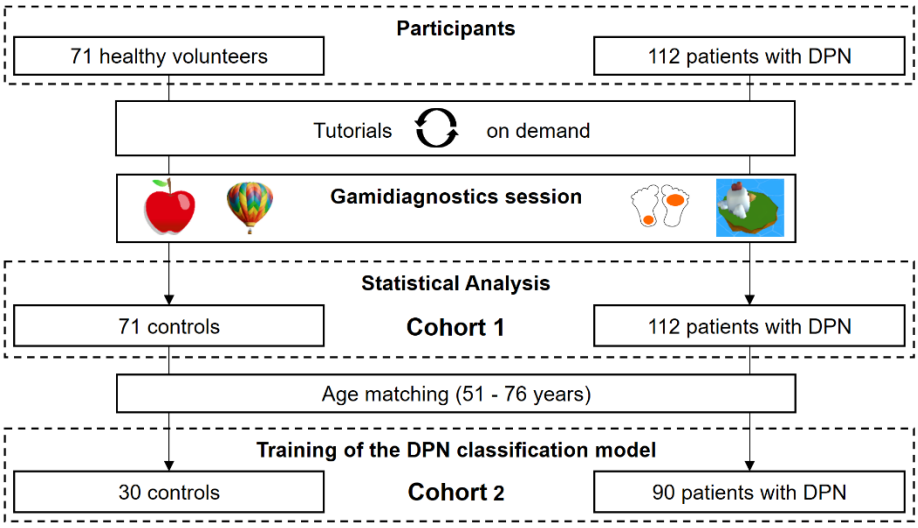

Figure 18. Study flow diagram. *Cohort 1 comprised of 71 healthy volunteers with absent neuropathy and 112 individuals diagnosed with diabetes and diabetic peripheral neuropathy. Participants were seated in a quiet room on a chair without armrests in front of a table with a standing tablet. Shoes harboring sensor-equipped insoles matched the participants' foot size (four sizes are available: S, M, L, and XL). A standardized tutorial explaining the challenges was provided, allowing the participants to familiarize themselves with the video games. The interactive tutorials were repeated on demand. The average duration per "Gamidiagnostics" session was 20 min including tutorials. To minimize age as a confounding factor, individuals of similar age in both groups were identified and combined in cohort 2 for further analyses. Statistical analyses were carried out with cohorts 1 and 2, and AI algorithm development was performed with age-matched cohort 2 only. DPN: diabetic peripheral neuropathy*

Table 3. Demographic characteristics and clinical diagnosis of study cohorts. *Data are means ± SD or n (%). DPN: diabetic peripheral neuropathy*

Cohort	**Cohort 1**		**Cohort 2**	
Group	Control	DPN	Control	DPN
N	71	112	30	90
Age (years)	45.5 ± 18.4	68.5 ± 8.1	64.9 ± 7.0	66.4 ± 5.9
Sex				
Female	48 (67.6%)	33 (29.5%)	18 (60%)	25 (27.8%)
Male	23 (32.4%)	79 (70.5%)	12 (40%)	65 (72.2%)
Body-mass index (BMI, kg/m²)	24.3 ± 2.9	29.7 ± 5.1	25.3 ± 2.9	30.3 ± 5.2
Diabetes type				
Type1	0	23 (20.5%)	0	19 (21.1%)
Type2	0	88 (78.6%)	0	70 (77.8%)
Type3	0	1 (0.9%)	0	1 (1.1%)
Diabetes duration (years)	0	20.5 ± 12.2	0	21.2 ± 12.6
Neuropathy symptoms score (NSS)				
Normal (0)	71 (100%)	17 (15.2%)	30 (100%)	15 (16.7%)
Mild (1–4)	0	6 (5.4%)	0	6 (6.7%)
Moderate (5-6)	0	22 (19.6%)	0	16 (17.8%)
Severe (7-10)	0	67 (59.8%)	0	53 (58.9%)
Neuropathy disability score (NDS)				
Normal (0)	71 (100%)	0	30 (100%)	0
Mild (2-5)	0	46 (41.1%)	0	37 (41.1%)
Moderate (6-8)	0	55 (49.1%)	0	45 (50.0%)
Severe (9-10)	0	11 (9.8%)	0	8 (8.9%)
Pinprick (left)				
Present	71 (100%)	90 (80.4%)	30 (100%)	72 (80.0%)
Reduced/Absent	0	22 (19.6%)	0	18 (20.0%)
Pinprick (right)				
Present	71 (100%)	88 (78.6%)	30 (100%)	70 (77.8%)
Reduced/Absent	0	24 (21.4%)	0	20 (22.2%)
Temperature sensation (Tip Therm, left)				
Present	71 (100%)	83 (74.1%)	30 (100%)	67 (74.4%)
Reduced/Absent	0	29 (25.9%)	0	23 (25.6%)
Temperature sensation (Tip Therm, right)				
Present	71 (100%)	81 (72.3%)	30 (100%)	65 (72.2%)
Reduced/Absent	0	31 (27.7%)	0	25 (27.8%)
Vibration perception (128 Hz tuning fork, left)				
Normal (6-8)	60 (84.5%)	0	19 (63.3%)	0
Mild (5)	11 (15.5%)	0	11 (36.7%)	0
Moderate (3-4)	0	22 (19.6%)	0	19 (21.1%)
Severe (0-2)	0	90 (80.4%)	0	71 (78.9%)
Vibration perception (128 Hz tuning fork, right)				
Normal (6-8)	66 (93.0%)	0	25 (83.3%)	0
Mild (5)	5 (7.0%)	0	5 (16.7%)	0
Moderate (3-4)	0	24 (21.4%)	0	20 (22.2%)
Severe (0-2)	0	88 (78.6%)	0	70 (77.8%)
10-g monofilament-test (left)				
Present	71 (100%)	92 (82.1%)	30 (100%)	73 (81.1%)
Reduced/Absent	0	20 (17.9%)	0	17 (18.9%)
10-g monofilament-test (right)				
Present	71 (100%)	90 (80.4%)	30 (100%)	71 (78.9%)
Reduced/Absent	0	22 (19.6%)	0	19 (21.1%)
Achilles tendon reflex (left)				
Normal	71 (100%)	20 (17.9%)	30 (100%)	15 (16.7%)
Reduced	0	31 (27.7%)	0	27 (30.0%)
Absent	0	61 (54.5%)	0	48 (53.3%)
Present with reinforcement	0	0	0	0
Achilles tendon reflex (right)				
Normal	71 (100%)	22 (19.6%)	30 (100%)	17 (18.9%)
Reduced	0	28 (25.0%)	0	25 (27.8%)
Absent	0	61 (54.5%)	0	48 (53.3%)
Present with reinforcement	0	1 (0.9%)	0	0

3.2. Hypothesis-driven game assessment

The six hypothesis-driven key capabilities from healthy volunteers and patients with diabetes and peripheral neuropathy were quantified in both cohorts. Most of these revealed significant differences between the DPN and Control group in cohort 1, except for reaction time and balance. Age matching of the datasets with cohort 2 markedly changed the results. The between-group differentiation of sensation, skillfulness, endurance, and finger reaction time remained significant (Figure 19). The decreased "skillfulness" in patients with diabetes and peripheral neuropathy was observed from a higher count of failed jumps in the IJ game. Their impaired "sensation" resulted in the increased "Minimal virtual distance smiley 4" (BF game) and "Deviation from the optimal pressure" (IJ game). The distinction of "endurance" between healthy controls and DPN patients was evidenced with different consecutive jumps without failures (n) in the IJ game. Finger reaction time presented a light difference between the Control and DPN group.

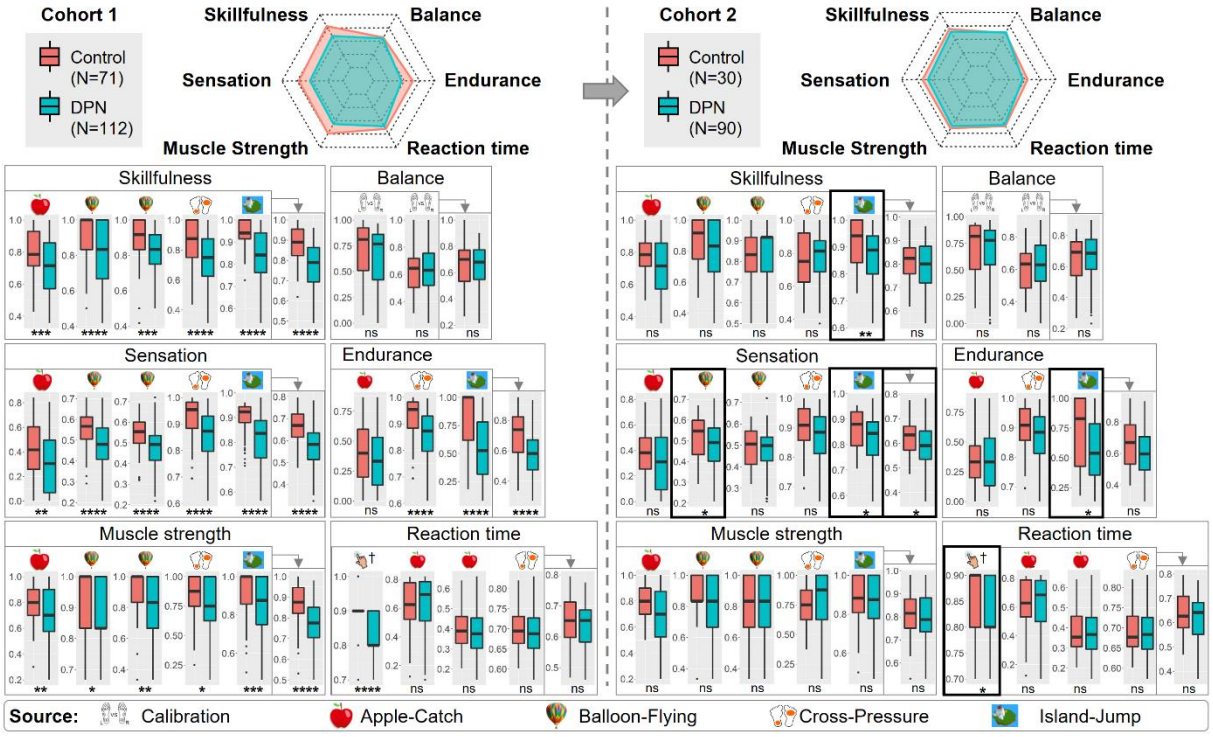

Figure 19. Results of intergroup difference test for hypothesis-driven key capabilities and scoring. *Following calculation of scores for the predefined key capabilities, significant differences were observed for skillfulness, finger reaction time, sensation, muscle strength, and endurance in cohort 1. For age-matched controls and DPN patients in cohort 2, differences remained significant for sensation, skillfulness, endurance, and finger reaction time. The annotations and extracted games of these key capabilities are provided, as well as the significance levels for intergroup differences (below boxplots). DPN: diabetic peripheral neuropathy. Differences between groups were calculated using Mann-Whitney U test or t test as appropriate. Significance levels: ns (p>0.05), * (p=0.01–0.05), ** (p=0.001–0.01), *** (p=0.0001–0.001), **** (p<0.0001). † Finger reaction time of one DPN patient is not available and replaced with the group mean value. All outliers were not included in density and boxplots.*

A logistic regression model with hypothesis-driven key capabilities discriminated healthy controls from DPN patients with a training accuracy of 71.8% (AUC-ROC: 0.66). The predictors

of this model are summarized in Figure 20 (F1–F6). The between-group differences are presented by density and box plots (excluding outliers), as well as mean values and SDs. The extracted games of each feature are provided in the last two columns.

	ID	Feature	Control (N=30)	DPN (N=90)	p	Game
	F1	Skillfulness	0.916 (0.085)	0.836 (0.151)	**	IJ
	F2	Finger reaction time [s] †	0.850 (0.073)	0.822 (0.061)	*	Reaction test
	F3	Sensation	0.626 (0.077)	0.586 (0.093)	*	All
	F4	Sensation	0.523 (0.103)	0.469 (0.132)	*	BF (L)
	F5	Sensation	0.860 (0.079)	0.815 (0.107)	*	IJ
	F6	Endurance	0.708 (0.295)	0.580 (0.271)	*	IJ

Figure 20. Features of the hypothesis-driven DPN classification using Logistic Regression (model 1b). *Six hypothesis-driven key capabilities scores (F1–F6) were treated as features and entered into a logistic regression model to differentiate between patients with peripheral neuropathy versus healthy controls. All predefined scores showed significant differences between the Control and DPN groups. The differences are presented by density and box plots. The extracted games and related task combinations of each feature are provided in the last two columns. Data are presented as means (SD). All outliers were excluded in density and boxplots. Differences between groups were calculated using the Mann-Whitney U test, t-test, or chi-square test as appropriate. Significance levels: ns (p>0.05), * (p=0.01–0.05), ** (p=0.001–0.01), *** (p=0.0001–0.001), **** (p<0.0001). F: feature; DPN: diabetic peripheral neuropathy; AC: Apple-Catch; BF: Balloon-Flying; L: Left; R: Right; CP: Cross-Pressure; IJ: Island-Jump. † Finger reaction time of one DPN patient was not available and replaced with the group mean value.*

3.3. Game feature analysis

The initial analysis with 183 gaming datasets acquired from the “Gamidiagnostics” sessions are summarized in a workflow diagram (Figure 21). For each dataset collected from a study participant, data preprocessing filtered out 701 dependent variables with strong correlations (correlation coefficients higher than 0.75) from all extracted game features. Subsequently, the rest of 1,179 variables were compared between the Control and DPN severity groups (mild, moderate, and severe) in Cohort 1 using appropriate statistical tests. The Kruskal-Wallis test was performed to identify the age influence on the game performance by comparing game features between younger, middle-aged, and elderly healthy controls. In the age-matched Cohort 2, the same parameters were compared between the Control and DPN groups as well. Separately, a data frame consisting of 120 observations (study participants from Cohort 2) and 1,179 variables was provided to train automatic DPN classification models. The performance of developed AI models is separately described in 3.4.

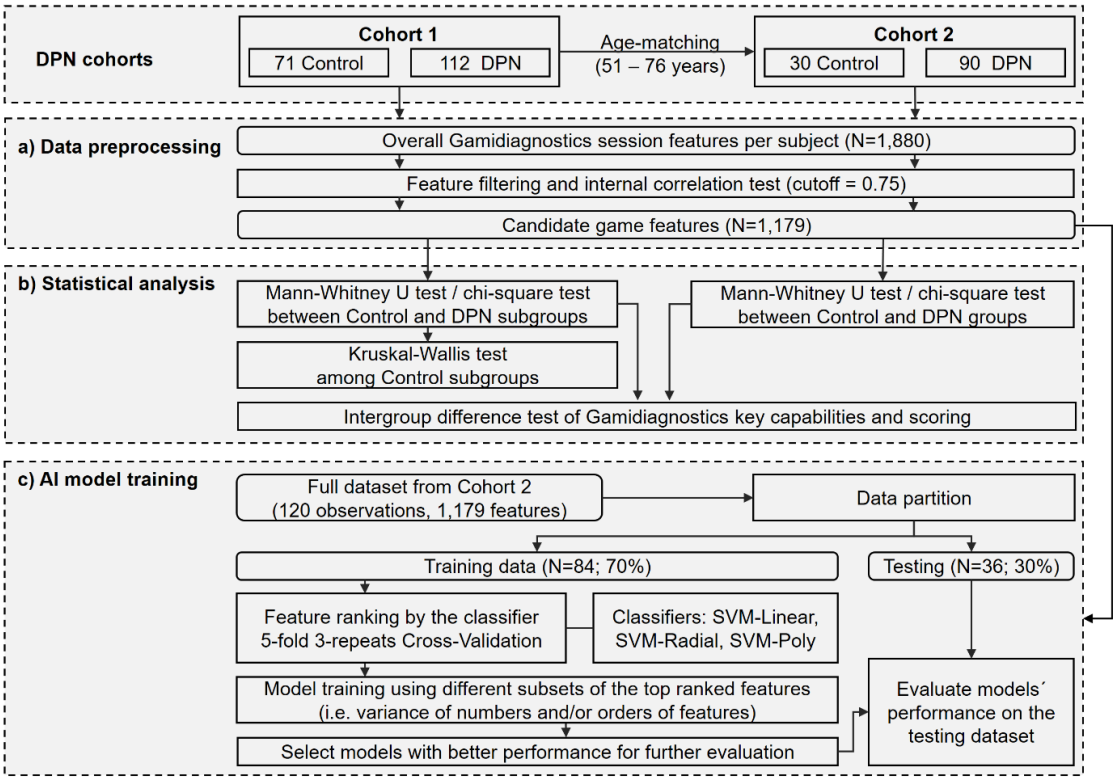

Figure 21. Flow diagram of data analyses. *(a) Data preprocessing filtered out parameters with zero variance or high inter-correlations from the feature matrix. (b) In cohort 1, three subgroups of participants with DPN were assigned according to NDS scores. 1,179 game features of the entire cohort were compared between healthy controls and patients with DPN to identify the effect of peripheral nerve damage on the "Gamidiagnostics" performance. Subsequently, the influence of age on the outcomes was tested for participants in the control group (subgroups: young, middle-aged, seniors). Participants aged 51 to 76 years were exported to cohort 2. Their game parameters (n=1,179) and predefined hypothesis-driven key capabilities were included in the comparisons and used as candidate features for machine learning algorithms. (c) Within cohort 2, candidate features were ranked by classifier-estimated importance. Different subsets of the top-ranked features were utilized for training classification models. Candidate models with higher Cohens Kappa values were selected to evaluate the predictive performance on the remaining (30%) of the sample. DPN: diabetic peripheral neuropathy; AI: artificial intelligence; SVM-Linear: support vector machines with a linear kernel function; SVM-Radial: support vector machines with a radial kernel function; SVM-Poly: support vector machines with a polynomial kernel function*

3.3.1. Game feature analysis in Cohort 1

In cohort 1, overall 1,179 independent game features were compared between healthy controls and DPN subgroups classified as mild, moderate, or severe neuropathy (according to NDS score). Amongst these, 314 features revealed significant differences. Representative examples of these game features are compared and visualized for each game (Figure 22a). In the AC game, the "Final virtual distance" (Feature 1) of task 8 was significantly lower in healthy controls compared to DPN patients ($p<0.0001$). It suggested that healthy subjects could more precisely modify their pressure on the foot and position the car precisely beneath the falling apple. However, another parameter named "Pressure gradients between successive frames" (Feature 2) of task 13 exhibited the opposite trend, that was a significantly reduced pressure gradient in DPN patients ($p<0.01$). It might be explained by the inability of DPN patients to dynamically adopt plantar pressure in real-time according to the distance between carriage and apple as healthy people due to lack of precise pressure sensation. In the CP

game, the “Normalized pressure” (Feature 3) of task 4 and “Time outside the optimal pressure zone [s]” (Feature 4) of TC 4 increased significantly in the DPN group. It indicated that DPN patients have more difficulties adjusting their foot pressure to reach the optimal pressure range. In the IJ game, the “Pressure differences between successive frames” (Feature 5) of TC 4 (tasks in which the bird jumps to the left) and “Anticipation time [s]” (Feature 6) of TC 3 (tasks in which the bird jumps to the right) were smaller in the Control group. It demonstrated that healthy controls react quicker and more precisely by switching from using both feet to one single foot (left or right) as the controlling unit. In the BF game, the standard deviation of maximal “Normalized pressure” (Feature 7) of TC 4 was lower in healthy controls compared to patients with peripheral neuropathy. The TC 4 consisted of tasks requiring high pressures. A lower standard deviation indicated better modification of pressures by healthy volunteers to control the balloon fly through the two highest obstacles in tasks 5 and 11. In task 6 that demanded the release of foot pressures, DPN patients had higher “Pressure-time integrals” (Feature 8) compared to healthy players. It indicated that DPN patients do not reduce plantar pressure as quickly and accurately as healthy participants due to their lack of reaction or pressure perception. A complete summary on 314 of these features and intergroup test results are provided in Supplementary Table 1.

Secondly, three age-related control subgroups were tested separately, 19 younger, 22 middle-aged, and 30 elderly adults. The same 314 features were tested among these three age groups, and 84 variables showed distinctions that associated with age (two examples are depicted in Figure 22b, other variables are presented in Supplementary Table 1, highlighted with a grey background). The first parameter, named “Virtual deviation of ideal flying route” (Feature 9, BF game, TC 3), calculated the deviation between the balloon’s real and ideal flying route while flying through middle-height obstacles using intermediate pressures. This variable was strongly correlated to the age of study participants. The “Anticipation time [s]” (Feature 10, CP game, TC 2) of healthy volunteers increased by the age in the control group. Therefore, age matching was quite necessary before modeling.

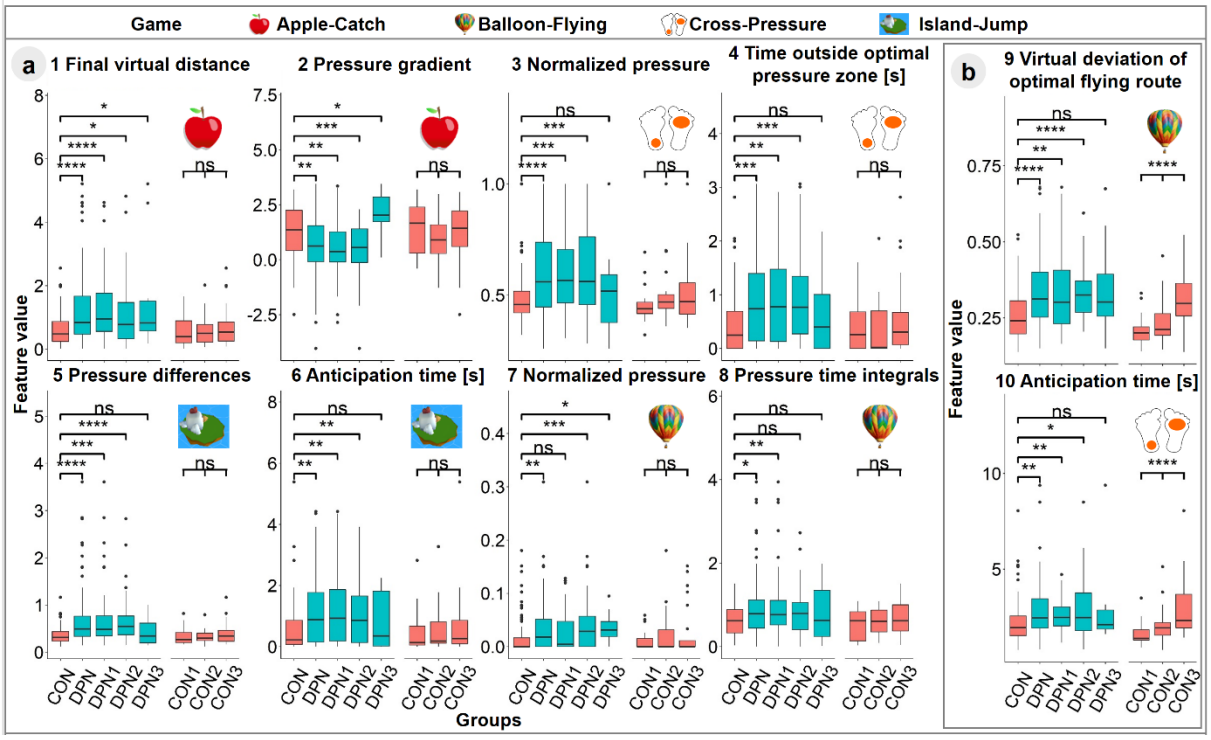

Figure 22. Results of intergroup difference tests of game features within cohort 1. *(a) According to the NDS score, 112 participants were assigned into mild, moderate, and severe DPN groups. After excluding highly inter-correlated parameters through preprocessing, the extracted game features from the entire DPN and its three subgroups (DPN1, DPN2, and DPN3) were compared with the game parameters from the Control group (CON). Ten examples of 314 significantly different features are presented here. (b) In the Control group, three subgroups were created by age to identify the influence of age on game performance. 84 of the 314 features observed from the horizontal comparison between the Control and DPN groups revealed apparent distinctions among the three age groups. Two representative parameters were "virtual deviation of the ideal flying route" in the BF game and "anticipation time [s]" in the CP game. CON: controls (N=71); CON1: controls aged 18-30 (N=19); CON2: controls aged 31—50 (N=22); CON3: controls aged 51—80 (N=30); DPN: diabetic peripheral neuropathy (N=112); DPN1: mild (NDS: 1—5, N=48); DPN2: moderate (NDS: 6-8, N=55); DPN3: severe (NDS: 9-10, N=11) Differences between groups were calculated using Mann-Whitney U test, t-test or chi-square test as appropriate. Significance levels: ns (p>0.05), * (p=0.01—0.05), ** (p=0.001—0.01), *** (p=0.0001—0.001), **** (p<0.0001).*

3.3.2. Game feature analysis in Cohort 2

Further analyses were carried out with 120 datasets collected from age-matched participants in cohort 2. Intergroup difference tests for the 1,179 game features between 30 healthy controls and 90 patients with DPN extracted 58 representative features with significant differences. Four examples are presented in Figure 23 modeling scheme 1, and all variables are summarized in Supplementary Table 2). As presented with boxplots and density curves, the "Anticipation time [s]" (Feature 1a, AC game, TC 2) was lower in the Control group compared to the DPN group. It measured the time that the player needed to bring the car into the catching area by modifying appropriate pressures on his/her feet. Similar trends were observed with the other three representative parameters. The intergroup difference of "Pressure differences between successive frames" (Feature 1b, BF game, Task 11) indicated that healthy subjects could modify their foot pressure more smoothly and precisely while controlling the balloon to fly through the highest obstacle (the cathedral in Task 11 of the BF game). The average "Time outside ideal pressure zone [s]" (Feature 1c, CP game, TC 6) in patients with DPN lasted about

0.8 seconds, twice as long as the value with healthy subjects. A number of DPN patients had even longer “Time outside ideal pressure zone [s]” than 1/4 of the entire execution phase (i.e., the phase required to maintain optimal pressure for 4.5 seconds). Thus, absence of pressure perception and difficulty maintaining constant pressure in patients with DPN existed. Moreover, the higher mean “Anticipation time [s]” (Feature 1d, IJ game, task 14) in DPN patients demonstrated that a majority of them needed longer time to identify the task target and to adjust foot pressure until reaching the optimal value that triggered a perfect jump of the virtual bird. From this perspective, the extracted game features were able to pinpoint peripheral nerve dysfunctions in patients with DPN.

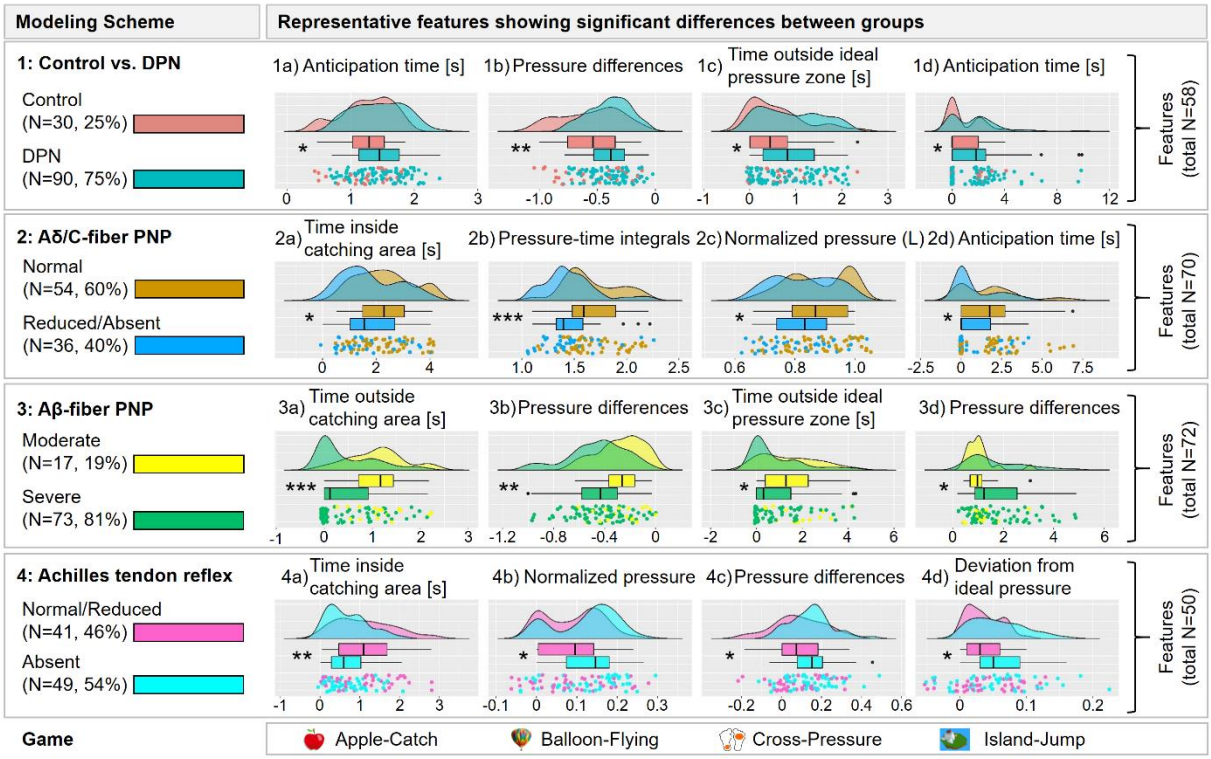

Figure 23. Classification modeling schemes and representative features extracted within cohort 2. *Model 1 was established to distinguish healthy controls and patients with diabetes and sensory neuropathy. Models 2-4 were developed to determine specific fiber subtype impairments (Aδ-, Aβ-/C-fibers). For each model, four representative features extracted from four different games were compared between groups. Data are n (%). Differences between groups were calculated using the Mann-Whitney U test, t-test, or chi-square test as appropriate. Significance levels: ns (p>0.05), * (p=0.01—0.05), ** (p=0.001—0.01), *** (p=0.0001—0.001), **** (p<0.0001). DPN: diabetic peripheral neuropathy; PNP: polyneuropathy*

In the DPN group, 70 game features were identified that predicted impaired pinprick or temperature sensation (Aδ-/C-fiber dysfunction). Four representative features are presented in Figure 23 modeling scheme 2, and all variables are summarized in Supplementary Table 3). The most significant parameter referred to “Pressure-time integrals” (Feature 2b) was calculated from task 3 of the BF game. Patients without small fiber impairments had smaller “Pressure-time integrals” than those with reduced or absent Aδ/C-fiber functions. The “Time inside catching area [s]” (Feature 2a, AC game, Task 8), the “Normalized pressure (L)”

(Feature 2c, CP game, Task 15), and the “Anticipation time [s]” (Feature 2d, IJ game, Task 3) were also lower in patients with diabetes and without small fiber neuropathy.

In addition, 72 game features indicating moderate or severe Aβ-fiber neuropathy are summarized in Supplementary Table 4. Four examples are presented in Figure 23 modeling scheme 3. The standard deviation of “Time outside catching area [s]” (Feature 3a, AC game, TC 12) was obviously higher in patients with diabetes and moderate compared to severe Aβ-fiber dysfunctions. A similar pattern was visible in “Pressure differences between successive frames” (Feature 3b, BF game, Task 7) and the “Time outside ideal pressure zone [s]” (Feature 3c, CP game, Task 2). However, patients with diabetes and severe Aβ-fiber impairment revealed increased “Pressure differences between successive frames” (Feature 3d, IJ game, Task 1).

Lastly, 50 game features correlated with absent Achilles tendon reflexes as shown in Supplementary Table 5, and four examples are shown in Figure 23 modeling scheme 4. The standard deviation “Time inside catching area [s]” (Feature 4a, AC game, TC3) in patients with diabetes and absent Achilles reflex was distinctly lower in those with normal or reduced reflexes. However, the standard deviation of “Normalized pressure” (Feature 4b, BF game, TC3), the “Pressure differences between successive frames (L)” (Feature 4c, CP game, Task 14), and the “Deviation from ideal pressure” (Feature 4d, IJ game, Task 9) in patients with diabetes and absent Achilles reflexes were relatively higher than those with normal or only decreased reflexes.

Overall, the intergroup difference tests confirmed that some extracted game features are associated with peripheral nerve damages caused by diabetes. Distinct features also indicated Aβ-fiber, Aδ-/C-fiber, and Achilles tendon reflex deficits in patients with diabetes. More details of these features are presented in chapter 2.4.

3.4. Predictive models of DPN

3.4.1. DPN classification model

Predictive models of DPN were trained with the original datasets from 120 participants in cohort 2 (Figure 21c). 70% of datasets (n=84) were utilized for model training, the remaining 30% (n=36) for testing. Five-fold three repeats cross-validation was applied in feature ranking using SVM-Linear, SVM-Radial, and SVM-Poly classifiers. Classification models using variant subsets of top-ranked features (n=25) were trained to search for the best predictor combinations. The final model was selected according to Cohen’s Kappa metric and evaluated using the heldout testing dataset.

The best prediction was observed with the SVM-Poly model (degree: 1, scale: 0.1, C: 0.5) utilizing 15 predictors (model 1a, Figure 24), reaching an adjusted accuracy of 85.2% (AUC-ROC 0.91, Kappa 0.70, sensitivity 92.6%, specificity 77.8%) on the heldout testing dataset. With this model, only four out of 36 participants were misclassified (two false positive and two false negative classifications). The performance of the unbiased predictive model exceeded by far the hypothesis-driven discrimination model (model 1b, Figure 24).

a) Models and setup of parameters

Model	N	Classifier	Features (N)	Tuning parameters	Validation
1a Control vs. DPN	120	SVM-Poly	**15**	degree: 1, scale: 0.1, C: 0.5	three repeats five-fold cross-validation
1b Control vs. DPN hypothesis-driven	120	LR	**6**	none	
2 Aδ/C-fiber PNP	90	SVM-Radial	**25**	sigma: 0.0252727957626335, C: 1	
3 Aβ-fiber PNP	90	SVM-Poly	**9**	degree: 1, scale: 0.01, C: 0.5	
4 Achilles tendon reflex	90	SVM-Radial	**13**	sigma: 0.0520043134564958, C: 1	

b) Training performance

Model	ACC (%, Range)	Kappa (Range)	AUC-ROC
1a Control vs. DPN	87.8 (100 – 70.6)	0.63 (1 – 0.10)	**0.91**
1b Control vs. DPN hypothesis-driven	71.8 (81.2 – 58.8)	0.10 (0.37 – -0.20)	0.66
2 Aδ/C-fiber PNP	81.2 (100 – 66.7)	0.60 (1 – 0.31)	**0.90**
3 Aβ-fiber PNP	90.5 (100 – 75.0)	0.60 (1 – -0.12)	**0.94**
4 Achilles tendon reflex	79.2 (92.3 – 61.5)	0.58 (0.85– 0.23)	**0.85**

c) ROC curve

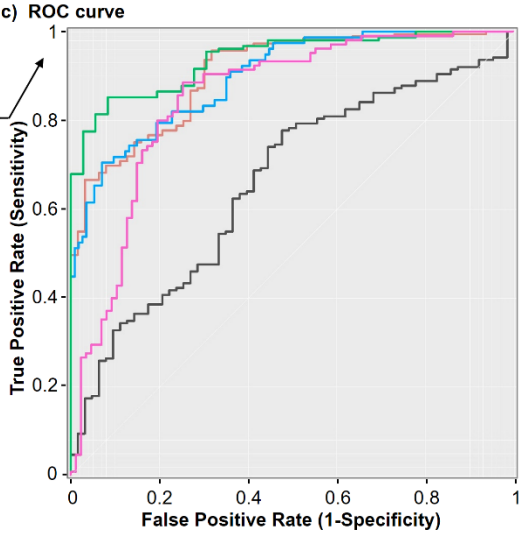

d) Predictive result

Model	Adjusted ACC (%)	Kappa	SEN (%)	SPE (%)
1a Control vs. DPN	**85.2**	0.70	92.6	77.8
1b Control vs. DPN hypothesis-driven	46.3	-0.10	92.6	0.0
2 Aδ/C-fiber PNP	**91.9**	0.84	90.0	93.8
3 Aβ-fiber PNP	**95.3**	0.78	90.5	100
4 Achilles tendon reflex	**88.1**	0.77	92.9	83.3

e) Confusion matrix

Model	TP (N)	TN (N)	FP (N)	FN (N)
1a Control vs. DPN	25	7	2	2
1b Control vs. DPN hypothesis-driven	25	0	9	2
2 Aδ/C-fiber PNP	9	15	1	1
3 Aβ-fiber PNP	19	5	0	2
4 Achilles tendon reflex	13	10	2	1

Figure 24. Performance of DPN classification models. *(a) Overview of models and setup parameters (class labels, sample sizes, classifiers, predictors, parameters, cross-validation). (b) Training performance of models with the comparison of subgroups and clinical findings summarizing calculated accuracies, Kappa, and AUC-ROC values of models. (c) Visualization of AUC-ROC curves for diagnosis of DPN and fiber damage. (d) Predictive performance of models on heldout testing dataset (adjusted testing accuracies ranged from 85.2 to 95.3 %). (e) Confusion matrix with absolute numbers of true positive/negative and false positive/negative classifications. DPN: diabetic peripheral neuropathy; PNP: Polyneuropathy; SVM: support vector machine; LR: logistic regression; ACC: accuracy; AUC-ROC: area under the receiver operating characteristic; SEN: sensitivity; SPE: specificity; TP: true positive; TN: true negative; FP: false positive; FN: false negative*

The predictors determined by the DPN classification models 1a are summarized in Figure 25 (F1–F15). The boxplots and density curves on the left presents between-group differences and distributions after excluding outliers. Data are presented as the means with standard deviations. The predictors were extracted from the games and TCs and are provided in the last two columns. Feature 11, named “Normalized pressure” (F11, AC game, TC 9), was the best predictor because it revealed significantly different distributions between the control and DPN groups.

	ID	Feature	Control (N=30)	DPN (N=90)	p	Game	Task/TC
	F1	Pressure gradients between successive frames (R)	0.039 (0.042)	0.066 (0.058)	*	CP	TC 8
	F2	Reaction time [s]	1.367 (0.781)	1.053 (0.773)	***	AC	Task 12
	F3	Final virtual distance	0.696 (0.622)	1.126 (1.074)	*	AC	Task 8
	F4	Anticipation time [s]	0.928 (1.382)	1.789 (1.739)	*	IJ	Task 9
	F5	Execution time [s]	0.825 (0.616)	1.775 (2.069)	**	IJ	TC 3
	F6	Pressure-time integrals of the reaction phase (L)	0.341 (0.316)	0.671 (1.308)	*	CP	Task 10
	F7	Normalized pressure	0.793 (0.158)	0.721 (0.159)	*	BF (L)	Task 7
	F8	Pressure differences between successive frames	1.589 (0.806)	2.425 (2.146)	*	IJ	Task 6
	F9	Pressure differences between successive frames	-0.556 (0.261)	-0.397 (0.179)	**	BF (R)	Task 11
	F10	Anticipation time [s]	0.678 (1.066)	1.130 (1.041)	*	IJ	TC 3
	F11	Normalized pressure	2.967 (0.972)	2.508 (1.301)	*	AC	TC 9
	F12	Anticipation time [s]	2.066 (0.752)	2.788 (1.515)	*	IJ	Task 12
	F13	Deviation from ideal pressure	0.021 (0.023)	0.048 (0.112)	**	IJ	Task 16
	F14	Minimal virtual distance smiley 1	0.549 (0.396)	0.562 (0.390)	ns	BF (R)	Task 6
	F15	Reaction time [s]	1.386 (1.182)	1.749 (1.567)	ns	CP	Task 13

Figure 25. Features for DPN classification using SVM-Poly (model 1a). *Fifteen game features (F1—F15) obtained by the SVM-Poly model for distinguishing patients with diabetes and peripheral neuropathy versus healthy controls are visualized with density and box plots. Most of the game features selected by the model showed significant differences between the Control and DPN groups. The differences are presented by density and box plots, as well as mean values and SDs. The extracted games and related task combinations of each feature are provided in the last two columns. Data are presented as means with standard deviation. All outliers were excluded in density and boxplots. Differences between groups were calculated using the Mann-Whitney U test, t-test, or chi-square test as appropriate. Significance levels: ns (p>0.05), * (p=0.01—0.05), ** (p=0.001—0.01), *** (p=0.0001—0.001), **** (p<0.0001). F: feature; DPN: diabetic peripheral neuropathy; AC: Apple-Catch; BF: Balloon-Flying; L: Left; R: Right; CP: Cross-Pressure; IJ: Island-Jump; TC: task combination*

3.4.2. Aδ-/C-fiber polyneuropathy classification model

Classification models to differentiate severity of dysfunction within the fiber types were built with datasets from 90 patients with diabetes within cohort 2. Overall, 36 out of 90 (40%) patients with diabetes had reduced/absent temperature sensation or pinprick (nociception), which is caused by Aδ-/C-fiber polyneuropathy (positive class). The obtained SVM-Radial model (sigma: 0.0252727957626335, C: 1) using 25 game predictors reached an adjusted accuracy of 91.9% for the classification of Aδ-/C-fiber polyneuropathy on a held out-testing dataset (model 2, Figure 24). The model misclassified two out of 26 cases (one false positive and one false negative classification). The final predictors of the model are presented in Figure 26 (F1—F25). Their distributions and between-group differences are visualized with boxplots and density curves on the left. The mean and standard deviation of these predictors were separately calculated between groups. The “Pressure-time integrals of the execution phase (R)” (F1, CP game, Task 4), the “Normalized pressure (R)” (F4, CP game, Task6), and the “Pressure differences between successive frames” (F18, BF game, Task 7) were optimal predictors that revealed distinct distributional differences between patients without and those with Aδ-/C-fiber dysfunctions. In addition, 21 out of all 25 predictors were significantly different in concordance with the results of the previous between-group difference tests.

	ID	Feature	Normal (N=54)	Absent (N=36)	p	Game	Task/TC
	F1	Pressure-time integrals of the execution phase (R)	2.104 (0.536)	1.876 (0.535)	ns	CP	Task 4
	F2	Pressure gradients between successive frames	0.353 (1.135)	1.104 (1.189)	**	AC	Task 13
	F3	Pressure-time integrals	0.991 (0.731)	0.674 (0.505)	*	BF (L)	Task 6
	F4	Normalized pressure (R)	0.567 (0.144)	0.508 (0.138)	*	CP	Task 6
	F5	Pressure-time integrals	1.668 (0.268)	1.471 (0.260)	***	BF (R)	Task 3
	F6	Minimal virtual distance smiley 2	0.623 (0.201)	0.547 (0.273)	ns	BF (L)	Task 4
	F7	Normalized pressure (R)	17.719 (4.053)	15.539 (3.841)	*	CP	Task 6
	F8	Pressure-time integrals of the reaction phase (L)	0.105 (0.144)	0.098 (0.295)	*	CP	Task 2
	F9	Normalized pressure	0.055 (0.022)	0.078 (0.033)	***	BF (R)	TC 2
	F10	Pressure differences between successive frames	0.052 (0.040)	0.037 (0.027)	*	IJ	TC 6
	F11	Normalized pressure	0.642 (0.155)	0.755 (0.174)	***	BF (R)	Task 4
	F12	Normalized pressure (R)	0.425 (0.026)	0.417 (0.022)	ns	CP	TC 3
	F13	Minimal virtual distance smiley 4	0.399 (0.334)	0.514 (0.301)	*	BF (L)	Task 12
	F14	Pressure differences between successive frames	0.281 (0.170)	0.375 (0.185)	*	AC	TC 9
	F15	Final virtual distance	0.908 (0.964)	0.586 (1.017)	*	AC	TC 8
	F16	Pressure differences between successive frames (L)	0.052 (0.030)	0.035 (0.018)	**	CP	TC 9
	F17	Minimal virtual distance smiley 2	0.163 (0.215)	0.078 (0.162)	*	BF (L)	TC 4
	F18	Pressure differences between successive frames	-0.383 (0.244)	-0.478 (0.202)	*	BF (R)	Task 7
	F19	Pressure differences between successive frames (R)	0.098 (0.057)	0.074 (0.068)	*	CP	TC 6
	F20	Minimal virtual distance smiley 3	0.586 (0.229)	0.377 (0.342)	*	BF (L)	Task 9
	F21	Normalized pressure (R)	0.475 (0.092)	0.409 (0.137)	*	CP	Task 7
	F22	Anticipation time [s]	0.980 (1.417)	2.118 (2.035)	**	IJ	Task 16
	F23	Virtual deviation of ideal flying route	0.057 (0.085)	0.174 (0.287)	*	BF (L)	Task 4
	F24	Pressure gradients between successive frames	3.032 (1.529)	2.319 (1.213)	*	BF (L)	Task 8
	F25	Pressure differences between successive frames (L)	0.071 (0.051)	0.053 (0.049)	ns	CP	Task 15

Figure 26. Features for Aδ-/C-fiber polyneuropathy classification using SVM-Radial (model 2). *Twenty-five game features (F1—F25) were obtained by SVM-Radial models that identified Aδ-/C-fiber polyneuropathy (absent pinprick or temperature sensation) in patients with diabetes. These are visualized by density and box plots. Most of the game features selected by the model showed significant differences between the "normal" and "absent" groups. The differences are presented by density and box plots, as well as mean values and standard deviations (SD). The extracted games and related task combinations of each feature are provided in the last two columns. Data are presented as means (SD). All outliers were excluded in density and boxplots. Differences between groups were calculated using the Mann-Whitney U test, t-test, or chi-square test as appropriate. Significance levels: ns (p>0.05), * (p=0.01—0.05), ** (p=0.001—0.01), *** (p=0.0001—0.001), **** (p<0.0001). F: feature; AC: Apple-Catch; BF: Balloon-Flying; L: Left; R: Right; CP: Cross-Pressure; IJ: Island-Jump; TC: task combination*

3.4.3. Aβ-fiber polyneuropathy classification model

In cohort 2, 73 out of 90 (81%) patients with diabetes had impaired vibration sensation (below 3/8) or an abnormal 10g monofilament-test result (reduced/absent), which was linked to Aβ-fiber polyneuropathy (positive class). The obtained SVM-Poly model (degree: 1, scale: 0.01, C: 0.5) using nine game predictors reached an adjusted accuracy of 95.3% for the classification of Aβ-fiber polyneuropathy on a held out-testing dataset (model 3, Figure 24). The model misclassified two out of 26 cases (two false negative cases). The final predictors of the model are presented in Figure 27 (F1—F9). Their distributions and between-group differences are visualized with boxplots and density curves on the left. The mean and standard deviation of these predictors were separately calculated between groups. Almost all predictors were significantly different in concordance with the results of the previous between-group difference test. The "Normalized pressure" (F9, BF game, TC3) was an optimal predictor that revealed significant distributional differences between patients without and those with Aβ-fiber dysfunctions.

	ID	Feature	Moderate (N=17)	Severe (N=73)	p	Game	Task/TC
	F1	Pressure differences between successive frames	-0.274 (0.180)	-0.455 (0.230)	**	BF (R)	Task 7
	F2	Frequency outside catching area (n)	0.779 (0.253)	0.476 (0.382)	**	AC	TC 12
	F3	Normalized pressure (L)	0.801 (0.098)	0.841 (0.140)	ns	CP	Task 13
	F4	Normalized pressure	0.090 (0.067)	0.130 (0.072)	*	AC	TC 6
	F5	Minimal virtual distance smiley 3	0.553 (0.264)	0.615 (0.203)	*	BF (L)	Task 10
	F6	Normalized pressure (L)	0.085 (0.052)	0.048 (0.035)	**	CP	Task 6
	F7	Pressure differences between successive frames (R)	0.003 (0.002)	0.002 (0.001)	**	CP	TC 8
	F8	Anticipation time [s]	1.245 (0.593)	1.890 (1.103)	**	AC	Task 7
	F9	Normalized pressure	1.239 (0.501)	1.635 (0.473)	**	BF (R)	TC 3

Figure 27. Features for the Aβ-fiber polyneuropathy classification using SVM-Poly (model 3). *The SVM-Poly model extracted nine game features (F1–F9) to classify the severity of Aβ-fiber polyneuropathy (moderate or severe, defined by vibration sensation testing and 10g monofilament-test results). Most of the game features selected by the model showed significant differences between the two severity groups. The differences are presented by density and box plots, as well as mean values (SD). The extracted games and related task combinations of each feature are provided in the last two columns. Data are presented as means (SD). All outliers were excluded in density and boxplots. Differences between groups were calculated using the Mann-Whitney U test, t-test, or chi-square test as appropriate. Significance levels: ns (p>0.05), * (p=0.01–0.05), ** (p=0.001–0.01), *** (p=0.0001–0.001), **** (p<0.0001). F: feature; AC: Apple-Catch; BF: Balloon-Flying; L: Left; R: Right; CP: Cross-Pressure; IJ: Island-Jump; TC: task combination*

3.4.4. Achilles tendon reflex classification model

In cohort 2, 49 out of 90 (54%) patients with diabetes exhibited absent Achilles tendon reflexes, which were considered as positive cases for AI models. The obtained SVM-Radial model (sigma: 0.0520043134564958, C: 1) using 13 game predictors reached an adjusted accuracy of 88.1% for the classification of Achilles tendon reflexes on a held out-testing dataset (model 4, Figure 24). The model misclassified three out of 26 cases (one false negative and two false positive cases). The final predictors identified in the model are presented in Figure 28 (F1–F13). Their distributions and between-group differences are visualized with boxplots and density curves on the left. The mean and standard deviation of these predictors were separately calculated between groups. Almost all predictors were significantly different in agreement with the results of the previous between-group difference test. The “Anticipation time [s]” (F6, AC game, TC10) and the “Pressure gradients between successive frames” (F11, AC game, TC 12) were optimal predictors that revealed significant distributional differences between diabetes with normal and absent Achilles tendon reflex status.

	ID	Feature	Present (N=41)	Absent (N=49)	p	Game	Task/TC
	F1	Minimal virtual distance smiley 3	0.630 (0.180)	0.561 (0.251)	*	BF (L)	Task 1
	F2	Pressure differences between successive frames	0.093 (0.090)	0.150 (0.115)	*	BF (R)	TC 4
	F3	Minimal virtual distance smiley 1	0.504 (0.409)	0.629 (0.362)	ns	BF (L)	Task 3
	F4	Normalized pressure	2.040 (1.520)	1.191 (0.870)	**	AC	TC 4
	F5	Time inside catching area [s]	0.631 (0.597)	0.304 (0.395)	**	AC	Task 6
	F6	Anticipation time [s]	1.345 (0.721)	1.682 (0.713)	*	AC	TC 10
	F7	Normalized pressure	7.278 (2.631)	5.105 (2.197)	****	AC	Task 8
	F8	Final virtual distance	1.088 (0.680)	0.836 (0.745)	*	AC	TC 9
	F9	Pressure-time integrals	8.509 (25.263)	2.166 (2.310)	**	IJ	Task 9
	F10	Pressure differences between successive frames (R)	0.003 (0.003)	0.005 (0.003)	**	CP	TC 5
	F11	Pressure gradients between successive frames	0.494 (0.361)	0.600 (0.341)	ns	AC	TC 12
	F12	Mean pressure of execution phase	0.171 (0.143)	0.117 (0.054)	*	IJ	TC 5
	F13	Pressure differences between successive frames (L)	0.088 (0.128)	0.148 (0.106)	*	CP	Task 14

Figure 28. Features for the Achilles tendon reflex classification using SVM-Radial (Model 4). *The SVM-Radial model selected 13 game features (F1—F13) to classify for absence or presence of Achilles tendon reflexes in diabetes patients. Most of the game features selected by the model showed significant differences between both classifications. The differences are presented by density and box plots, as well as mean values (SD). The extracted games and related task combinations of each feature are provided in the last two columns. Data are presented as means (SD). All outliers were excluded in density and boxplots. Differences between groups were calculated using the Mann-Whitney U test, t-test, or chi-square test as appropriate. Significance levels: ns (p>0.05), * (p=0.01—0.05), ** (p=0.001—0.01), *** (p=0.0001—0.001), **** (p<0.0001). F: feature; AC: Apple-Catch; BF: Balloon-Flying; L: Left; R: Right; CP: Cross-Pressure; IJ: Island-Jump; TC: task combination*

4. Discussion

The primary hypothesis of this thesis is that “a Gamidiagnostics application with video-based playful elements combining sensor-equipped insoles and machine learning algorithms is feasible to screen for peripheral neuropathy in patients with diabetes”. Following the outlined methodological developments and standardization of the test the “Gamidiagnostics” application indeed allowed to perform a highly predictive screening for peripheral neuropathy. This was assessed in a selected cohort of patients with clinically diagnosed severe neuropathy and healthy volunteers as comparator cohort. The system was designed for peripheral nerve function assessment with a low complexity setup allowing for a quick introduction into all games and an easy understanding of control functions of the sensor equipped insoles. Standardized calibration steps and interactive tutorials before each game allowed the participants to perform initial steering attempts to familiarize with the games. Motivational elements were combined to encourage completion of tasks and endurance over 15 minutes. Standardized data acquisition processes with time stamps linked sensor data throughout games, even with failed efforts (preset maximum allowance of three failed efforts per game). Challenges in the games provided information on movement control of both feet to determine muscle strength, sensation, balance, and coordination. “Immediate feedback to the participants on gaming results and overall performance was offered after the game was completed. Furthermore, the datasets were introduced into machine learning algorithms to predict peripheral neuropathy and phenotype affected nerve fiber subtypes.

Similarly, the second hypothesis was confirmed by the findings, that is “predefined hypothesis-driven parameters (reaction time, sensation, skillfulness, endurance, balance, muscle strength) correlate with the clinical status, e.g., the nerve disability score (NDS)”. In the age-matched cohort, the between-group differentiation of sensation, skillfulness, endurance, and finger reaction time remained significant. However, the logistic regression model using the hypothesis-driven indicators was less predictive of DPN than machine learning algorithms.

Notably, hypothesis three (“feature extraction methodology may be applied to determine representative game features and calculate key capabilities correlating with NDS”) and four (“the AI models may identify relevant game parameters, make predictions on DPN and possibly achieve phenotyping of impaired nerve fibers”) were confirmed. Feature extraction methodologies were able to identify representative game features and to calculate key capabilities that correlated to clinical ground truth (NDS). Game features were extracted from different game tasks and task combinations, which was possible due to the aforementioned standardization of the games, predefined game scenarios and time stamps. An unexpected key finding of this work was that the trained classification models were able to identify game

features that allowed to phenotype impaired nerve fibers. The feature ranking techniques classified Aδ/C- and Aβ-fiber polyneuropathy and Achilles tendon reflex impairment. The classification models were obtained with training data sets from 120 patients. On the heldout testing dataset, an adjusted testing accuracy of 85.2% with a sensitivity of 92.6% and specificity of 77.8% (Cohen's Kappa 0.70) in classifying peripheral small and large nerve functions was achieved. Furthermore, the SVM models allowed to differentiate between small (Aδ-/C-fibers) as well as large Aβ-fiber damage with high accuracy (adjusted accuracies of 91.9% and 95.3%, respectively).

To this end, all subgoals of the study were achieved, that have been defined in the aims section: design and development of a "Gamidiagnostics" application with real-time data acquisition using sensor-equipped insoles, automatic data transmission to a remote server, implementation of an online platform for visualizations and database exchange, validation of the "Gamidiagnostics" application in a pilot exploratory study with healthy volunteers and patients diagnosed with peripheral neuropathy, determination of representative game features and predefined key capabilities correlating to clinical ground truth, training and optimization of AI models to assess severity of dysfunction for fiber subtypes Aβ-, Aδ-/C and Achilles tendon reflexes.

4.1. Performance of the neuropathy "Gamidiagnostics" App in comparison to other studies

A literature search reveals that only few research groups have chosen similar approaches. Learning models calculating risk for peripheral nerve function on the basis of clinical data and past medical history impairment was reported by Kazemi et al., who enrolled 600 subjects (175 healthy volunteers and 425 patients with different severities of DPN). On the basis of the NDS score as the ground truth the best-performance was achieved with the SVM-OAO-RBF kernel model yielding an accuracy of 76% in predicting the DPN severity (none, mild, moderate, severe). The 13 features included age, type of diabetes, education level, BMI, history of elevated blood pressure, actual systolic blood pressure, history of foot ulcer, medication, weight, history of laser photocoagulation, duration of diabetes, average blood glucose level and height (75). Dubey et al. established a Neural Network to predict the diabetic neuropathy risk level using the following seven features: duration of diabetes mellitus, age, height, weight, urinary albumin-to-creatinine ratio, glycated hemoglobin (HbA1c) and cholesterol. They selected vibration perception thresholds to identify different severity groups. The accuracy was 70.1% with simulated patient data (4,158 cases) using mean and covariance of patients´ data obtained from a clinical database (n=5,088) (91). Corpin et al. introduced plantar pressure data as predictors to distinguish healthy subjects, patients with only T2DM, and patients with

T2DM and DPN. The authors performed a rather small study with 36 patients that performed repeated measurements (sample size: 288). Michigan Neuropathy Screening Instrument-questionnaire (MNSI-q) and Nerve Conduction Velocity (NCV) measurements were performed to stratify patients into subgroups. 29 features were extracted from 13 plantar pressure parameters on 16 different foot regions. The SVM algorithm exhibited the highest accuracy with 91.9%, the MLP model yielded an accuracy of 89.8% (92).

However, a study with dynamic data acquisition from patients and multiple challenges that does not rely on clinical parameters at forehand was not identified in the literature.

The plethora of data obtained by the “Gamidiagnostics” App offered numerous advantages:

1. Data acquisition for AI model development. The “Gamidiagnostics” application provided features with high quantity and quality for AI models. The obtained models in this work were trained with predefined game indicators and sensor data. These included amongst others reaction time, anticipation time, time inside the catching area, frequency outside of the catching area, virtual distance. Similar to Corpin et al. (2019), we extracted multiple pressure parameters by calculating maximum, minimum, mean, standard deviation, pressure differences and gradients between successive frames, and pressure time integration. The pressure parameters were subdivided into specific game scenarios and task combinations that reached far beyond the simple integration of the measurement process. Thus, more than 1,800 distinctive parameters were extracted as potential predictors according to the proposed feature extraction methodology from each dataset. Moreover, intergroup difference tests and feature ranking methods both identified many features that significantly correlated with clinical findings, confirming that game features were associated with underlying sensory and motor dysfunctions resulting from peripheral neuropathy.

2. Widely used neuropathy disability score as comparator. The chosen comparator neuropathy disability score (NDS) (93, 94) is widely used as a tool in clinical practice with scores ranging from 0 to 10. Mild (score 3–5), moderate (score 6–8), and severe neuropathy (score 9–10) may subclassified, the latter posing the highest risk of developing foot ulcerations (95). DPN is often diagnosed at a very late, pre-ulcerative stage due to a lack of systematic screening. Monofilament-testing identified advanced neuropathy only. Similarly, the NSS cannot reliably identify DPN (93, 96). The enrolled diabetes cohort included patients with mild (41.1%), moderate (49.1%), and severe (9.8%) peripheral neuropathy according to the NDS (see Table 3). Severe damage of Aδ-/C-fibers was assumed in patients with reduced/absent pinprick (nociception) or temperature sensation. The presence of severe Aβ-fiber polyneuropathy was assumed with impaired vibration sensation (below 3/8) or an abnormal 10g monofilament-test result (reduced/absent). The remaining patients in the DPN group were classified as moderate

Aβ-fiber polyneuropathy (impaired vibration sensation: 3-4/8). The absence of Achilles tendon reflexes was considered as a positive label in the model training. A negative label was assigned to normal or mildly impaired reflexes.

3. Age as bias for neuropathy. We only entered datasets from age-matched participants to AI models because the comparison of game features among young, middle-aged, and elderly control groups confirmed that age has a significant effect on game performance of study participants.

In the study of Kazemi et al. (2016), age itself was included as a predictor for DPN classification. Such a choice may misguide machine learning models to make determinations that are very close to objective facts only based on age since the age distribution of their samples correlated significantly with DPN severity (normal: 43.98±15.20 years, mild: 54.7±12.02 years, moderate: 61.91±11.20 years, severe: 62.67±10.27 years). In the study of Corpin et al. (2019) the age of healthy subjects differed from those who had diabetes mellitus and/or peripheral neuropathy (49.5±8.07 versus 57.6±4.39 and 49.5±8.07 versus 56.8±10.90, respectively).

4. Model predictors were improved by feature ranking and selection. The work flow of the game feature extraction excluded those with high intercorrelations. This ensured that only independent variables were utilized for modeling. Thereafter, the dataset was split into a training and a testing set with a ratio of 7:3. The testing dataset was held out only for final model evaluation. Machine learning algorithms estimated the feature importance with the training dataset only. The applied feature ranking approach was proposed by Kuhn et al. within the caret R package (89). It maintains the exact meaning of features and ranks them according to their calculated association with the class distribution. The feature ranking is an effective solution to select features from datasets that often consist of fewer observations than variables (small sample size but high dimensionality) (97). It is different from the Principal Components Analysis (PCA) that was performed by Corpin et al. (2019) on their pressure dataset that combines multiple variables to principles with a maximum variance but no specific meaning or definition, which brings difficulties for the model explanation.

5. Cross-validation in the model training avoided overfitting. Specifically, five-fold three repeats cross-validation were utilized in the model training, avoiding overfitting and deriving a more accurate model performance estimate. Similar statistical methods were also used for model validation in the above-mentioned studies (10-fold cross-validation) (75, 91).

6. Subanalyses on specific fiber damage. Impressive accuracy was achieved in classifying peripheral small and large nerve functions in patients diagnosed with moderate to advanced sensorimotor neuropathy and diabetes. The classification model to distinguish healthy controls and patients with diabetes and peripheral neuropathy achieved an adjusted testing accuracy

of 85.2% (sensitivity 92.6%, specificity 77.8%, and Cohen's Kappa 0.70) on a heldout testing dataset. This dataset was split only for final evaluation that enhanced the reliability of the obtained classification mode. Compared to the above-mentioned studies, only Dubey et al. (2020) created a testing dataset (15%) for model evaluation. Kazemi et al. (2016) and Corpin et al. (2019) reported their model training performance only with 10-fold cross-validation. The training accuracy represents a certain degree of model performance, but it is not comparable to the testing accuracy. Moreover, we also performed phenotyping of nerve dysfunctions in model training. The obtained models were able to differentiate Aδ-/C-fiber versus Aβ-fiber polyneuropathy, and the absence of Achilles tendon reflexes in diabetes with adjusted accuracies of 91.9%, 95.3%, and 88.1%, respectively. None of the aforementioned studies considered detailed phenotyping of small or large fiber dysfunctions. Thus, the presented polyneuropathy "Gamidiagnostics" set allowed to apply AI models in subclassifying neuropathy.

7. Considerations on video game design for polyneuropathy diagnosis. The study cohort of patients with diabetes mostly represented elderly people with a duration of diabetes mostly exceeding 15 years. These participants have specific demands when they perform games, which were addressed as follows:

- The pantolettes were easy to use, with open design, nice fit and relaxed foot wear.
- Participants were seated in comfortable chairs with arm rests and at a table of normal height.
- Tablets were positioned at comfortable distance to the participants with good vision.
- Speakers were tuned high volume to allow easy listening.
- Special large fonts were chosen to enable better reading.
- Eye-catching background colors and larger sizes for navigation buttons were configured to simplify on-screen navigation.

Such standardization and addressing specific demands are prerequirements for game-based diagnostic approaches and comparability (98, 99).

All study participants judged the "Gamidiagnostics" App as simple to carry out. The barrier to completion of this study was low, even for those with little or no experience in games. The immediate response of the study participants upon completion of the games was overwhelmingly positive. More than 90% wished to repeat the sessions, however, the second-course results were not included in this study to exclude learning effects.

8. Future developments and autonomous usage. The "Gamidiagnostics" application in combination with the database platform IQ-Trial incorporates the opportunity for regular screening of peripheral neuropathy in a home-based environment of high-risk populations such as patients with diabetes. Care providers would be able to receive the data sets remotely within

a telemedicine framework. Trained classification models may be implemented as online diagnostic platforms (online prediction). The models itself could be iteratively improved by labeled datasets (online learning) (100, 101). Ultimately, a game-based assessment in the outpatient setting would open the window for screening of a broader population. It could be combined with other applications, such as gait analysis (102), real-time fall detection (103, 104), and diabetic foot ulcer prevention (105).

4.2. Limitations of the pilot study

Noteworthy, our study did not address the diagnosis of minor polyneuropathy. It remains unclear whether game-based diagnostics (i.e., incorporation of game-playing elements into the diagnosis of neuropathy) will be similarly sensitive in detecting isolated Aδ-/C-fiber neuropathy. Given that small-fiber deficits are believed to be precursors of large fiber impairment in DPN (21, 44), testing of nerve function impairment by electroneurography should be performed, even in patients with prediabetes (51). These findings may be correlated with game-based diagnostics patterns in follow-up studies. Notably, with early diagnosis, preventive measures may be taken. Small fibers are believed to degenerate first and are most likely to be repaired. Interventions may comprise body weight control or normalization of hyperglycemia (106, 107). Foreseeable, preventive measures may also include supplementation with vitamin B12, e.g., in patients that commonly take metformin (108). Drugs with a potential protective action on nerve integrity may also be included (109).

In addition, there are only a few studies that performed a comparable approach. The majority of studies established classification models for DPN using clinical biomarkers (e.g. age, duration of diabetes, BMI, HbA1c, etc.) without considering any wearable sensor data or video game parameters. Corpin et al. (2019) involved plantar pressure values in classification algorithms, but only 36 healthy volunteers and patients with diabetes were included. The reliability of our work will likely be improved in large cohorts that utilize wearable sensors and video games for DPN detection in the future (110, 111).

Furthermore, the cohorts may not be entirely representative for the general population. The diabetes group were relatively elder than other study cohorts with long duration of diabetes and high BMI values (75, 111–113). Specifically, there was a strong bias towards male participants in the diabetes group, which may translate into differing gaming skills. In addition, no diabetes without peripheral neuropathy was included in the study, as well as patients with other types of peripheral neuropathy (e.g. alcoholic polyneuropathy). Analyses on hidden alcohol-toxicity and other causes of neuropathy were not performed.

The between-group comparison of game features in the entire cohort showed that age had an impact on the game performance. Cognitive impairment in addition to the normal aging process

may also influence on the execution of the games. Therefore, a systematic analyses of aging and cognitive impairment on game performance have been initiated.

Moreover, the established models require further evaluation with larger and balanced datasets. The effect of limited sample size is evidenced by the deviation between the predictive performance and the training metrics even though three repeats five-fold cross-validation was applied in model training. For example, the accuracy of model 1a decreased from 87.8% (maximal 100% in cross-validation) in the training dataset to 85.2% with the testing dataset. With a larger dataset, classifier-based feature importance estimation would target the optimal features more precisely. In addition, the imbalance in the number of healthy individuals and DPN patients in the dataset (ratio 1:3) lead to a significant gap between the sensitivity and specificity of the classification models. A larger control sample will improve AI modeling to identify differences in game performance of healthy individuals compared to DPN patients (114, 115).

4.3. Conclusion and outlook

The game-based polyneuropathy diagnosis App (“Gamidiagnostics”) combining smart footwear sensors is able to diagnose advanced peripheral nerve malfunction with high accuracy in a time-saving, examiner-independent, self-administered enjoyable manner, which has the potential to be established as a telemedical device.

This approach bears the potential to be implemented as telemedical App within an online diagnostic platform for automatic prediction of DPN and dynamic learning with more labeled datasets. Participants may receive immediate feedback on their gaming performance, capabilities and peripheral nerve status. Care providers would receive similar information enriched with details on fiber type impairment.

The findings of our study are encouraging. Nevertheless further trials are required to enrich the sample size and also to include more objective clinical examinations, such as nerve conduction measurements and corneal confocal microscopy. A cohort with early-stage peripheral neuropathy (i.e., only absent temperature sensation or nociception) should be recruited to evaluate the feasibility of the “Gamidiagnostics” application to detect small fiber polyneuropathy. Patients diagnosed with diabetes and without peripheral neuropathy should be enrolled as another reference group for comparison with the DPN group. Patients with mild cognitive impairment, subjective cognitive impairment, or Alzheimer´s disease may also be tested to investigate the feasibility of game-based assessment of cognitive impairment.

Furthermore, gaming sessions may be offered as exergaming sessions to improve balance, postural stability and physical capabilities. The scope of such developments is unlimited.

5. Summary

Given an overall prevalence rate of 40% for diabetes-associated polyneuropathy in patients and elevated risk for complications, such as diabetic foot syndrome, the disease management program diabetes has adopted a surveillance strategy for neuropathy. Diagnosis of peripheral neuropathy (DPN) is routinely achieved through clinical examination, that are standardized procedures (pinprick test, vibration perception, Tip Therm, reflexes, muscle function). However, the performance is time-consuming and an investigator-related bias may confound findings.

The goal of this thesis is to explore the potentials of a video game-based approach to assess polyneuropathy ("Gamidiagnostics"). The hypothesis is tested that the proposed "Gamidiagnostics" application is able to provide a meaningful assessment of small and large fiber function in a self-administered, examiner-independent manner and therefore may be suited as as telemedical application. To this end a gaming platform was set up. A pilot study with 71 healthy volunteers and 112 patients diagnosed with diabetes and peripheral neuropathy by clinical examination (neuropathy disability score, NDS, for phenotyping of Aδ-, Aβ- and C-fiber function as well as the Achilles tendon reflex) evaluated the feasibility of this approach. Participants utilized pressure sensor-equipped insoles as control units and played four games specifically designed to test for reaction time, sensation, skillfulness, endurance, balance, and muscle strength.

Unbiased training of prediction algorithms with datasets identified 15 independent variables with discriminatory functions that indicated polyneuropathy (training with five-fold three repeats cross-validation). In age-matched cohorts, the support vector machines achieved a training accuracy of 87.8% (AUC-ROC 0.91) and an adjusted accuracy of 85.2% on a heldout testing dataset (sensitivity 92.6%, specificity 77.8%). Distinct variables were identified for each nerve fiber deficit and allowed correct classification with adjusted accuracies of 88.1%, 91.9%, and 95.3% for Achilles tendon reflex, Aδ-/C-fiber, and Aβ-fiber impairment, respectively. In contrast, biased hypothesis-driven discrimination only resulted in the accurate classification of polyneuropathy in 71.8% (AUC-ROC 0.66) of participants.

Thus, the established game-based diagnostics approach combining video games and smart footwear sensors was able to diagnose advanced peripheral nerve malfunction with high accuracy in an examiner-independent manner, which has the potential to be established as a telemedical device.

6. References

1. Akinrodoye MA, Lui F (Eds.). *StatPearls [Internet],* StatPearls Publishing, 2021
2. Romero-Ortega M. Peripheral Nerves, Anatomy and Physiology of. In *Encyclopedia of Computational Neuroscience.* Jaeger D, Jung R, Eds. New York, NY, Springer New York, 2020, p. 1–5
3. Azhary H, Farooq MU, Bhanushali M, Majid A, Kassab MY. Peripheral Neuropathy: Differential Diagnosis and Management. 0002-838X 2010;81:887–92
4. Callaghan BC, Price RS, Feldman EL. Distal Symmetric Polyneuropathy: A Review. 1538-3598 2015;314:2172–81
5. Callaghan B, McCammon R, Kerber K, Xu X, Langa KM, Feldman E. Tests and expenditures in the initial evaluation of peripheral neuropathy. 1538-3679 2012;172:127–32
6. Hanewinckel R, Drenthen J, van Oijen M, Hofman A, van Doorn PA, Ikram MA. Prevalence of polyneuropathy in the general middle-aged and elderly population. Neurology 2016;87:1892–8
7. Savettieri G, Rocca WA, Salemi G, Meneghini F, Grigoletto F, Morgante L et al. Prevalence of diabetic neuropathy with somatic symptoms: a door-to-door survey in two Sicilian municipalities. Sicilian Neuro-Epidemiologic Study (SNES) Group. Neurology 1993;43:1115–20
8. Bharucha NE, Bharucha AE, Bharucha EP. Prevalence of peripheral neuropathy in the Parsi community of Bombay. Neurology 1991;41:1315–7
9. Ylitalo KR, Sowers M, Heeringa S. Peripheral vascular disease and peripheral neuropathy in individuals with cardiometabolic clustering and obesity: National Health and Nutrition Examination Survey 2001-2004. 1935-5548 2011;34:1642–7
10. Visser NA, Notermans NC, Linssen RSN, van Berg LH den, Vrancken, Alexander F. J. E. Incidence of polyneuropathy in Utrecht, the Netherlands. Neurology 2015;84:259–64
11. Ziegler D, Strom A, Lobmann R, Reiners K, Rett K, Schnell O. High prevalence of diagnosed and undiagnosed polyneuropathy in subjects with and without diabetes participating in a nationwide educational initiative (PROTECT study). Journal of diabetes and its complications 2015;29:998–1002

12. Pfannkuche A, Alhajjar A, Ming A, Walter I, Piehler C, Mertens PR. Prevalence and risk factors of diabetic peripheral neuropathy in a diabetics cohort: Register initiative “diabetes and nerves”. Endocrine and Metabolic Science 2020;1:100053

13. Research, Markets. *Diabetic Peripheral Neuropathy (DPN) Epidemiology Forecast (2020 to 2030) - Key Assessments, Patient Segmentation and Disease Risk & Burden.* Research and Markets 2020 Feb 13. Available from https://www.globenewswire.com/news-release/2020/02/13/1984758/0/en/Diabetic-Peripheral-Neuropathy-DPN-Epidemiology-Forecast-2020-to-2030-Key-Assessments-Patient-Segmentation-and-Disease-Risk-Burden.html. Accessed 25 January 2022

14. Kostev K, Jockwig A, Hallwachs A, Rathmann W. Prevalence and risk factors of neuropathy in newly diagnosed type 2 diabetes in primary care practices: a retrospective database analysis in Germany and U.K. Primary care diabetes 2014;8:250–5

15. Watson JC, Dyck PJB. Peripheral Neuropathy: A Practical Approach to Diagnosis and Symptom Management. Mayo Clinic proceedings 2015;90:940–51

16. Won JC, Park TS. Recent Advances in Diagnostic Strategies for Diabetic Peripheral Neuropathy. Endocrinology and Metabolism 2016;31:230–8

17. Nold CS, Nozaki K. Peripheral neuropathy: Clinical pearls for making the diagnosis. 1547-1896 2020;33:9–15

18. Wettasinghe AH, Dissanayake DWN, Allet L, Katulanda P, Lord SR. Sensorimotor impairments, postural instability, and risk of falling in older adults with diabetic peripheral neuropathy. 1998-3832 2020;40:547–54

19. Feldman EL, Callaghan BC, Pop-Busui R, Zochodne DW, Wright DE, Bennett DL et al. Diabetic neuropathy. Nature reviews. Disease primers 2019;5:41

20. Cho NH, Shaw JE, Karuranga S, Huang Y, da Rocha Fernandes JD, Ohlrogge AW et al. IDF Diabetes Atlas: Global estimates of diabetes prevalence for 2017 and projections for 2045. Diabetes research and clinical practice 2018;138:271–81

21. Callaghan BC, Cheng HT, Stables CL, Smith AL, Feldman EL. Diabetic neuropathy: clinical manifestations and current treatments. The Lancet Neurology 2012;11:521–34

22. Selvarajah D, Kar D, Khunti K, Davies MJ, Scott AR, Walker J et al. Diabetic peripheral neuropathy: advances in diagnosis and strategies for screening and early intervention. The Lancet Diabetes & Endocrinology 2019;7:938–48

23. Armstrong DG, Boulton AJM, Bus SA. Diabetic Foot Ulcers and Their Recurrence. The New England journal of medicine 2017;376:2367–75

24. Richard J-L, Lavigne J-P, Got I, Hartemann A, Malgrange D, Tsirtsikolou D et al. Management of patients hospitalized for diabetic foot infection: results of the French OPIDIA study. Diabetes & metabolism 2011;37:208–15

25. Singh N, Armstrong DG, Lipsky BA. Preventing foot ulcers in patients with diabetes. JAMA 2005;293:217–28

26. Pop-Busui R, Boulton AJM, Feldman EL, Bril V, Freeman R, Malik RA et al. Diabetic Neuropathy: A Position Statement by the American Diabetes Association. Diabetes care 2017;40:136–54

27. Lipsky BA, Berendt AR, Cornia PB, Pile JC, Peters EJG, Armstrong DG et al. 2012 infectious diseases society of america clinical practice guideline for the diagnosis and treatment of diabetic foot infections. Journal of the American Podiatric Medical Association 2013;103:2–7

28. Devigili G, Tugnoli V, Penza P, Camozzi F, Lombardi R, Melli G et al. The diagnostic criteria for small fibre neuropathy: from symptoms to neuropathology. Brain : a journal of neurology 2008;131:1912–25

29. Schiff E, Eisenberg E. Can quantitative sensory testing predict the outcome of epidural steroid injections in sciatica? A preliminary study. Anesthesia and analgesia 2003;97:828–32

30. Li Z-F, Niu X-L, Nie L-L, Chen L-P, Cao C-F, Guo L. Diagnostic value of clinical deep tendon reflexes in diabetic peripheral neuropathy. Archives of medical science : AMS 2020

31. Won JC, Kwon HS, Kim CH, Lee JH, Park TS, Ko KS et al. Prevalence and clinical characteristics of diabetic peripheral neuropathy in hospital patients with Type 2 diabetes in Korea. 1464-5491 2012;29:e290-296

32. Callaghan BC, Little AA, Feldman EL, Hughes RAC. Enhanced glucose control for preventing and treating diabetic neuropathy. 1469-493X 2012:CD007543

33. Dyck PJ. Detection, characterization, and staging of polyneuropathy: assessed in diabetics. Muscle & nerve 1988;11:21–32

34. Feldman EL, Stevens MJ, Thomas PK, Brown MB, Canal N, Greene DA. A practical two-step quantitative clinical and electrophysiological assessment for the diagnosis and staging of diabetic neuropathy. Diabetes care 1994;17:1281–9

35. Weintrob N, Amitay I, Lilos P, Shalitin S, Lazar L, Josefsberg Z. Bedside neuropathy disability score compared to quantitative sensory testing for measurement of diabetic

neuropathy in children, adolescents, and young adults with type 1 diabetes. Journal of diabetes and its complications 2007;21:13–9

36. Uddin Z, MacDermid JC. Quantitative Sensory Testing in Chronic Musculoskeletal Pain. Pain medicine (Malden, Mass.) 2016;17:1694–703

37. Yu Y. Gold Standard for Diagnosis of DPN. Frontiers in endocrinology 2021;12:719356

38. Dyck PJ, Lais A, Karnes JL, O'Brien P, Rizza R. Fiber loss is primary and multifocal in sural nerves in diabetic polyneuropathy. Annals of neurology 1986;19:425–39

39. Behse F, Buchthal F, Carlsen F. Nerve biopsy and conduction studies in diabetic neuropathy. Journal of neurology, neurosurgery, and psychiatry 1977;40:1072–82

40. Tesfaye S, Boulton AJM, Dyck PJ, Freeman R, Horowitz M, Kempler P et al. Diabetic neuropathies: update on definitions, diagnostic criteria, estimation of severity, and treatments. Diabetes care 2010;33:2285–93

41. Richard J-L, Reilhes L, Buvry S, Goletto M, Faillie J-L. Screening patients at risk for diabetic foot ulceration: a comparison between measurement of vibration perception threshold and 10-g monofilament test. International wound journal 2014;11:147–51

42. Weisman A, Bril V, Ngo M, Lovblom LE, Halpern EM, Orszag A et al. Identification and prediction of diabetic sensorimotor polyneuropathy using individual and simple combinations of nerve conduction study parameters. PloS one 2013;8:e58783

43. England JD, Gronseth GS, Franklin G, Miller RG, Asbury AK, Carter GT et al. Distal symmetric polyneuropathy: a definition for clinical research: report of the American Academy of Neurology, the American Association of Electrodiagnostic Medicine, and the American Academy of Physical Medicine and Rehabilitation. Neurology 2005;64:199–207

44. Breiner A, Lovblom LE, Perkins BA, Bril V. Does the prevailing hypothesis that small-fiber dysfunction precedes large-fiber dysfunction apply to type 1 diabetic patients? Diabetes care 2014;37:1418–24

45. Papanas N, Ziegler D. New vistas in the diagnosis of diabetic polyneuropathy. Endocrine 2014;47:690–8

46. Lee JA, Halpern EM, Lovblom LE, Yeung E, Bril V, Perkins BA. Reliability and validity of a point-of-care sural nerve conduction device for identification of diabetic neuropathy. PloS one 2014;9:e86515

47. Chatzikosma G, Pafili K, Demetriou M, Vadikolias K, Maltezos E, Papanas N. Evaluation of sural nerve automated nerve conduction study in the diagnosis of peripheral

neuropathy in patients with type 2 diabetes mellitus. Archives of medical science : AMS 2016;12:390–3

48. Ziegler D, Siekierka-Kleiser E, Meyer B, Schweers M. Validation of a novel screening device (NeuroQuick) for quantitative assessment of small nerve fiber dysfunction as an early feature of diabetic polyneuropathy. Diabetes care 2005;28:1169–74
49. Papanas N, Giassakis G, Papatheodorou K, Papazoglou D, Monastiriotis C, Christakidis D et al. Sensitivity and specificity of a new indicator test (Neuropad) for the diagnosis of peripheral neuropathy in type 2 diabetes patients: a comparison with clinical examination and nerve conduction study. Journal of diabetes and its complications 2007;21:353–8
50. Pritchard N, Edwards K, Russell AW, Perkins BA, Malik RA, Efron N. Corneal confocal microscopy predicts 4-year incident peripheral neuropathy in type 1 diabetes. Diabetes care 2015;38:671–5
51. Ziegler D, Papanas N, Zhivov A, Allgeier S, Winter K, Ziegler I et al. Early detection of nerve fiber loss by corneal confocal microscopy and skin biopsy in recently diagnosed type 2 diabetes. Diabetes 2014;63:2454–63
52. Mao F, Liu S, Qiao X, Zheng H, Xiong Q, Wen J et al. Sudoscan is an effective screening method for asymptomatic diabetic neuropathy in Chinese type 2 diabetes mellitus patients. Journal of diabetes investigation 2017;8:363–8
53. Selvarajah D, Cash T, Davies J, Sankar A, Rao G, Grieg M et al. SUDOSCAN: A Simple, Rapid, and Objective Method with Potential for Screening for Diabetic Peripheral Neuropathy. PloS one 2015;10:e0138224
54. Ponirakis G, Petropoulos IN, Fadavi H, Alam U, Asghar O, Marshall A et al. The diagnostic accuracy of Neuropad for assessing large and small fibre diabetic neuropathy. Diabetic medicine : a journal of the British Diabetic Association 2014;31:1673–80
55. Hertz P, Bril V, Orszag A, Ahmed A, Ng E, Nwe P et al. Reproducibility of in vivo corneal confocal microscopy as a novel screening test for early diabetic sensorimotor polyneuropathy. Diabetic medicine : a journal of the British Diabetic Association 2011;28:1253–60
56. Mayaudon H, Miloche P-O, Bauduceau B. A new simple method for assessing sudomotor function: relevance in type 2 diabetes. Diabetes & metabolism 2010;36:450–4
57. Gasparotti R, Padua L, Briani C, Lauria G. New technologies for the assessment of neuropathies. Nature reviews. Neurology 2017;13:203–16

58. Tolks D, Lampert C, Dadaczynski K, Maslon E, Paulus P, Sailer M. Spielerische Ansätze in Prävention und Gesundheitsförderung: Serious Games und Gamification. Bundesgesundheitsblatt, Gesundheitsforschung, Gesundheitsschutz 2020;63:698–707

59. Meloni W, Gruener W. *Gamification in 2012: Market Update Consumer and Enterprise Market Trends,* 2012. Available from https://www.docsity.com/pt/Gamification-in-2012/4799762/

60. Cotton V, Patel MS. Gamification Use and Design in Popular Health and Fitness Mobile Applications. American journal of health promotion : AJHP 2019;33:448–51

61. Patel MS, Small DS, Harrison JD, Fortunato MP, Oon AL, Rareshide CAL et al. Effectiveness of Behaviorally Designed Gamification Interventions With Social Incentives for Increasing Physical Activity Among Overweight and Obese Adults Across the United States: The STEP UP Randomized Clinical Trial. JAMA internal medicine 2019;179:1624–32

62. Kempf K, Martin S. Autonomous exercise game use improves metabolic control and quality of life in type 2 diabetes patients - a randomized controlled trial. BMC endocrine disorders 2013;13:57

63. Morrison S, Simmons R, Colberg SR, Parson HK, Vinik AI. Supervised Balance Training and Wii Fit-Based Exercises Lower Falls Risk in Older Adults With Type 2 Diabetes. Journal of the American Medical Directors Association 2018;19:185.e7-185.e13

64. Tong T, Chignell M, Tierney MC, Lee J. A Serious Game for Clinical Assessment of Cognitive Status: Validation Study. JMIR serious games 2016;4:e7

65. Zygouris S, Iliadou P, Lazarou E, Giakoumis D, Votis K, Alexiadis A et al. Detection of Mild Cognitive Impairment in an At-Risk Group of Older Adults: Can a Novel Self-Administered Serious Game-Based Screening Test Improve Diagnostic Accuracy? Journal of Alzheimer's disease : JAD 2020;78:405–12

66. Samuel A. Some Studies in Machine Learning Using the Game of Checkers. undefined 1959

67. Luxton DD (Ed.). *Artificial Intelligence in Behavioral and Mental Health Care.* San Diego, Academic Press, 2016

68. Bhavsar P, Safro I, Bouaynaya N, Polikar R, Dera D. Machine Learning in Transportation Data Analytics. In *Data Analytics for Intelligent Transportation Systems,* Elsevier, 2017, p. 283–307

69. Handelman GS, Kok HK, Chandra RV, Razavi AH, Lee MJ, Asadi H. eDoctor: machine learning and the future of medicine. Journal of internal medicine 2018;284:603–19

70. Amisha, Malik P, Pathania M, Rathaur VK. Overview of artificial intelligence in medicine. Journal of family medicine and primary care 2019;8:2328–31

71. Xia Y, Gao Q, Ye Q. Classification of gait rhythm signals between patients with neuro-degenerative diseases and normal subjects: Experiments with statistical features and different classification models. Biomedical Signal Processing and Control 2015;18:254–62

72. Nukala BT, Nakano T, Rodriguez A, Tsay J, Lopez J, Nguyen TQ et al. Real-Time Classification of Patients with Balance Disorders vs. Normal Subjects Using a Low-Cost Small Wireless Wearable Gait Sensor. Biosensors 2016;6

73. Araújo T, Aresta G, Castro E, Rouco J, Aguiar P, Eloy C et al. Classification of breast cancer histology images using Convolutional Neural Networks. PloS one 2017;12:e0177544

74. Li C, Zhi X, Ma J, Cui Z, Zhu Z, Zhang C et al. Performance comparison between Logistic regression, decision trees, and multilayer perceptron in predicting peripheral neuropathy in type 2 diabetes mellitus. Chinese medical journal 2012;125:851–7

75. Kazemi M, Moghimbeigi A, Kiani J, Mahjub H, Faradmal J. Diabetic peripheral neuropathy class prediction by multicategory support vector machine model: a cross-sectional study. Epidemiology and health 2016;38:e2016011

76. Ming A, Walter I, Alhajjar A, Leuckert M, Mertens PR. Study protocol for a randomized controlled trial to test for preventive effects of diabetic foot ulceration by telemedicine that includes sensor-equipped insoles combined with photo documentation. Trials 2019;20:521

77. Liu X, Xu Y, An M, Zeng Q. The risk factors for diabetic peripheral neuropathy: A meta-analysis. PloS one 2019;14:e0212574

78. Koo TK, Li MY. A Guideline of Selecting and Reporting Intraclass Correlation Coefficients for Reliability Research. Journal of chiropractic medicine 2016;15:155–63

79. Udovicic M, Bazdaric K, Bilic-Zulle L, Petrovecki M. What we need to know when calculating the coefficient of correlation? Biochem Med 2007:10–5

80. Holm S. A Simple Sequentially Rejective Multiple Test Procedure 1979

81. Hamel L (Ed.). *Knowledge Discovery with Support Vector Machines.* Hoboken, NJ, USA, John Wiley & Sons, Inc, 2009

82. Ma Y. *Support Vector Machines Applications.* 1st ed. Cham, Springer International Publishing AG, 2014. Available from https://ebookcentral.proquest.com/lib/kxp/detail.action?docID=1698112

83. Gandhi R. Support Vector Machine — Introduction to Machine Learning Algorithms, 2018. Available from https://towardsdatascience.com/support-vector-machine-introduction-to-machine-learning-algorithms-934a444fca47

84. Alexander EK, Kennedy GC, Baloch ZW, Cibas ES, Chudova D, Diggans J et al. Preoperative diagnosis of benign thyroid nodules with indeterminate cytology. The New England journal of medicine 2012;367:705–15

85. Claassen J, Doyle K, Matory A, Couch C, Burger KM, Velazquez A et al. Detection of Brain Activation in Unresponsive Patients with Acute Brain Injury. The New England journal of medicine 2019;380:2497–505

86. Sim J, Wright CC. The kappa statistic in reliability studies: use, interpretation, and sample size requirements. Physical therapy 2005;85:257–68

87. Landis JR, Koch GG. The measurement of observer agreement for categorical data. Biometrics 1977;33:159–74

88. Fawcett T. An introduction to ROC analysis. Pattern Recognition Letters 2006;27:861–74

89. Kuhn M. Variable Selection Using The caret Package. R 2010;2010

90. R Core Team. R: A Language and Environment for Statistical Computing. R Foundation for Statistical Computing 2020

91. Dubey VN, Dave JM, Beavis J, Coppini DV. Predicting Diabetic Neuropathy Risk Level Using Artificial Neural Network and Clinical Parameters of Subjects With Diabetes. Journal of diabetes science and technology 2020:1932296820965583

92. Corpin RRA, Guingab HAR, Manalo ANP, Sampana MLB, Abello ANA, dela Cruz AR et al. Prediction of Diabetic Peripheral Neuropathy (DPN) using Plantar Pressure Analysis and Learning Models. In *2019 IEEE 11th International Conference 11/29/2019,* p. 1–6

93. Dyck PJ, Sherman WR, Hallcher LM, Service FJ, O'Brien PC, Grina LA et al. Human diabetic endoneurial sorbitol, fructose, and myo-inositol related to sural nerve morphometry. Annals of neurology 1980;8:590–6

94. Yang Z, Chen R, Zhang Y, Huang Y, Hong T, Sun F et al. Scoring systems to screen for diabetic peripheral neuropathy. Cochrane Database of Systematic Reviews 2018

95. Shalitin S, Josefsberg Z, Lilos P, de-Vries L, Phillip M, Weintrob N. Bedside scoring procedure for the diagnosis of diabetic peripheral neuropathy in young patients with type

1 diabetes mellitus. Journal of pediatric endocrinology & metabolism : JPEM 2002;15:613–20

96. Dyck PJ, Davies JL, Litchy WJ, O'Brien PC. Longitudinal assessment of diabetic polyneuropathy using a composite score in the Rochester Diabetic Neuropathy Study cohort. Neurology 1997;49:229–39

97. Wei Y, Gu F, Zhang W. A two-phase iterative machine learning method in identifying mechanical biomarkers of peripheral neuropathy. Expert Systems with Applications 2021;169:114333

98. Apiquian R, Ulloa RE, Victoria G, Gómez-Tello MF, Morales E, García-Covarrubias L. Standardization and validity of Chefmania, a video game designed as a cognitive screening test for children. Humanit Soc Sci Commun 2020;7

99. Kelle S, Klemke R, Gruber M, Specht M. Standardization of Game Based Learning Design. In *Computational Science and Its Applications - ICCSA 2011.* Murgante B, Gervasi O, Iglesias A, Taniar D, Apduhan BO, Eds. Berlin, Heidelberg, Springer Berlin Heidelberg, 2011, p. 518–532 (Lecture Notes in Computer Science; vol. 6785)

100. Aboueid S, Liu RH, Desta BN, Chaurasia A, Ebrahim S. The Use of Artificially Intelligent Self-Diagnosing Digital Platforms by the General Public: Scoping Review. JMIR medical informatics 2019;7:e13445

101. Collingwood J. Artificial Intelligence in Medical Diagnosis, 2021. Available from https://sma.org/ai-in-medical-diagnosis/

102. Domingues MF, Alberto N, Leitao CSJ, Tavares C, Rocon de Lima E, Radwan A et al. Insole Optical Fiber Sensor Architecture for Remote Gait Analysis—An e-Health Solution. IEEE Internet Things J. 2019;6:207–14

103. Gschwind YJ, Schoene D, Lord SR, Ejupi A, Valenzuela T, Aal K et al. The effect of sensor-based exercise at home on functional performance associated with fall risk in older people - a comparison of two exergame interventions. European review of aging and physical activity : official journal of the European Group for Research into Elderly and Physical Activity 2015;12:11

104. Ayena JC, Zaibi H, Otis MJ-D, Menelas B-AJ. Home-Based Risk of Falling Assessment Test Using a Closed-Loop Balance Model. IEEE transactions on neural systems and rehabilitation engineering : a publication of the IEEE Engineering in Medicine and Biology Society 2016;24:1351–62

105. Abbott CA, Chatwin KE, Foden P, Hasan AN, Sange C, Rajbhandari SM et al. Innovative intelligent insole system reduces diabetic foot ulcer recurrence at plantar sites: a prospective, randomised, proof-of-concept study. The Lancet Digital Health 2019;1:e308-e318

106. Azmi S, Jeziorska M, Ferdousi M, Petropoulos IN, Ponirakis G, Marshall A et al. Early nerve fibre regeneration in individuals with type 1 diabetes after simultaneous pancreas and kidney transplantation. Diabetologia 2019;62:1478–87

107. Smith AG, Russell J, Feldman EL, Goldstein J, Peltier A, Smith S et al. Lifestyle intervention for pre-diabetic neuropathy. Diabetes care 2006;29:1294–9

108. Singh AK, Kumar A, Karmakar D, Jha RK. Association of B12 deficiency and clinical neuropathy with metformin use in type 2 diabetes patients. Journal of postgraduate medicine 2013;59:253–7

109. Romeo-Guitart D, Forés J, Herrando-Grabulosa M, Valls R, Leiva-Rodríguez T, Galea E et al. Neuroprotective Drug for Nerve Trauma Revealed Using Artificial Intelligence. Scientific reports 2018;8:1879

110. *2009 9th International Conference*

111. Ziegler D, Landgraf R, Lobmann R, Reiners K, Rett K, Schnell O et al. Painful and painless neuropathies are distinct and largely undiagnosed entities in subjects participating in an educational initiative (PROTECT study). 1872-8227 2018;139:147–54

112. Bansal D, Gudala K, Muthyala H, Esam HP, Nayakallu R, Bhansali A. Prevalence and risk factors of development of peripheral diabetic neuropathy in type 2 diabetes mellitus in a tertiary care setting. Journal of diabetes investigation 2014;5:714–21

113. Li L, Chen J, Wang J, Cai D. Prevalence and risk factors of diabetic peripheral neuropathy in Type 2 diabetes mellitus patients with overweight/obese in Guangdong province, China. Primary care diabetes 2015;9:191–5

114. Johnstone IM, Titterington DM. Statistical challenges of high-dimensional data. Philosophical transactions. Series A, Mathematical, physical, and engineering sciences 2009;367:4237–53

115. Vabalas A, Gowen E, Poliakoff E, Casson AJ. Machine learning algorithm validation with a limited sample size. PloS one 2019;14:e0224365

7. Acknowledgements

Die Danksagung ist in der Version aus Datenschutzgründen nicht enthalten.

8. Erklärung

Ich erkläre, dass ich die der Medizinischen Fakultät der Otto-von-Guericke-Universität zur

Promotion eingereichte Dissertation mit dem Titel:

“Game-based assessment of peripheral neuropathy in patients with diabetes by combining sensor-equipped insoles with video games and machine learning algorithms”

in der Universitätsklinik für Nieren- und Hochdruckkrankheiten, Diabetologie und Endokrinologie der

Otto-von-Guericke-Universität Magdeburg

ohne sonstige Hilfe durchgeführt und bei der Abfassung der Dissertation keine anderen als im Methodenteil aufgeführten Hilfsmittel benutzt habe.

Bei der Abfassung der Dissertation sind Rechte Dritter nicht verletzt worden.

Ich habe diese Dissertation bisher an keiner in- oder ausländischen Hochschule zur Promotion eingereicht. Ich übertrage der Medizinischen Fakultät das Recht, weitere Kopien meiner Dissertation herzustellen und zu vertreiben.

Magdeburg, den 06.07.2023

Unterschrift

9. Curriculum Vitae

Der Lebenslauf ist in der Version aus Datenschutzgründen nicht enthalten.

Magdeburg, den 06.07.2023

Unterschrift

10. Publications

A patent application related to this work was submitted to the European Patent Office on June 1, 2022, entitled "Method and device for nerve function assessment" (application number: EP22176811.2).

Parts of this work has been published in the following manuscripts:

- Ming A, Walter I, Alhajjar A, Leuckert M, Mertens PR. Study protocol for a randomized controlled trial to test for preventive effects of diabetic foot ulceration by telemedicine that includes sensor-equipped insoles combined with photo documentation. Trials. 2019;20(1):521.

- Niemann U*, Spiliopoulou M*, Malanowski J*, Kellersmann J, Szczepanski T, Klose S, Dedonaki E, Walter I, Ming A*, Mertens PR. Plantar temperatures in stance position: A comparative study with healthy volunteers and diabetes patients diagnosed with sensoric neuropathy. EBioMedicine. 2020;54:102712. (*divided first authorship)

- Pfannkuche A, Alhajjar A, Ming A, Walter I, Piehler C, Mertens PR. Prevalence and risk factors of diabetic peripheral neuropathy in a diabetics cohort: Register initiative “diabetes and nerves”. Endocrine and Metabolic Science. 2020;1(1):100053.

- Niemann U, Spiliopoulou M, Szczepanski T, Samland F, Grützner J, Senk D, Ming A, Kellersmann J, Malanowski J, Klose S, Mertens PR. Comparative clustering of plantar pressure distributions in diabetics with polyneuropathy may be applied to reveal inappropriate biomechanical stress. PLOS ONE. 2016;11(8):e0161326.

- Alhajjar A, Ming A, Clemens V, Mertens PR. Potenzielles Frühwarnsystem für diabetische Fußschädigungen durch sensorbestückte Einlegesohlen (Early Warning System for Diabetic Foot Damage with Sensor-Equipped Insoles). Diabetischer Fuß. 2020.

- Ravindran R, Niemann U, Klose S, Walter I, Ming A, Mertens PR, Spiliopoulou M. Transformation of Temperature Timeseries into Features that Characterize Patients with Diabetic Autonomic Nerve Disorder. In: 2018 IEEE 31st International Symposium on Computer-Based Medical Systems (CBMS). 2018;65-70.

- Niemann U, Spiliopoulou M, Samland F, Szczepanski T, Grützner J, Ming A, Kellersmann J, Malanowski J, Klose S, Mertens PR. Learning Pressure Patterns for Patients with Diabetic Foot Syndrome. In: 2016 IEEE 29th International Symposium on Computer-Based Medical Systems (CBMS). 2016;54-59.

The comprehensive results of the further work have now been compiled into another manuscript and submitted.

11. Supplementary Appendix

11.1. Approval of the Ethics Committee

UNIVERSITÄTSKLINIKUM MAGDEBURG A.ö.R. OTTO VON GUERICKE UNIVERSITÄT MAGDEBURG MEDIZINISCHE FAKULTÄT

Ethik-Kommission der Otto-von-Guericke-Universität an der Medizinischen Fakultät und am Universitätsklinikum Magdeburg A.ö.R.

Univ.-Prof. Dr. med. Christof Huth
Vorsitzender

Dr. med. Norbert Beck
Geschäftsführer

Telefon: +49 391 67-14314
Telefax: +49 391 67-14354
elektr.Fax: +49 391 67-290185
eMail: ethikkommission@ovgu.de

Ethik-Kommission, Medizinische Fakultat / Universitatsklinikum, Leipziger Str. 44 Haus 28, 39120 Magdeburg

Herrn Prof. Dr. med. P. Mertens
Medizinische Fakultät
Universitätsklinik für Nieren- und Hochdruckkrankheiten
Universitätsklinikum Magdeburg A.ö.R.
Haus 60b, Leipziger Str. 44
39120 Magdeburg

Datum
13.03.2017

Unser Zeichen: **28/17**

Gamification bei Patienten mit und ohne sensomotorische Neuropathie: Diagnostik mittels einer Einlegesohle mit Sensoren für Druck und Temperatur in Verbindung mit einer mobilen App

Sehr geehrter Herr Prof. Dr. Mertens,
sehr geehrte Kolleginnen und Kollegen,

die Ethik-Kommission der Otto-von-Guericke-Universität an der Medizinischen Fakultät und am Universitätsklinikum Magdeburg hat die übergebenen Unterlagen zur o. g. Studie überprüft, in der letzten Kommissionssitzung eingehend erörtert und ist zu der Auffassung gekommen, dass gegen die Durchführung keine ethischen Bedenken bestehen.
Diese **zustimmende Bewertung** ergeht unter dem Vorbehalt gleichbleibender Gegebenheiten.

Die Verantwortlichkeit des jeweiligen Prüfwissenschaftlers / behandelnden Prüfarztes bleibt in vollem Umfang erhalten und wird durch diese Entscheidung nicht berührt. Alle zivil- oder haftungsrechtlichen Folgen, die sich ergeben könnten, verbleiben uneingeschränkt beim Projektleiter und seinen Mitarbeitern.

Beim Monitoring sind die Bestimmungen des Bundes- und Landesdatenschutzgesetzes sowie die sich aus der ärztlichen Schweigepflicht ergebenden Einschränkungen zu beachten, was eine Aushändigung kompletter Patientenakten zum Monitoring ausschließt.
Ein Monitoring personen- und studienbezogener Daten wird dadurch nicht beeinträchtigt.

Um die Übersendung von studienbezogenen Jahresberichten / Abschlussberichten / Publikationen wird unter Nennung unserer Registraturnummer gebeten.

Mit freundlichen Grüßen

(i. A. Dr. med. Norbert Beck, Geschäftsführer)
Prof. Dr. med. C. Huth
Vorsitzender der Ethik-Kommission

Ethik-Kommission
der Otto-von-Guericke-Universität an der Medizinischen Fakultät
und am Universitätsklinikum Magdeburg A.ö.R.
Vorsitzender: Univ.-Prof. Dr. med. C. Huth

Anlage zum Votum der Studie 28/17 vom 13.03.2017

Zum Zeitpunkt der Bewertung der vorstehenden Studie waren folgende Damen und Herren Mitglied der Ethik-Kommission der Otto-von-Guericke-Universität an der Medizinischen Fakultät und am Universitätsklinikum Magdeburg:

Herr Prof. Dr. med. Norbert Bannert	Medizinische Fakultät / Universitätsklinikum, Pädiater
Frau Prof. Dr. phil. Eva Brinkschulte	Medizinische Fakultät / Universitätsklinikum, Bereich Geschichte, Ethik und Theorie der Medizin
Herr Prof. Dr.-Ing. Rolf Findeisen	Fakultät für Elektrotechnik und Informationstechnik, Institut für Automatisierungstechnik
Herr Prof. Dr. med. Christof Huth	Medizinische Fakultät / Universitätsklinikum, Universitätsklinik für Herz- und Thoraxchirurgie
Frau Assessorin Ute Klanten	Medizinische Fakultät / Universitätsklinikum, Stabsstelle Recht
Herr Prof. Dr. rer. nat. Siegfried Kropf	Medizinische Fakultät / Universitätsklinikum, Mathematiker, Biometriker
Herr Dr. med. Werner Kuchheuser	Medizinische Fakultät / Universitätsklinikum, Institut für Rechtsmedizin
Herr Prof. Dr. med. Frank Peter Meyer	Medizinische Fakultät / Universitätsklinikum, Klinischer Pharmakologe
Herr Prof. Dr. med. Jens Schreiber	Medizinische Fakultät / Universitätsklinikum, Universitätsklinik für Pneumologie
Herr Prof. Dr.-Ing. Klaus Tönnies	Fakultät für Informatik, Institut für Simulation und Graphik, AG Bildverarbeitung/Bildverstehen

Mitglieder der Ethik-Kommission, die in eine Studie eingebunden sind, haben für die Votierung der betreffenden Studie kein Stimmrecht.

Die Ethik-Kommission der Otto-von-Guericke-Universität an der Medizinischen Fakultät und am Universitätsklinikum Magdeburg ist unter Beachtung entsprechender internationaler Richtlinien (ICH, GCP) und nationaler Richtlinien (AMG, GCP-V, MPG, MPKPV) tätig, nach Landesrecht (Hochschulmedizingesetz des Landes Sachsen-Anhalt § 1 Abs. 4, Verordnung über Ethik-Kommissionen zur Bewertung klinischer Prüfungen von Arzneimitteln - Ethik-Kom-VO LSA - i. d. akt. Fassung) legitimiert. Weiterhin besteht eine Registrierung der Ethik-Kommission beim Bundesamt für Strahlenschutz nach § 28g Röntgenverordnung (EK-043/R) und § 92 Strahlenschutzverordnung (EK-046/S) sowie beim Office for Human Research Protections, reg. no. IRB00006099, Rockville, MD, U.S.A.

Dr. med. Norbert Beck
Geschäftsführer der Ethik-Kommission

UNIVERSITÄTSKLINIKUM
MAGDEBURG A.ö.R.

OTTO VON GUERICKE
UNIVERSITÄT
MAGDEBURG

TOP
2021
FOCUS

Ethik-Kommission, Medizinische Fakultät / Universitätsklinikum, Leipziger Str. 44 Haus 28, 39120 Magdeburg

Herrn Prof. Dr. med. P. Mertens
Universitätsklinik für Nieren- und Hochdruckkrankheiten,
Diabetologie und Endokrinologie
Universitätsklinikum Magdeburg A.ö.R.
Haus 60b, Leipziger Str. 44
39120 Magdeburg

Ethik-Kommission der
Otto-von-Guericke-
Universität an der
Medizinischen Fakultät un
am Universitätsklinikum
Magdeburg A.ö.R.

Univ.-Prof. Dr. med. Christof Huth
Vorsitzender

Dr. med. Norbert Beck
Geschäftsführer

Telefon: +49 391 67-14314
Telefax: +49 391 67-14354
elektr.Fax: +49 391 67-290185
eMail: ethikkommission@ovgu.de

Datum
14.10.2021

Unser Zeichen: **28/17**

Gamification bei Patienten mit und ohne sensomotorische Neuropathie: Diagnostik mittels einer Einlegesohle mit Sensoren für Druck und Temperatur in Verbindung mit einer mobilen App

Sehr geehrter Herr Prof. Mertens,
sehr geehrte Kolleginnen und Kollegen,

zur vorstehend genannte Studie ist bei uns am 31.08.2021 / 08.09.2021 ein Amendment eingegangen. Nach Umlauf zwischen den Kommissionsmitgliedern und Beantwortung der Fragen kann dem Amendment zugestimmt werden.

Die zustimmende Bewertung – positives Votum – vom 13.03.2017 bleibt gültig.

Mit freundlichem Gruß

Prof. Dr. med. C. Huth
Vorsitzender der Ethik-Kommission

11.2. Patient information and consent forms

UNIVERSITÄTSKLINIKUM MAGDEBURG A.ö.R.

Zentrum Innere Medizin

Universitätsklinik für Nieren- und Hochdruckkrankheiten
Diabetologie und Endokrinologie

Direktor: Univ.-Prof. Dr. med. Peter R. Mertens

Adresse: Otto-von-Guericke-Universität Magdeburg, Leipziger Str. 44, 39120 Magdeburg, Tel 0391-6713236

http://www.med.uni-magdeburg.de/
***Klinikdirektor*:**
Univ.-Prof. Dr. med. Peter R. Mertens
Tel.: 0391/67-13236
nephrologie@med.ovgu.de
Sekretariat:
Claudia Kluge
Tel.: 0391/67-13236
Fax: 0391/67-15440
Claudia.kluge@med.ovgu.de

Name des Prüfarztes…….....

Tel. Nr. …….

Patienteninformation und Einwilligungserklärung zur Teilnahme an der klinischen Studie: „Gamification bei Patienten mit und ohne sensomotorische Neuropathie: Diagnostik mittels einer Einlegesohle mit Sensoren für Druck und Temperatur in Verbindung mit einer mobilen App“

Sehr geehrte Patientin, sehr geehrter Patient,

Wir laden Sie ein, an der oben genannten klinischen Studie teilzunehmen. Die Aufklärung darüber erfolgt in einem ausführlichen ärztlichen Gespräch. Ihre Teilnahme an dieser klinischen Studie erfolgt freiwillig. Sie können jederzeit ohne Angabe von Gründen Ihre Teilnahme an der Studie beenden. Die Ablehnung der Teilnahme oder ein vorzeitiges Ausscheiden aus dieser Studie hat keine nachteiligen Folgen für Ihre medizinische Betreuung.

Diese klinische Prüfung soll an gesunden Probanden, Diabetikern mit Nervenschäden oder ohne Nervenschäden und an Probanden mit einem sogenannten Metabolischen Syndrom durchgeführt werden.

Klinische Prüfungen sind notwendig, um verlässliche neue medizinische Forschungsergebnisse zu gewinnen. Unverzichtbare Voraussetzung für die Durchführung

einer klinischen Prüfung ist jedoch, dass Sie Ihr Einverständnis zur Teilnahme an dieser klinischen Prüfung schriftlich erklären. Bitte lesen Sie den nachfolgenden Text sorgfältig durch. Ihr Studienarzt wird mit Ihnen auch direkt über diese klinische Prüfung sprechen. Bitte fragen Sie Ihren Prüfarzt, wenn Sie etwas nicht verstehen oder wenn Sie zusätzlich etwas wissen möchten.

Bitte unterschreiben Sie die Einwilligungserklärung nur

- wenn Sie Art und Ablauf der klinischen Prüfung vollständig verstanden haben,

- wenn Sie bereit sind der Teilnahme zuzustimmen und

- wenn Sie sich über Ihre Rechte als Teilnehmer an dieser klinischen Prüfung im

Klaren sind.

Zu dieser klinischen Prüfung sowie zur Patienteninformation und Einwilligungserklärung wurde von der zuständigen Ethikkommission eine befürwortende Stellungnahme abgegeben.

1. Was ist der Zweck der klinischen Prüfung?

In dem geplanten Projekt soll eine neue Untersuchungsmethode für die Nervenfunktion in den Füßen bei Probanden (vor allem Diabetiker) mit und ohne Nervenschäden erprobt werden.

Hierbei wird der Ansatz der Gamification (deutsch: Spielifizierung) verwendet, um spielerisch Daten zu sammeln.

Dabei wird die „intelligente Einlegesohle“ verwendet, welche über Druck und Temperatursensoren verfügt und *via* Bluetooth mit einem Android-Tablet verbunden ist. Auf diese Weise werden Sie vier Spiele absolvieren, die mit den Füßen gesteuert werden.

Ergänzend zur bestehenden Untersuchungen können durch die Ergebnisse der in dieser Studie durchgeführten Tests die Leistungsfähigkeit des Fußes und die Nervenfunktion möglicherweise genauer differenziert werden.

Es werden Messungen erfolgen, die sowohl Auskünfte über die Reaktionsgeschwindigkeit und die Druckausübung als auch über die Links-Rechts-Koordination der Füße, die Feinmotorik und das Lernvermögen liefern sollen. Außerdem werden unterschiedliche Fußbereiche (Vorfuß und Ferse) bei den Tests beansprucht. Dadurch kann eine genauere Untersuchung und Analyse der Füße erfolgen. Weiterhin wollen wir ihre Merkfähigkeit und kognitive Leistungsfähigkeit mit einem Fragebogen und kurzen Aufgaben erfassen. Dieses Testsystem ist an einer großen Zahl von Probanden getestet worden und soll einen Anhalt über die Merkfähigkeit und Gedächtnisfunktionen geben (Montreal Cognitive Assessment Test, MoCA).

Durch eine begleitende Untersuchung von ihrem Blut und Urin wollen wir erfassen, ob es Änderungen in der Immunzellzusammensetzung und Aktivierung gibt. Desweiteren wollen wir herausfinden, ob in Ihrem Blut eine veränderte Zusammensetzung besteht, die auf eine Einschränkung der kognitiven Leistungsfähigkeit hinweist.

Die aus dem Projekt gewonnenen Daten werden pseudonymisiert ausgewertet, um neue Erkenntnisse hinsichtlich krankheitsspezifischer Unterschiede zu erhalten. Hierzu werden wir eine Reihe von gesunden Probanden ebenso rekrutieren, um eine Vergleichbarkeit herzustellen. Die Ergebnisse der Gamification-Anwendung werden ihnen unmittelbar nach der Teilnahme übermittelt. Die weiteren Ergebnisse werden durch uns derart ermittelt, dass eine Zuordnung zu einzelnen Probanden nicht mehr möglich ist. Daher werden wir Ihnen diese Ergebnisse nicht übermitteln können.

2. Welche anderen Diagnosemöglichkeiten für Nervenschäden an den Füßen gibt es?

Im klinischen Alltag wird die umfassende Untersuchung des Fußes wie folgt durchgeführt:

Zuerst wird eine Anamnese erhoben. Dabei werden Informationen zu Diabetes mellitus, Nebenerkrankungen (wie z.B. periphere arterielle Verschlusskrankheiten), Schlaganfällen, Gefühlsstörungen sowie Risikofaktoren gesammelt.

Symptome wie Taubheitsgefühle, sensible Reizerscheinungen, Schmerzen und Krämpfe werden erfasst. Zusätzlich erfolgt eine neurologische Untersuchung durch den Arzt, die den Status der Reflexe, des Vibrationsempfindens (Stimmgabel), des Berührungs- und Druckempfindens erhebt.

3. Wie läuft die klinische Prüfung ab?

Es wird ein Fragebogen erhoben, bei dem die persönlichen Informationen (Name, Geburtsdatum, aktueller Beruf etc.), die medizinischen Hintergrundinformationen zu Vorerkrankungen und vor allem einer bestehenden Zuckerkrankheit (Diabetes mellitus; falls eine Diagnose vorliegt: Typ, Therapie, Begleitschäden etc., die diabetischen Nervenschäden (Gefühlsstörungen, Beschwerden, Bewegungseinschränkung im täglichen Leben), autonome diabetische Neuropathie (Herzrhythmusstörungen, gastrointestinale Beschwerden) und bedeutsame Nebenerkrankungen (Schlaganfall, M. Parkinson, Operationen an der Wirbelsäule etc.), Metabolisches Syndrom (Bluthochdruck, Gicht), App-Erfahrung, Aktivität (Sportarten, Händigkeit, Füßigkeit), Erfragung von historischen HbA1c- sowie Nüchternblutzuckerwerten erfragt.

Desweiteren folgt eine körperliche Untersuchung mit Messung des Taillenumfangs. Zudem wird die Untersuchung der unteren Extremität erfolgen. Diese Untersuchung beinhaltet: Die

Testung des Achillessehnen-Reflex, die Fußpulse, Empfindung von Vibration einer Stimmgabel, die Empfindung von einem dünnen Faden sowie Temperaturunterschieden (kalt, warm).

Eine Blutdruckmessung an den Unterschenkeln und Armen erfolgt. Im Anschluss werden Sie gebeten auf der Stelle einige Schritte zu gehen, zu Beginn mit offenen Augen und im Anschluss mit geschlossenen Augen. Ihre Sehfähigkeit wird mit einem Sehtest untersucht.

Eine Blutentnahme von 10 ml EDTA-Blut für eine FACS Analyse (zur Aktivitätsbestimmung von Immunzellen, insbesondere Monozyten und Granulozyten, die bei der Entstehung einer Polyneuropathie von Bedeutung sein kann). Zudem soll 5 ml Blut für die Bestimmung des aktuellen HbA1c-Wertes, von Kreatinin und Harnstoff zur Bestimmung der Nierenwerte, und die Elektrolyte (Kalium und Natrium) erfolgen. Die Probanden sollen zudem eine Urin-Probe zur Ermittlung der Proteinurie abgeben. Aus der gewonnenen Blutprobe sollen Entzündungsbotenstoffe des Körpers bestimmt werden und eine Untersuchung auf demenzielle Erkrankungen erfolgen.

Vorstellung der Gamification Spiele

Vier „Spiele“ wurden für die Studie konzipiert, welche auf einem Android-Tablet installiert sind: Ein „Belastungsspiel“, ein „Apfelfangspiel“, ein „Ballonfahrtspiel“ und ein „Sprungspiel“.

Diese Spiele können durch die Verbindung mit der „intelligenten Einlegesohle“ mit den Füßen gespielt werden.

In dem **Belastungsspiel** werden die Füße in jeweils 2 Quadranten (Vorfuß und Ferse) unterschieden. Es gibt zwei Druckbereiche (leicht und mittel), welche durch zwei Farben visuell kodiert sind. Ein leichter Druckbereich entspricht der Farbe Grün und ein mittlerer Druck der gelben Farbe. Sie sollen mit Ihren Füßen den Druckbereich einstellen, welcher auf dem Bildschirm erscheint und einige Sekunden halten. Ziel des Spiels ist es, so schnell wie möglich den richtigen Quadranten im angezeigten Druckbereich einzustellen.

In dem **Apfelfangspiel** geht es darum, vom Baum fallende Äpfel mit einem rollenden Wagen zu sammeln. Die Äpfel fallen nacheinander nach einer definierten Zeit auf den Boden. Ein Wagen wird mit den Füßen, welche die Sohle bedienen, gesteuert und kann unter die fallenden Äpfel gelenkt werden. Eine Druckausübung des linken Fußes auf die Sohle bewirkt, dass der Wagen sich nach links bewegt, eine Druckausübung auf die rechte Sohle steuert den Wagen nach rechts. Um die Äpfel zu sammeln muss der angezeigte Druck gehalten werden, damit der Wagen am gewünschten Ort stehen bleibt. Wird kein Druck ausgeübt, fährt der Apfelwagen automatisch in die Mitte des Bildschirms zurück. Ziel ist es, so viele Äpfel wie möglich einzusammeln.

Belastungsspiel

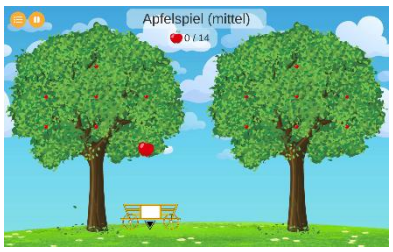

Apfelfangspiel

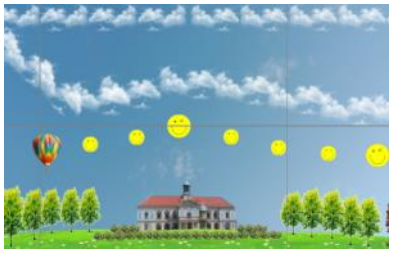

Ballonfahrtspiel

Sprungspiel

Abbildung 1. Muster alle vier Spiele in Rahmen der Gamification Studie

In dem **Ballonfahrtspiel** steuern Sie einen Heißluftballon, welcher über verschiedene Stadtlandschaften fliegt. Der Ballon fliegt automatisch mit einer konstanten Geschwindigkeit vorwärts. Auf der Flugbahn tauchen diverse Hindernisse, wie zum Beispiel Gebäude oder Wolken auf, denen Sie ausweichen müssen, um ins Ziel zu gelangen. Während des Fluges tauchen Smileys auf, die Sie einsammeln sollten, um einen hohen Score zu erreichen. Der Test kann wahlweise mit dem rechten oder mit dem linken Vorfuß durchgeführt werden. Bei Druckausübung des gewählten Vorfußes wird der Ballon aufsteigen. Wird kein oder wenig Druck ausgeübt, verliert der Ballon an Höhe und sinkt ab. Gelingt es Ihnen für einen bestimmten Zeitraum fehlerfrei zu fliegen, so wird der Schwierigkeitsgrad automatisch um eine Stufe erhöht. Insgesamt gibt es drei Stufen, welche durch eine erhöhte Fluggeschwindigkeit des Ballons definiert sind. Sollten Sie mit einem Hindernis kollidieren, wird die Geschwindigkeit wieder zum Ausgangswert herabgesetzt. Kommt es zu einer Kollision mit einem Hindernis, haben Sie 5 Sekunden Zeit, um den Fehler zu korrigieren. Sofern dies nicht gelingt, wird der Parkour neu gestartet und Sie starten von vorne. Insgesamt sind drei Kollisionen erlaubt, bevor der Parkour neu gestartet wird. Des Weiteren wird die optimale Flugroute bzw. Ideallinie durch Smileys angedeutet, die Sie einsammeln sollen, um eine hohe Punktzahl zu erreichen.

Im **Sprungspiel** steuert der Spieler einen Hahn namens "Gockel" (eine 3D-Spielfigur), um nacheinander durch mehrere Inseln zu springen, bis er seine Heimat erreicht. Die Sprungweite hängt von der Zeitdauer ab, die der Spieler den erforderlichen Druck (über 20% des gesamten Druckbereichs) auf seinen linken Vorderfuß (Sprung nach links), rechten Vorderfuß (Sprung

nach rechts) oder auf beide (Sprung nach vorne) einstellt. Wendet der Spieler den Druck zu lange oder zu kurz an, fällt der "Gockel" ins Wasser. Dann wird das Spiel wiederholt von der letzten Insel.

4. Was ist die Gaming-Einlegesohle?

In der Studie wurden drei Arten von Gaming-Einlegesohlen in Pantoletten zur Erfassung der Druck-, Temperatur-, Beschleunigung, Gyroskope- (Objektrotationen), und Kompass-Daten (Objektrichtungen) verwendet. Sie liefern qualitativ hochwertige RAW-Daten in Echtzeit und/oder zur Nachbearbeitung über Bluetooth.

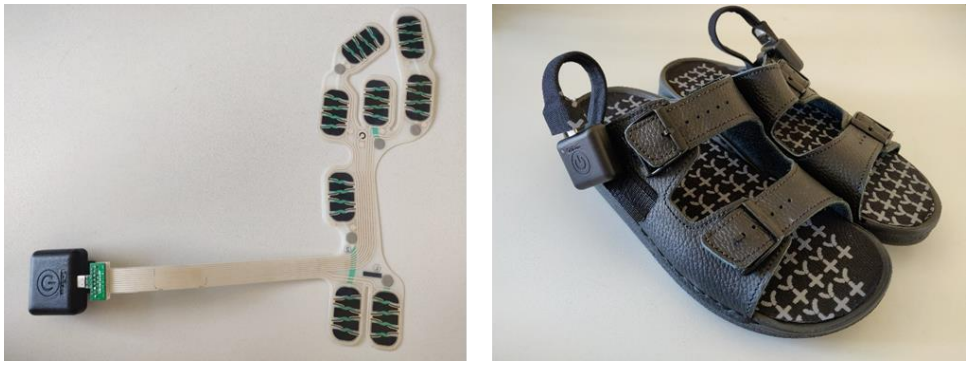

Abbildung 2. Ein Paar Gaming-Einlegesohlen

5. Worin liegt der Nutzen einer Teilnahme an der Klinischen Prüfung?

Es ist nicht zu erwarten, dass Sie aus Ihrer Teilnahme an dieser klinischen Prüfung gesundheitlichen Nutzen ziehen werden.

Die in dieser Studie gesammelten Daten könnten aufschlussreich in Bezug auf die Diagnostik von Nervenschäden in den Füßen sein und in Zukunft zu einer Verbesserung der Untersuchung für den klinischen Alltag beitragen.

6. Gibt es Risiken, Beschwerden und Begleiterscheinungen?

Die Anwendung der intelligenten sensorbestückten Einlegesohle in Verbindung mit den App-Tests ist prinzipiell gefahrlos. Die Entstehung von scharfen Kanten wird durch die Herstellung über den Schuhmacher ausgeschlossen.

7. Wer wird für die klinische Prüfung gesucht?

- gesunde Probanden
- Probanden mit Übergewicht, Fettstoffwechselstörungen, Bluthochdruck oder Vorstufen einer Zuckerkrankheit
- Diabetiker ohne Nervenschäden
- Diabetiker mit Nervenschäden
- Patienten mit Schwindelsymptomatik

8. Wann wird die klinische Prüfung vorzeitig beendet?

Sie können jederzeit auch ohne Angabe von Gründen Ihre Teilnahmebereitschaft widerrufen und aus der klinischen Prüfung ausscheiden, ohne dass Ihnen dadurch irgendwelche Nachteile für Ihre weitere medizinische Betreuung entstehen.

9. In welcher Weise werden die im Rahmen dieser klinischen Prüfung gesammelten Daten verwendet?

Nachdem Sie die Einwilligungserklärung unterzeichnet haben, wird Ihnen ein Pseudoynym (dient zur Verschleierung Ihrer Identität) zugewiesen. Sobald Sie ein Pseudonym haben, können Sie die Spiele starten. Die Daten werden zunächst auf dem Tablet gespeichert. Das Spielergebnis umfasst neben dem eigentlichen Spielerfolg unter anderem auch Sensordaten, Reaktionszeiten und Schwierigkeitsgrade. Die entstandene Datei, welche nur pseudonymisierte Daten enthält, wird auf einem Rechner der Uniklinik importiert und in eine Datenbank, in welcher alle Spiele pseudonymisierter Probanden gesammelt werden, geschrieben. Weiterhin gibt es eine separate Datenbank, welche Ihre persönlichen Daten sowie die Pseudonymzuordnung enthält. Zu dieser Datenbank hat ausschließlich das betreuende Studienpersonal Zugriff, welches zur Verschwiegenheit verpflichtet ist. Es gibt sowohl von den Pseudonymen als auch den Spieledaten ein Backup-System (Datensicherungs-System), sodass ein großer technischer Schaden nicht zum Verlust der Daten führen kann. Die Backup-Systeme sind ebenfalls zugriffsgeschützt. Die Datenbanken sind gegen externe Angriffe geschützt.

Sie können jederzeit Auskunft über Ihre gespeicherten Daten verlangen. Sie haben das Recht, fehlerhafte Daten berichtigen zu lassen. Sie haben das Recht zu jeder Zeit die Einwilligung zur Verarbeitung Ihrer personenbezogenen Daten zu widerrufen oder Daten löschen zu lassen, soweit nicht gesetzliche Bestimmungen dem entgegenstehen.

10. Entstehen für die Teilnehmer Kosten? Gibt es einen Kostenersatz oder eine Vergütung?

Durch Ihre Teilnahme an dieser klinischen Prüfung entstehen für Sie keine zusätzlichen Kosten. Eine Vergütung für die Teilnahme an der Studie ist nicht vorgesehen.

11. Möglichkeit zur Diskussion weiterer Fragen

Für weitere Fragen im Zusammenhang mit dieser klinischen Testung stehen Ihnen Ihr Prüfarzt und seine Mitarbeiter gern zur Verfügung. Auch Fragen, die Ihre Rechte als Patient und Teilnehmer an dieser klinischen Testung betreffen, werden Ihnen gerne beantwortet.

Adressen und Telefonnummern Ihrer Ansprechpartner:

Ahmad Alhajjar (Studienarzt)

Saskia Häberer (Studienärztin)

Claudia Piehler (Studienassistentin)

Antao Ming (Wissenschaftlicher Mitarbeiter)

Prof. Dr. med. Peter R. Mertens **(**Studienleiter)

Klinik für Nieren- und Hochdruckkrankheiten, Diabetologie und Endokrinologie

Telefon 0391-6721745

Telefax 0391-6715440

Prüfung erfolgt freiwillig und kann jederzeit widerrufen werden.

Bitte lesen Sie die gesamte Patienteninformation sorgfältig durch!

12. Einwilligungserklärung

Ich wurde durch ……. ausführlich über die klinische Prüfung mit dem Titel „***Gamification bei Patienten mit und ohne sensomotorische Neuropathie: Diagnostik mittels einer Einlegesohle mit Sensoren für Druck und Temperatur in Verbindung mit einer mobilen App***“ aufgeklärt. Ich hatte die Gelegenheit und ausreichend Zeit, Fragen zu stellen. Diese wurden zufriedenstellend beantwortet. Zusätzlich zu der schriftlichen Information wurden folgende Punkte besprochen:

Ich wurde darauf hingewiesen, dass meine Teilnahme an der klinischen Prüfung freiwillig ist und dass ich das Recht habe, diese jederzeit ohne Angabe von Gründen zu beenden, ohne dass dadurch Nachteile für mich entstehen.

Ich wurde ausführlich – mündlich und schriftlich – über das Ziel und den Verlauf der klinischen Prüfung, sowie über die Freiwilligkeit der Teilnahme aufgeklärt und mir wurde zugesichert, dass diese Aufklärung vollständig war.

Ich habe die schriftliche Patienteninformation zur o. g. klinischen Prüfung erhalten, und ich werde nach meiner Unterschrift eine Kopie meiner unterschriebenen Einwilligungserklärung zur Teilnahme erhalten. Mit meiner Unterschrift bestätige ich dann auch, dass ich beide Dokumente gelesen und verstanden habe.

Ich erkläre hiermit meine freiwillige Teilnahme an der o. g. klinischen Prüfung.

_____,_____

(Ort, Datum - von Patient/in einzutragen)

(Unterschrift Patient/in)

_____

_____

Vor- und Nachname - Patient/in in Druckbuchstaben

Die Patientin/der Patient wurde von mir über Ziel, Dauer, Ablauf, Nutzen, der klinischen Prüfung mündlich und schriftlich aufgeklärt.

Aufgetretene Fragen wurden von mir verständlich und ausreichend beantwortet.

Die Patientin/der Patient hat ohne Zwang seine Einwilligung erteilt.

Eine schriftliche Patienteninformation und eine Kopie dieser Patienteneinwilligung habe ich der Patientin/dem Patienten ausgehändigt.

_____

(Ort, Datum - vom Prüfer/in einzutragen)

_____

Vor und Nachname - Prüfer/in in Druckbuchstaben

11.3. Gamification study questionaire

„Fragebogen Gamification“	
Persönliche Informationen	
Name	
Vorname	
Geburtsdatum	
Geschlecht	☐ männlich ☐ weiblich
Anschrift	
E-Mail-Adresse	
Telefonnummer	
Größe:	**cm**
Gewicht:	**Kg**
Schuhgröße	**EU- Norm**

Diabetes mellitus: Erfassungsfragen	
Diabetiker	☐ Ja ☐ Nein ☐ unbekannt
Erstdiagnose des Diabetes mellitus?	Jahr: _____ ☐ unbekannt.
Typ des Diabetes mellitus	☐ Typ 1 ☐ Typ 2 (Alterszucker) ☐ Zuckerkrankheit nach Bauchspeicheldrüsen-entzündung**/** Zuckerkrankheit nach Operation an der Bauchspeicheldrüse

	☐ Schwangerschaftsdiabetes ☐ Vordiabetes/Zuckertoleranzstörung ☐ nicht insulinabhängiger Diabetes im Jugendalter (MODY) ☐ anderer Typ ☐ unbekannt

Metabolisches Syndrom: Erfassungsfragen		
Bluthochdruck	☐ Ja	☐ Nein
Gicht	☐ Ja	☐ Nein

Relevante Nebenerkrankungen: Erfassungsfragen		
Liegen bei Ihnen Krankheiten des Nervensystems vor? (Schlaganfall, M. Parkinson, Multiple Sklerose, Polyneuropathie)	☐ Ja	☐ Nein (nicht bekannt)
Wenn ja, welche?		
Seit wann?		
Therapie? (z.B. bei PNP Schmerzmittel, Antidepressiva)		
Liegen bei Ihnen Erkrankungen der Muskeln vor? (angeborene Defizite, Entzündungen, Verletzungen)	☐ Ja	☐ Nein (nicht bekannt)
Wenn ja, welche?		
Seit wann?		
Therapie?		
Liegen bei Ihnen Krankheiten der Wirbelsäule oder Beine vor? (Bandscheibenvorfälle, Einengung des Spinalkanals, Arthrose,	☐ Ja	☐ Nein (nicht bekannt)

Entzündungen, Verletzungen, Ulzerationen)	
Wenn ja, welche?	
Seit wann?	
Therapie?	
Hatten Sie Fußgeschwüre?	☐ Ja ☐ Nein (nicht bekannt)

Gamificationfragen	
Wie ist Ihre Händigkeit?	☐ Rechtshänder ☐ Linkshänder ☐ Beidhändig
Wie ist Ihre Füßigkeit (dominanter Fuß beim Sport)?	☐ Rechtsfuß ☐ Linksfuß ☐ beidfüßig
Haben Sie einen Führerschein (Fahren Sie Auto), wenn ja km/Jahr ?	☐ Nein ☐ Ja, _____ km/Jahr
Liegen bei Ihnen Bewegungs-einschränkungen vor (im täglichen Leben)? bspw. beim Glas halten? oder Schneiden der Fußnägel?	☐ Ja ☐ Nein _____ _____
Treiben Sie Sport?	☐ Nein, ☐ unregelmäßig, ☐ regelmäßig
Welche Sportarten	☐ Fahrrad fahren / _____ km/Jahr ☐ Andere:

Haben Sie App – Erfahrung? (Spielerfahrung)	☐ Nein ☐ Ja, und zwar: - ☐ soziale Medien, Nachrichten etc. - ☐ Spiele sehr selten (wenige h im Monat) - ☐ Spiele ab und zu (wöchentlich) - ☐ Spiele häufig (mehrmals die Woche/ tgl. etc.) - ☐ Andere _____

Nervenschädigung: Erfassungsfragen	
Gibt es in Ihren Beinen Gefühlsstörungen? (Mehrfachnennung mögl..)	☐Nein ☐ Ja und zwar: (Auswahl) - ☐ Brennen (2 Punkte) - ☐ Taubheit (fehlendes Gefühl) (2) - ☐ Missempfindungen/Ameisenlaufen/ Kribbeln (2 Punkte) - ☐ Schmerzen (1Punkt) - ☐ Krämpfe (1Punkt) - ☐ Schwächegefühl, Schwäche im Bein (1) ☐ Weiß nicht
Wenn ja, wo sind Ihre Beschwerden lokalisiert?	☐ Füße (2 Punkte), ☐ distaler Unterschenkel (1 Punkt), ☐ proximaler Unterschenkel (1 Punkt), ☐ Oberschenkel, ☐ Hände, ☐ Unterarme, ☐ andere Beschwerden_____
Wann treten die Beschwerden auf?	☐ Nachts (2 Punkte), ☐ Tag und Nacht (1 Punkt),

	☐ nur am Tag (keine Punkte), ☐ Patient wacht nachts wegen seinen Beschwerden auf, ☐ keine Angabe
Wann bessern sich Ihre Beschwerden?	☐ Gehen (2 Punkte), ☐ Stehen (1 Punkt), ☐ Sitzen oder Hinlegen (keinen Punkt), ☐ sonstiges _____
Score	/10

Metabolisches Syndrom/ Diabetes mellitus: Untersuchung	
Nahvisus c.c.	
Taillenumfang	_____cm (> 94cm bei Männern, > 80 cm bei Frauen)
letzter HBA1c- Wert	_____Prozent oder in _____mmol/mol, ☐ unbekannt
HDL	☐ ≤ 40mg/dl (≤ 1,05 mmol/l), ☐ 40-50mg/dl (1,06-1,24 mmol/l), ☐ > 50mg/dl (> 1,25 mmol/l), ☐ nicht durchgeführt
Triglyzeride	☐ <150mg/dl (<1,7 mmol/l), ☐ >150mg/dl (>1,7 mmol/l), ☐ unbekannt
letzter Nüchternblutzucker?	☐ <100mg/dl (<5,6mmol/l), ☐ 100-109mg/dl (5,6-6,0 mmol/l), ☐ ≥110mg/dl (≥6,1mmol/l)

	☐ unbekannt

Motorik / Koordination Untersuchung	
Motorik grob	
Bein-Halteversuch	☐ normal ☐ rechts pathologisch ☐ links pathologisch
Koordination/Zielmotorik	
Knie-Hacke-Versuch	☐ normal ☐ rechts pathologisch ☐ links pathologisch
Koordination/Ataxie	
Romberg Stand	☐ normal ☐ Fallneigung
Unterberger Tretversuch	☐ normal ☐ Abweichung nach rechts ☐ Abweichung nach links
Nervenschädigung: Untersuchung	
Puls A. dorsales pedis	Pulsqualität / rechts / links Kräftig ☐ ☐ Schwach ☐ ☐ fehlend ☐ ☐
ABI-Messung A. dorsalis pedis rechts	☐ ≥1,3(Mönkeberg), ☐ >0,9 (gesund),

<table>
<tr><td>RR Brachial:_____/_____

RR Ankle: _____

☐ Angaben für A. tibialis post.</td><td>☐ ≤0,9-0,75 (leichte pAVK),
☐ <0,75-0,5 (mittelschwere pAVK)
☐ ≤0,5 (kritische Ischämie)
☐ nicht messbar</td></tr>
<tr><td>ABI-Messung A. dorsalis pedis links

RR Brachial:_____/_____

RR Ankle: _____

☐ Angaben für A. tibialis post.</td><td>☐ ≥1,3(Mönkeberg),
☐ >0,9 (gesund),
☐ ≤0,9-0,75 (leichte pAVK),
☐ <0,75-0,5 (mittelschwere pAVK)
☐ ≤0,5 (kritische Ischämie)
☐ nicht messbar</td></tr>
<tr><td>Achillessehnenreflex</td><td><table><tr><td>Qualität</td><td>rechts</td><td>links</td></tr><tr><td>Normal/lebhaft</td><td>☐</td><td>☐</td></tr><tr><td>Vermindert</td><td>☐(1)</td><td>☐(1)</td></tr><tr><td>Fehlend</td><td>☐(2)</td><td>☐(2)</td></tr><tr><td>gesteigert</td><td>☐</td><td>☐</td></tr></table></td></tr>
<tr><td>Vibrationsempfindung (Messung am Großzehengrundgelenk)

Rechts_____ / ___8___

Links _____ / ___8___</td><td><table><tr><td>Qualität</td><td>rechts</td><td>links</td></tr><tr><td>≥6/8</td><td>☐</td><td>☐</td></tr><tr><td>5/8</td><td>☐</td><td>☐</td></tr><tr><td>≤4/8</td><td>☐(1)</td><td>☐(1)</td></tr><tr><td>≤2/8</td><td>☐(1)</td><td>☐(1)</td></tr></table></td></tr>
<tr><td>Schmerzempfinden</td><td><table><tr><td>Qualität</td><td>rechts</td><td>links</td></tr><tr><td>Normal/lebhaft</td><td>☐(1)</td><td>☐(1)</td></tr><tr><td>Vermindert/ Fehlend</td><td>☐(1)</td><td>☐(1)</td></tr></table></td></tr>
<tr><td>Temperaturempfinden</td><td><table><tr><td>Qualität</td><td>rechts</td><td>links</td></tr><tr><td>Normal/lebhaft</td><td>☐(0)</td><td>☐(0)</td></tr></table></td></tr>
</table>

	Vermindert/ Fehlend	☐(1)	☐(1)	
Sensibilitätsprüfung (mit 10g Monofilament)	Qualität	rechts	links	
	Normal/lebhaft	☐	☐	
	Vermindert	☐	☐	
	Fehlend	☐	☐	
Punkte gesamt	/10			

Fußstatus / Beinstatus				
Muskeln	Qualität	rechts	links	
	Normal	☐	☐	
	Atrophie	☐	☐	
	Hypertrophie	☐	☐	
Deformitäten	Qualität	rechts	links	
	nein	☐	☐	
	ja	☐	☐	
Kommentar:				

Höhere Kognitive Funktionen: Untersuchung	
Aktueller Beruf	
Reaktionszeit (aus App)	

Status Autonome Nervenfunktion		
Kommt es zu Schwindelgefühlen beim Lagewechsel (z. B. beim Aufstehen)	☐ Ja	☐ Nein (nicht bekannt)

Sind Herzrhythmus-Störungen bekannt? (Herzrasen, Herzstolpern, Herzklopfen) Welche Diagnose besteht?	☐ Ja	☐ Nein (nicht bekannt)
Haben Sie regelmäßig Stuhlgang ohne Abführmittel?	☐ Ja	☐ Nein (nicht bekannt)
Leiden Sie an Blasenentleerungsstörungen?	☐ Ja	☐ Nein (nicht bekannt)
Schwitzen sie verstärkt?	☐ Ja	☐ Nein (nicht bekannt)

11.4. Supplementary figures

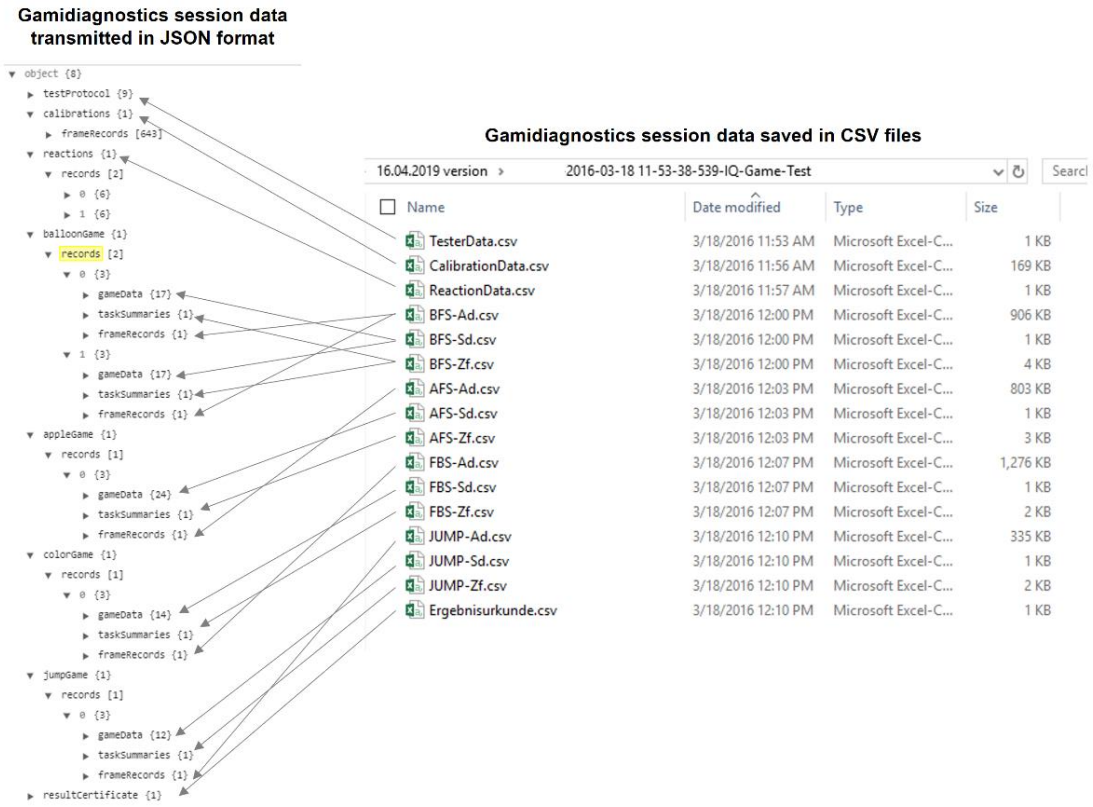

Supplementary Figure 1. Organization of exported data sets from the "Gamidiagnostics" session as CSV files and JSON objects. For each gamidiagnostic session, 16 tables were generated as data sets, all of which were automatically exported to local CSV files. The test identifier, the timestamp when the game session started, the study participant ID, the study personel supervising the test session, the software and hardware versions were documented in the first table for tracking game sessions on the remote server. The following files saved calibration thresholds, finger reaction time, game settings (version, tutorial, pressure thresholds, tasks parameters, etc.), task summaries (scores and points achieved in every task), and sensor data (recorded from each sample). A last file sumarized the results on the six hypothesis-driven key capabilities and provided feedback to study participants on their overall performance.

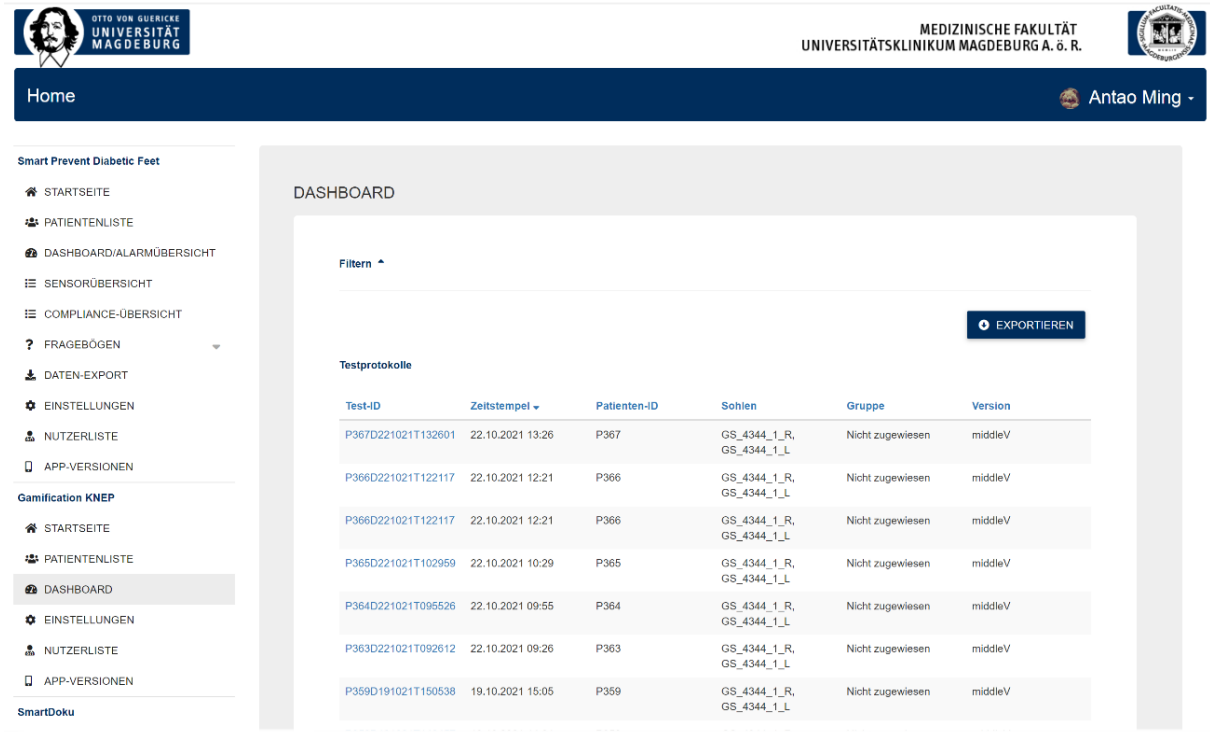

Supplementary Figure 2. IQ-Trial dashboard. On the dashboard of the IQ-Trial webpage the test identifier ("Test-ID", e.g., P367D221021T132601), timestamp ("Zeitstempel", e.g., 22.10.2021 13:26), study participant ID ("Patienten-ID", e.g., P367), insole identifier ("Sohlen", e.g., GS_4344_1_R and GS_4344_1_L), group ("Gruppe", e.g., Control or DPN), and game version ("Version", e.g., middle version) were presented. Users could filter, sort, and export datasets on demand. The exported dataset had a structure resembling the one on the gaming tablet.

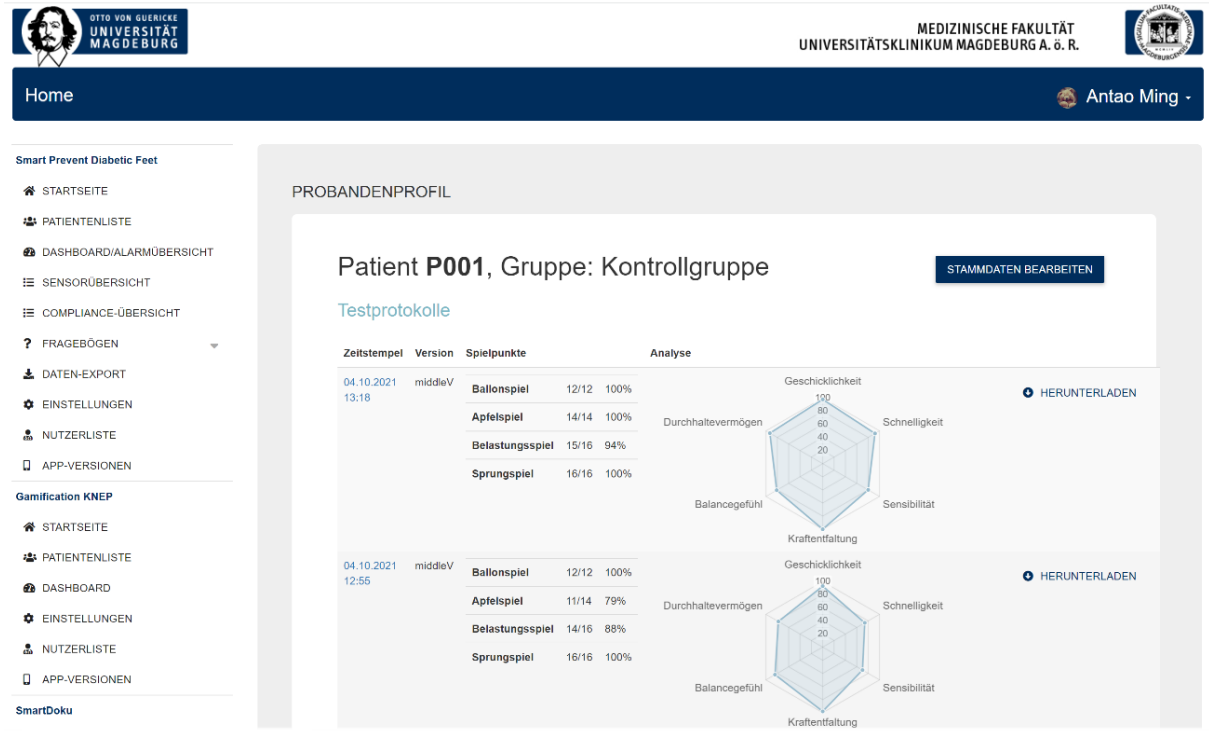

Supplementary Figure 3. Profiles on individual participants. Two game session datasets collected from a healthy volunteer are visualized, including time stamp, game version, achieved scores in different games, and calculated key capabilities (skillfulness, reaction time, sensation, endurance, muscle strength, and balance). According to the spider chart, P001 performed better in his second session.

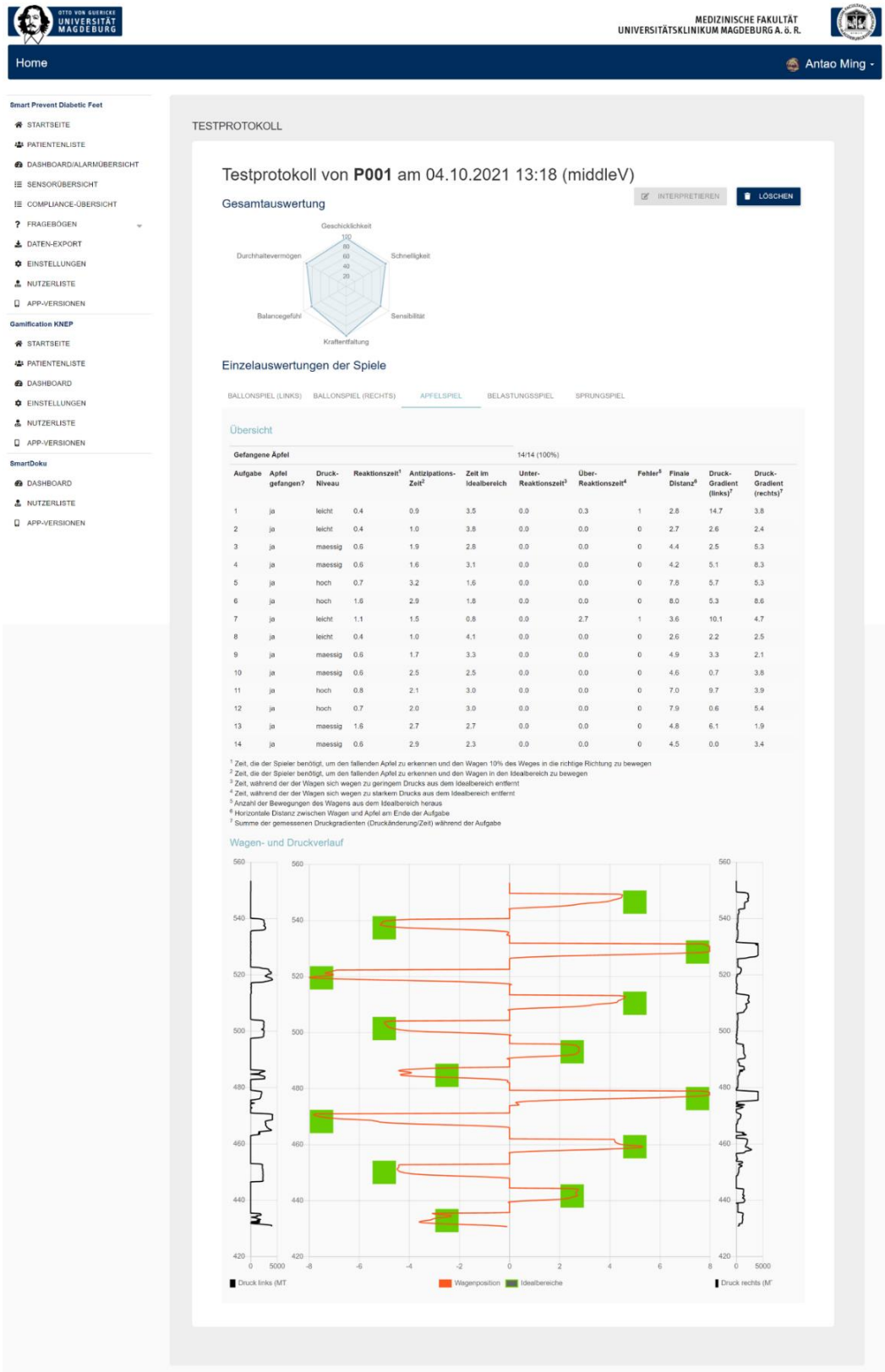

Aufgabe	Apfel gefangen?	Druck-Niveau	Reaktionszeit[1]	Antizipations-Zeit[2]	Zeit im Idealbereich	Unter-Reaktionszeit[3]	Über-Reaktionszeit[4]	Fehler[5]	Finale Distanz[6]	Druck-Gradient (links)[7]	Druck-Gradient (rechts)[7]
1	ja	leicht	0.4	0.9	3.5	0.0	0.3	1	2.8	14.7	3.8
2	ja	leicht	0.4	1.0	3.8	0.0	0.0	0	2.7	2.6	2.4
3	ja	maessig	0.6	1.9	2.8	0.0	0.0	0	4.4	2.5	5.3
4	ja	maessig	0.6	1.6	3.1	0.0	0.0	0	4.2	5.1	8.3
5	ja	hoch	0.7	3.2	1.6	0.0	0.0	0	7.8	5.7	5.3
6	ja	hoch	1.8	2.9	1.8	0.0	0.0	0	8.0	5.3	8.6
7	ja	leicht	1.1	1.5	0.8	0.0	2.7	1	3.6	10.1	4.7
8	ja	leicht	0.4	1.0	4.1	0.0	0.0	0	2.6	2.2	2.5
9	ja	maessig	0.6	1.7	3.3	0.0	0.0	0	4.9	3.3	2.1
10	ja	maessig	0.6	2.5	2.5	0.0	0.0	0	4.6	0.7	3.8
11	ja	hoch	0.8	2.1	3.0	0.0	0.0	0	7.0	9.7	3.9
12	ja	hoch	0.7	2.0	3.0	0.0	0.0	0	7.9	0.6	5.4
13	ja	maessig	1.6	2.7	2.7	0.0	0.0	0	4.8	6.1	1.9
14	ja	maessig	0.6	2.9	2.3	0.0	0.0	0	4.5	0.0	3.4

[1] Zeit, die der Spieler benötigt, um den fallenden Apfel zu erkennen und den Wagen 10% des Weges in die richtige Richtung zu bewegen
[2] Zeit, die der Spieler benötigt, um den fallenden Apfel zu erkennen und den Wagen in den Idealbereich zu bewegen
[3] Zeit, während der der Wagen sich wegen zu geringem Drucks aus dem Idealbereich entfernt
[4] Zeit, während der der Wagen sich wegen zu starkem Drucks aus dem Idealbereich entfernt
[5] Anzahl der Bewegungen des Wagens aus dem Idealbereich heraus
[6] Horizontale Distanz zwischen Wagen und Apfel am Ende der Aufgabe
[7] Summe der gemessenen Druckgradienten (Druckänderung/Zeit) während der Aufgabe

Supplementary Figure 4. Standardized assessment page of the Apple-Catch game. The top spider chart shows six hypothesis-driven key capabilities (skillfulness, reaction time, sensation, endurance, muscle strength, and balance). The table below summarizes the study participant's performance in every task, including collected apples (n), pressure level, reaction time [s], anticipation time [s], time inside catching area [s], time outside catching area [s], frequency outside catching area, and pressure gradients between successive frames of the left and right foot. The vertical line chart visualizes the position changes of the car (red line) and apples (green boxes), as well as pressure-time curves measured by insoles (black line charts on both sides).

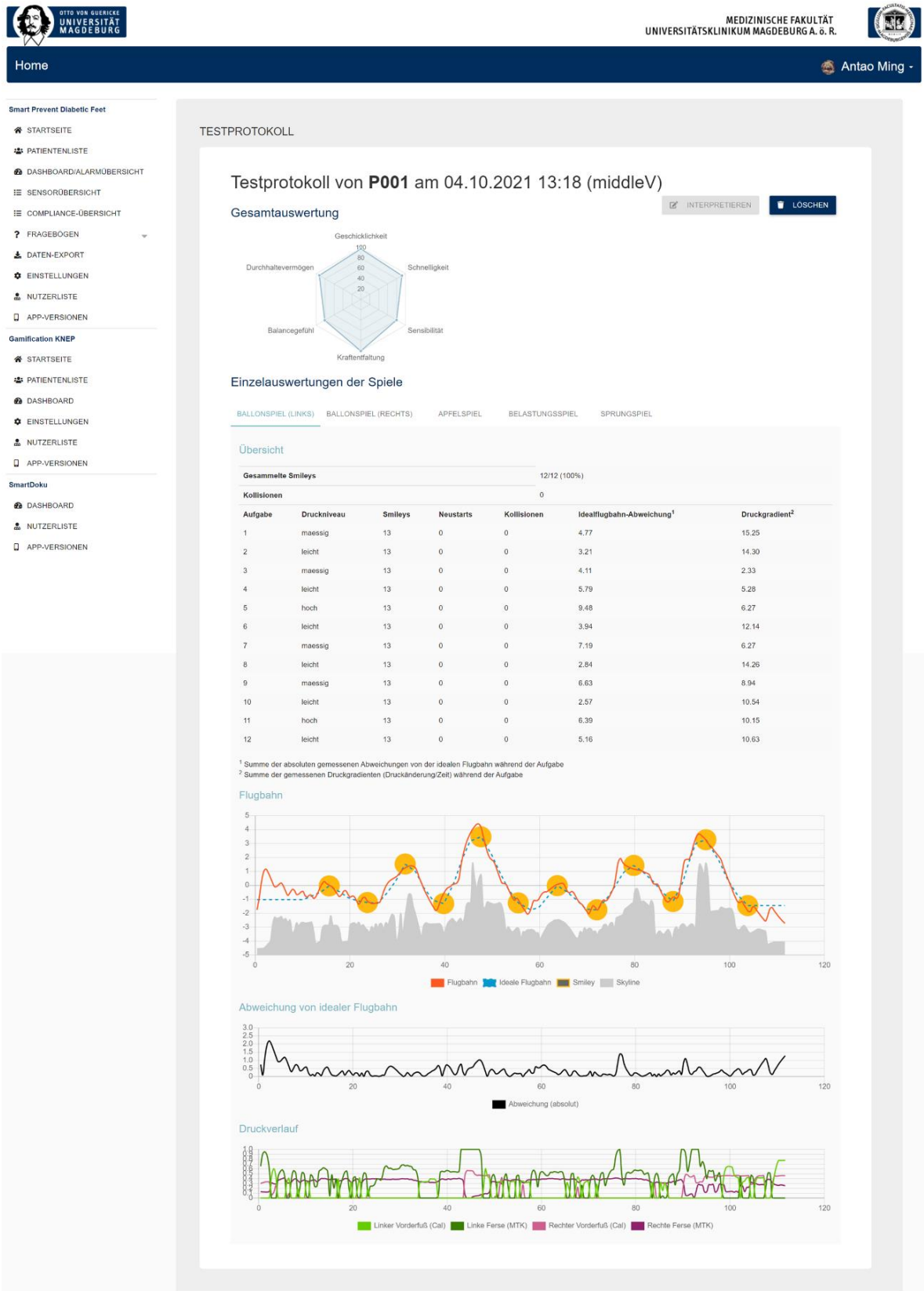

Supplementary Figure 5. Standardized assessment page of the Balloon-Flying game. The top spider chart shows six hypothesis-driven key capabilities (skillfulness, reaction time, sensation, endurance, muscle strength, and balance). The table below summarizes the study participant's performance in every task, including collected smileys (n), restarts (n), collisions (n), virtual deviation of the ideal flying route, and pressure-time integrals. Three graphics visualize obstacles, smileys, skyline, deviation of the real and the optimal flying route, and pressure-time curves.

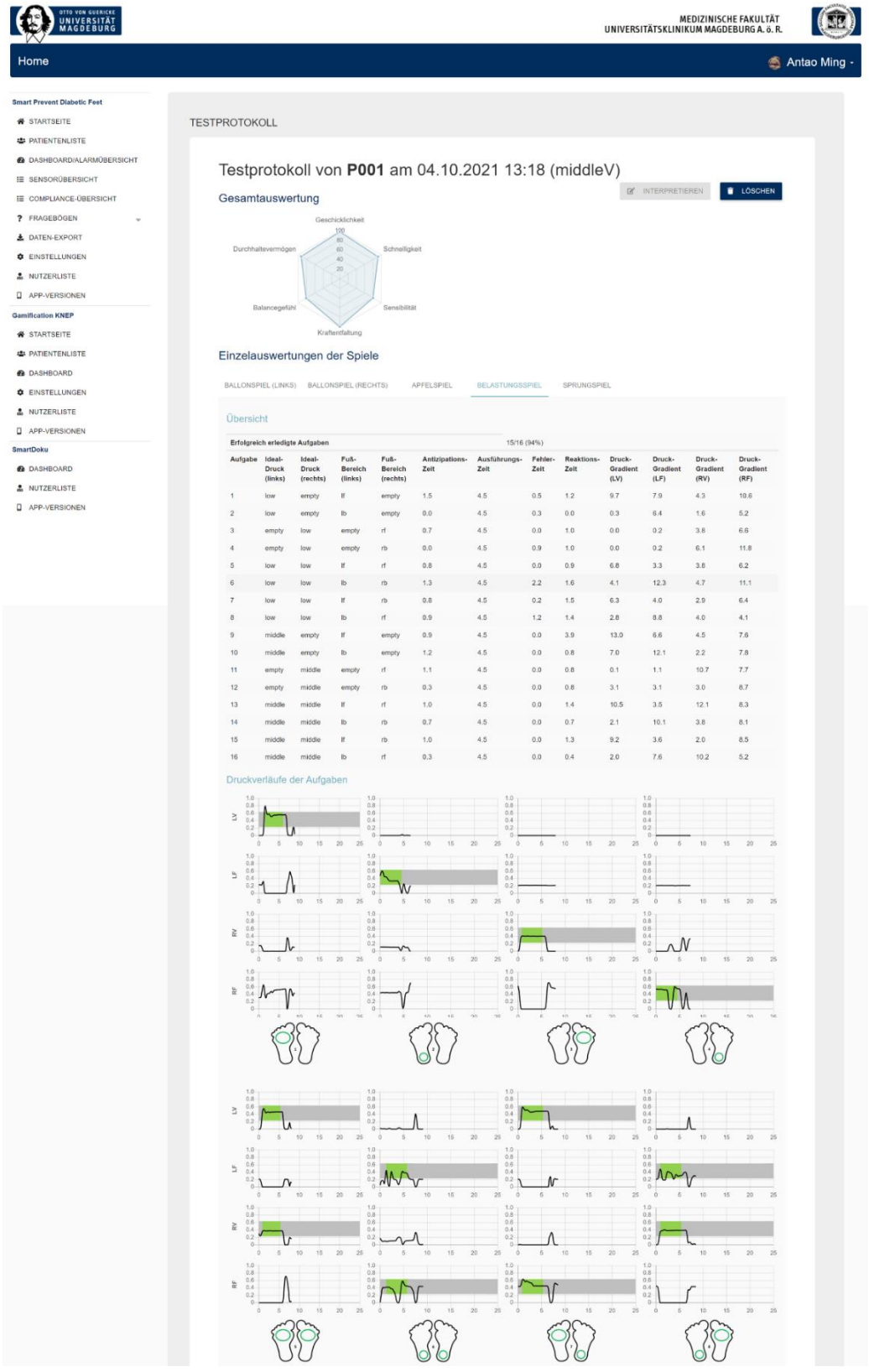

Supplementary Figure 6. Standardized assessment page of the Cross-Pressure game. The top spider chart shows six hypothesis-driven key capabilities (skillfulness, reaction time, sensation, endurance, muscle strength, and balance). The table below shows the total count of collected smileys and the study participant's performance in every task, including anticipation time [s], execution time [s], time outside optimal pressure range [s], time for releasing pressure [s], smileys (n), restarts (n), collisions (n), virtual deviation of the ideal flying route, and pressure gradients between successive frames of different foot areas. In each task, the line charts present pressure-time profiles of different plantar regions (left forefoot, left heel, right forefoot, and right heel).

Supplementary Figure 7. Standardized assessment page of the Island-Jump game. The top spider chart shows six hypothesis-driven key capabilities (skillfulness, reaction time, sensation, endurance, muscle strength, and balance). The table below shows the total count of jump attempts and the study participant's performance in every task, including deviation from optimal pressure, anticipation time [s], pressure gradients between successive frames, and pressure time integrals. The bar plots below present the deviation from optimal pressure, and the line plots demonstrate pressure-time curves of the left and right insole in each task.

11.5. Supplementary tables

*Supplementary Table 1. Results of intergroup difference tests of game features within cohort 1. Differences between groups were calculated using Kruskal test, Mann-Whitney U test, t-test or chi-square test as appropriate. Significance levels: ns (p>0.05), * (p=0.01–0.05), ** (p=0.001–0.01), *** (p=0.0001–0.001), **** (p<0.0001). CF: candidate features; AC: Apple-Catch; BF: Balloon-Flying; CP: Cross-Pressure; IJ: Island-Jump; TC: task combination; CON: controls (N=71); CON1: controls aged 18-30 (N=19); CON2: controls aged 31–50 (N=22); CON3: controls aged 51–80 (N=30); DPN: diabetic peripheral neuropathy (N=112); DPN1: mild (NDS: 1–5, N=48); DPN2: moderate (NDS: 6-8, N=55); DPN3: severe (NDS: 9-10, N=11);*

ID	Game	Task/TC	Feature Name	P CON vs. DPN	P CON vs. DPN1	P CON vs. DPN2	P CON vs. DPN3	P CON1, CON2, vs. CON3
CF1	AC	Task 8	Final virtual distance	****	****	*	*	ns
CF2	AC	Task 12	Reaction time [s]	***	*	***	ns	ns
CF3	AC	Task 12	Apple caught (yes/no)	**	***	*	ns	ns
CF4	AC	TC 12	Time outside catching area [s]	**	***	ns	ns	ns
CF5	AC	Task 13	Pressure gradients between successive frames	**	**	***	*	ns
CF6	AC	TC 1	Anticipation time [s]	**	**	**	ns	ns
CF7	AC	Task 5	Apple caught (yes/no)	**	**	*	ns	ns
CF8	AC	TC 11	Time outside catching area [s]	**	**	*	ns	ns
CF9	AC	TC 12	Final virtual distance	**	**	*	ns	ns
CF10	AC	Task 5	Time inside catching area [s]	**	**	*	ns	ns
CF11	AC	Task 6	Pressure gradients between successive frames	**	**	*	ns	ns
CF12	AC	TC 2	Final virtual distance	**	**	ns	*	ns
CF13	AC	TC 3	Time outside catching area [s]	**	*	*	ns	ns
CF14	AC	Task 7	Time outside catching area [s]	**	*	*	ns	ns
CF15	AC	Task 11	Pressure gradients between successive frames	**	*	*	ns	ns
CF16	AC	Task 13	Normalized pressure	**	ns	***	ns	ns
CF17	AC	TC 11	Normalized pressure	**	ns	**	ns	ns
CF18	AC	TC 12	Time inside catching area [s]	**	ns	**	ns	ns
CF19	AC	Task 8	Time inside catching area [s]	**	ns	**	ns	ns
CF20	AC	TC 11	Pressure differences between successive frames	**	ns	*	ns	ns
CF21	AC	Task 3	Time outside catching area [s]	**	ns	*	ns	ns
CF22	AC	Task 8	Normalized pressure	*	***	ns	ns	ns
CF23	AC	TC 4	Normalized pressure	*	**	ns	ns	ns
CF24	AC	TC 9	Anticipation time [s]	*	**	ns	ns	ns
CF25	AC	Task 2	Normalized pressure	*	**	ns	ns	ns
CF26	AC	Task 3	Apple caught (yes/no)	*	**	ns	ns	ns
CF27	AC	Task 8	Anticipation time [s]	*	**	ns	ns	ns
CF28	AC	TC 8	Reaction time [s]	*	*	*	ns	ns
CF29	AC	Task 2	Normalized pressure	*	*	*	ns	ns
CF30	AC	Task 3	Time inside catching area [s]	*	*	*	ns	ns
CF31	AC	Task 6	Reaction time [s]	*	*	*	ns	ns
CF32	AC	Task 9	Time outside catching area [s]	*	*	*	ns	ns
CF33	AC	TC 7	Final virtual distance	*	*	ns	ns	ns
CF34	AC	TC 5	Normalized pressure	*	*	ns	ns	ns
CF35	AC	TC 9	Time inside catching area [s]	*	*	ns	ns	ns
CF36	AC	Task 3	Final virtual distance	*	*	ns	ns	ns
CF37	AC	Task 8	Apple caught (yes/no)	*	*	ns	ns	ns
CF38	AC	Task 12	Pressure gradients between successive frames	*	*	ns	ns	ns
CF39	AC	TC 5	Normalized pressure	*	ns	**	ns	ns
CF40	AC	TC 5	Pressure differences between successive frames	*	ns	**	ns	ns
CF41	AC	Task 6	Time inside catching area [s]	*	ns	**	ns	ns
CF42	AC	Task 12	Time inside catching area [s]	*	ns	**	ns	ns
CF43	AC	Task 12	Final virtual distance	*	ns	**	ns	ns
CF44	AC	Task 13	Reaction time [s]	*	ns	**	ns	ns
CF45	AC	TC 2	Anticipation time [s]	*	ns	*	ns	ns
CF46	AC	TC 7	Normalized pressure	*	ns	*	ns	ns

CF47	AC	TC 10	Pressure differences between successive frames	*	ns	*	ns	ns
CF48	AC	Task 9	Normalized pressure	*	ns	*	ns	ns
CF49	AC	Task 9	Pressure gradients between successive frames	*	ns	*	ns	ns
CF50	AC	Task 13	Pressure gradients between successive frames	*	ns	*	ns	ns
CF51	AC	TC 3	Normalized pressure	*	ns	ns	ns	ns
CF52	AC	TC 4	Time outside catching area [s]	*	ns	ns	ns	ns
CF53	AC	Task 5	Normalized pressure	*	ns	ns	ns	ns
CF54	BF (L)	TC 1	Minimal virtual distance smiley 4	****	****	****	ns	***
CF55	BF (L)	Task 7	Virtual deviation of ideal flying route	****	***	****	*	***
CF56	BF (R)	TC 1	Minimal virtual distance smiley 4	****	***	***	ns	*
CF57	BF (R)	TC 2	Virtual deviation of ideal flying route	****	***	***	ns	ns
CF58	BF (L)	Task 5	Normalized pressure	****	***	**	ns	**
CF59	BF (L)	Task 7	Virtual deviation of ideal flying route	****	**	****	*	**
CF60	BF (R)	TC 1	Minimal virtual distance smiley 2	****	**	****	ns	**
CF61	BF (R)	TC 3	Virtual deviation of ideal flying route	****	**	****	ns	****
CF62	BF (R)	Task 3	Virtual deviation of ideal flying route	****	**	**	*	ns
CF63	BF (L)	Task 4	Virtual deviation of ideal flying route	***	**	****	ns	ns
CF64	BF (R)	TC 3	Minimal virtual distance smiley 2	***	**	***	*	ns
CF65	BF (L)	Task 11	Virtual deviation of ideal flying route	***	**	***	ns	**
CF66	BF (R)	TC 1	Minimal virtual distance smiley 1	***	**	***	ns	****
CF67	BF (L)	Task 8	Virtual deviation of ideal flying route	***	**	***	ns	*
CF68	BF (L)	TC 2	Minimal virtual distance smiley 4	***	**	***	ns	ns
CF69	BF (L)	Task 6	Virtual deviation of ideal flying route	***	**	***	ns	ns
CF70	BF (L)	TC 1	Minimal virtual distance smiley 3	***	**	**	ns	*
CF71	BF (L)	Task 9	Virtual deviation of ideal flying route	***	**	**	ns	*
CF72	BF (R)	Task 8	Virtual deviation of ideal flying route	***	**	**	ns	*
CF73	BF (L)	TC 3	Virtual deviation of ideal flying route	***	**	**	ns	ns
CF74	BF (L)	TC 3	Minimal virtual distance smiley 2	***	*	***	ns	*
CF75	BF (R)	Task 10	Virtual deviation of ideal flying route	***	*	**	**	***
CF76	BF (L)	TC 3	Minimal virtual distance smiley 1	**	****	ns	ns	ns
CF77	BF (L)	Task 5	Collision frequency (n)	**	***	**	ns	*
CF78	BF (L)	TC 3	Collision frequency (n)	**	**	**	*	**
CF79	BF (L)	TC 2	Collision frequency (n)	**	**	**	*	*
CF80	BF (L)	Task 9	Virtual deviation of ideal flying route	**	**	**	ns	**
CF81	BF (L)	Task 12	Virtual deviation of ideal flying route	**	**	**	ns	ns
CF82	BF (R)	TC 2	Collision frequency (n)	**	**	*	*	*
CF83	BF (R)	TC 2	Minimal virtual distance smiley 4	**	**	*	ns	*
CF84	BF (L)	TC 4	Collision frequency (n)	**	**	*	ns	ns
CF85	BF (R)	Task 2	Virtual deviation of ideal flying route	**	**	*	ns	ns
CF86	BF (L)	Task 5	Virtual deviation of ideal flying route	**	**	*	ns	ns
CF87	BF (L)	Task 5	Normalized pressure	**	**	*	ns	ns
CF88	BF (L)	Task 3	Minimal virtual distance smiley 1	**	**	ns	*	ns
CF89	BF (R)	Task 11	Virtual deviation of ideal flying route	**	*	***	ns	*
CF90	BF (L)	TC 2	Virtual deviation of ideal flying route	**	*	***	ns	*
CF91	BF (L)	Task 5	Virtual deviation of ideal flying route	**	*	***	ns	*
CF92	BF (L)	Task 6	Normalized pressure	**	*	**	**	ns
CF93	BF (R)	TC 1	Normalized pressure	**	*	**	ns	*
CF94	BF (R)	TC 4	Collision frequency (n)	**	*	**	ns	*
CF95	BF (R)	Task 1	Virtual deviation of ideal flying route	**	*	**	ns	ns
CF96	BF (R)	Task 3	Virtual deviation of ideal flying route	**	*	**	ns	**
CF97	BF (L)	Task 3	Minimal virtual distance smiley 2	**	*	**	ns	ns
CF98	BF (R)	Task 8	Minimal virtual distance smiley 2	**	*	**	ns	ns
CF99	BF (R)	TC 4	Minimal virtual distance smiley 3	**	*	*	ns	**
CF100	BF (L)	Task 5	Minimal virtual distance smiley 4	**	*	*	ns	*
CF101	BF (R)	TC 2	Minimal virtual distance smiley 2	**	*	*	ns	**
CF102	BF (L)	Task 3	Virtual deviation of ideal flying route	**	*	*	ns	**
CF103	BF (L)	Task 10	Virtual deviation of ideal flying route	**	*	*	ns	ns
CF104	BF (R)	TC 3	Minimal virtual distance smiley 2	**	*	ns	**	ns
CF105	BF (L)	TC 4	Normalized pressure	**	ns	***	*	ns
CF106	BF (R)	TC 1	Minimal virtual distance smiley 3	**	ns	***	ns	***
CF107	BF (R)	Task 7	Virtual deviation of ideal flying route	**	ns	***	ns	***
CF108	BF (L)	Task 10	Virtual deviation of ideal flying route	**	ns	***	ns	ns
CF109	BF (L)	TC 3	Minimal virtual distance smiley 3	**	ns	**	*	*
CF110	BF (L)	TC 4	Virtual deviation of ideal flying route	**	ns	**	*	ns
CF111	BF (L)	Task 1	Minimal virtual distance smiley 3	**	ns	**	**	ns
CF112	BF (R)	TC 3	Virtual deviation of ideal flying route	**	ns	**	ns	****
CF113	BF (L)	TC 2	Minimal virtual distance smiley 1	**	ns	**	ns	**
CF114	BF (R)	TC 3	Collision frequency (n)	**	ns	**	ns	***
CF115	BF (L)	Task 4	Minimal virtual distance smiley 4	**	ns	**	ns	*

CF116	BF (R)	Task 5	Virtual deviation of ideal flying route	**	ns	**	ns	*
CF117	BF (R)	Task 3	Minimal virtual distance smiley 2	**	ns	**	ns	ns
CF118	BF (R)	Task 5	Collision frequency (n)	**	ns	*	ns	**
CF119	BF (L)	TC 3	Minimal virtual distance smiley 4	**	ns	*	ns	*
CF120	BF (R)	TC 2	Minimal virtual distance smiley 3	**	ns	*	ns	ns
CF121	BF (L)	Task 3	Normalized pressure	*	**	ns	ns	**
CF122	BF (L)	Task 6	Pressure-time integrals	*	**	ns	ns	ns
CF123	BF (L)	Task 3	Normalized pressure	*	*	*	ns	**
CF124	BF (L)	TC 2	Pressure gradients between successive frames	*	*	*	ns	ns
CF125	BF (R)	TC 4	Minimal virtual distance smiley 1	*	*	*	ns	ns
CF126	BF (R)	Task 7	Minimal virtual distance smiley 2	*	*	*	ns	ns
CF127	BF (L)	Task 11	Minimal virtual distance smiley 4	*	*	ns	ns	**
CF128	BF (L)	TC 2	Minimal virtual distance smiley 3	*	*	ns	ns	ns
CF129	BF (L)	TC 2	Pressure differences between successive frames	*	*	ns	ns	ns
CF130	BF (L)	Task 1	Virtual deviation of ideal flying route	*	*	ns	ns	ns
CF131	BF (L)	Task 4	Pressure differences between successive frames	*	*	ns	ns	ns
CF132	BF (L)	Task 6	Minimal virtual distance smiley 1	*	*	ns	ns	ns
CF133	BF (L)	Task 11	Minimal virtual distance smiley 3	*	*	ns	ns	ns
CF134	BF (L)	Task 11	Virtual deviation of ideal flying route	*	*	ns	ns	ns
CF135	BF (R)	Task 8	Minimal virtual distance smiley 1	*	*	ns	ns	ns
CF136	BF (R)	Task 9	Virtual deviation of ideal flying route	*	ns	***	ns	**
CF137	BF (L)	Task 7	Minimal virtual distance smiley 2	*	ns	**	ns	*
CF138	BF (L)	Task 10	Virtual deviation of ideal flying route	*	ns	**	ns	ns
CF139	BF (R)	Task 2	Virtual deviation of ideal flying route	*	ns	**	ns	ns
CF140	BF (L)	Task 7	Minimal virtual distance smiley 3	*	ns	*	*	ns
CF141	BF (R)	Task 12	Virtual deviation of ideal flying route	*	ns	*	*	ns
CF142	BF (L)	Task 11	Normalized pressure	*	ns	*	**	ns
CF143	BF (R)	Task 4	Virtual deviation of ideal flying route	*	ns	*	ns	****
CF144	BF (R)	TC 2	Virtual deviation of ideal flying route	*	ns	*	ns	**
CF145	BF (R)	Task 4	Minimal virtual distance smiley 4	*	ns	*	ns	ns
CF146	BF (L)	Task 1	Virtual deviation of ideal flying route	*	ns	*	ns	*
CF147	BF (L)	Task 4	Minimal virtual distance smiley 3	*	ns	*	ns	ns
CF148	BF (R)	Task 11	Collision frequency (n)	*	ns	*	ns	ns
CF149	BF (R)	Task 9	Virtual deviation of ideal flying route	*	ns	*	ns	*
CF150	BF (L)	TC 1	Normalized pressure	*	ns	*	ns	ns
CF151	BF (L)	Task 2	Virtual deviation of ideal flying route	*	ns	*	ns	ns
CF152	BF (L)	Task 6	Pressure differences between successive frames	*	ns	*	ns	ns
CF153	BF (L)	Task 7	Normalized pressure	*	ns	*	ns	ns
CF154	BF (R)	TC 2	Pressure differences between successive frames	*	ns	*	ns	ns
CF155	BF (R)	Task 5	Minimal virtual distance smiley 1	*	ns	*	ns	ns
CF156	BF (R)	Task 5	Minimal virtual distance smiley 4	*	ns	*	ns	ns
CF157	BF (R)	Task 5	Normalized pressure	*	ns	*	ns	ns
CF158	BF (R)	Task 5	Pressure differences between successive frames	*	ns	*	ns	ns
CF159	BF (R)	Task 6	Virtual deviation of ideal flying route	*	ns	*	ns	ns
CF160	BF (L)	Task 4	Virtual deviation of ideal flying route	*	ns	ns	*	ns
CF161	BF (R)	Task 10	Minimal virtual distance smiley 3	*	ns	ns	***	*
CF162	BF (R)	TC 3	Virtual deviation of ideal flying route	*	ns	ns	ns	****
CF163	BF (R)	Task 1	Normalized pressure	*	ns	ns	ns	ns
CF164	BF (R)	Task 2	Normalized pressure	*	ns	ns	ns	*
CF165	BF (R)	Task 11	Minimal virtual distance smiley 3	*	ns	ns	ns	**
CF166	BF (L)	Task 5	Pressure differences between successive frames	*	ns	ns	ns	ns
CF167	BF (L)	Task 12	Minimal virtual distance smiley 3	*	ns	ns	ns	ns
CF168	BF (R)	TC 1	Normalized pressure	*	ns	ns	ns	ns
CF169	BF (R)	TC 4	Normalized pressure	*	ns	ns	ns	ns
CF170	BF (R)	Task 5	Minimal virtual distance smiley 3	*	ns	ns	ns	ns
CF171	BF (L)	Task 11	Normalized pressure	ns	ns	*	ns	ns
CF172	BF (L)	Task 11	Normalized pressure	ns	ns	*	ns	ns
CF173	CP	TC 6	Time outside ideal pressure zone [s]	****	****	****	*	*
CF174	CP	Task 1	Reaction time [s]	****	****	***	ns	ns
CF175	CP	Task 2	Reaction time [s]	****	***	****	ns	ns
CF176	CP	Task 8	Time outside ideal pressure zone [s]	****	***	****	ns	ns
CF177	CP	Task 9	Normalized pressure (L)	****	***	***	ns	***
CF178	CP	Task 4	Normalized pressure (R)	****	***	***	ns	ns
CF179	CP	Task 6	Time outside ideal pressure zone [s]	****	***	**	*	ns
CF180	CP	TC 6	Anticipation time [s]	****	***	**	ns	*

CF181	CP	TC 5	Reaction time [s]	****	**	***	*	**
CF182	CP	Task 7	Reaction time [s]	****	**	***	*	ns
CF183	CP	Task 4	Pressure differences between successive frames (R)	***	****	**	ns	ns
CF184	CP	Task 9	Reaction time [s]	***	****	*	ns	ns
CF185	CP	TC 4	Time outside ideal pressure zone [s]	***	**	***	ns	ns
CF186	CP	TC 6	Normalized pressure (L)	***	**	***	ns	ns
CF187	CP	Task 6	Reaction time [s]	***	**	***	ns	ns
CF188	CP	TC 1	Normalized pressure (L)	***	**	**	*	ns
CF189	CP	TC 6	Normalized pressure (L)	***	**	**	ns	ns
CF190	CP	TC 4	Reaction time [s]	***	**	**	ns	*
CF191	CP	TC 6	Pressure differences between successive frames (L)	***	**	**	ns	ns
CF192	CP	Task 4	Reaction time [s]	***	**	**	ns	ns
CF193	CP	Task 8	Normalized pressure (L)	***	**	**	ns	ns
CF194	CP	TC 2	Normalized pressure (R)	***	**	*	*	ns
CF195	CP	Task 13	Normalized pressure (L)	**	***	ns	ns	ns
CF196	CP	Task 7	Anticipation time [s]	**	**	**	ns	***
CF197	CP	TC 2	Anticipation time [s]	**	**	*	ns	****
CF198	CP	TC 6	Normalized pressure (L)	**	**	*	ns	ns
CF199	CP	Task 1	Time outside ideal pressure zone [s]	**	**	*	ns	ns
CF200	CP	TC 5	Pressure gradients between successive frames (R)	**	**	ns	*	**
CF201	CP	Task 12	Reaction time [s]	**	**	ns	*	ns
CF202	CP	Task 10	Reaction time [s]	**	**	ns	ns	ns
CF203	CP	Task 12	Normalized pressure (R)	**	**	ns	ns	ns
CF204	CP	TC 5	Time outside ideal pressure zone [s]	**	*	**	*	ns
CF205	CP	TC 6	Pressure differences between successive frames (L)	**	*	**	*	ns
CF206	CP	Task 8	Normalized pressure (R)	**	*	**	ns	ns
CF207	CP	TC 6	Normalized pressure (R)	**	*	**	ns	ns
CF208	CP	Task 4	Time outside ideal pressure zone [s]	**	*	**	ns	ns
CF209	CP	Task 7	Time outside ideal pressure zone [s]	**	*	**	ns	ns
CF210	CP	Task 8	Reaction time [s]	**	*	*	*	ns
CF211	CP	Task 14	Reaction time [s]	**	*	*	*	ns
CF212	CP	Task 5	Reaction time [s]	**	*	*	ns	**
CF213	CP	TC 6	Normalized pressure (R)	**	*	*	ns	ns
CF214	CP	Task 7	Pressure differences between successive frames (L)	**	*	*	ns	ns
CF215	CP	TC 5	Pressure differences between successive frames (R)	**	*	ns	*	**
CF216	CP	TC 7	Pressure differences between successive frames (L)	**	*	ns	*	ns
CF217	CP	Task 5	Pressure-time integrals of the reaction phase (R)	**	*	ns	*	ns
CF218	CP	Task 12	Pressure-time integrals of the reaction phase (R)	**	ns	***	*	ns
CF219	CP	TC 7	Pressure differences between successive frames (L)	**	ns	**	ns	ns
CF220	CP	TC 6	Reaction time [s]	**	ns	**	ns	*
CF221	CP	TC 6	Normalized pressure (R)	**	ns	**	ns	ns
CF222	CP	TC 7	Normalized pressure (L)	**	ns	*	**	ns
CF223	CP	TC 6	Pressure differences between successive frames (R)	**	ns	*	ns	ns
CF224	CP	Task 7	Pressure-time integrals of the reaction phase (R)	**	ns	*	ns	ns
CF225	CP	Task 8	Pressure differences between successive frames (L)	*	**	ns	*	ns
CF226	CP	TC 6	Pressure differences between successive frames (R)	*	*	*	ns	ns
CF227	CP	TC 6	Pressure-time integrals of the execution phase (R)	*	*	*	ns	ns
CF228	CP	Task 4	Pressure-time integrals of the execution phase (R)	*	*	*	ns	ns
CF229	CP	Task 15	Normalized pressure (L)	*	*	ns	*	ns
CF230	CP	TC 9	Normalized pressure (L)	*	*	ns	*	ns
CF231	CP	TC 9	Reaction time [s]	*	*	ns	*	ns
CF232	CP	TC 5	Normalized pressure (R)	*	*	ns	ns	ns
CF233	CP	Task 5	Anticipation time [s]	*	*	ns	ns	**
CF234	CP	Task 8	Anticipation time [s]	*	*	ns	ns	**
CF235	CP	TC 5	Anticipation time [s]	*	*	ns	ns	ns
CF236	CP	TC 5	Normalized pressure (R)	*	*	ns	ns	ns

CF237	CP	Task 5	Time outside ideal pressure zone [s]	*	*	ns	ns	ns
CF238	CP	Task 6	Normalized pressure (R)	*	*	ns	ns	ns
CF239	CP	Task 7	Pressure differences between successive frames (R)	*	*	ns	ns	ns
CF240	CP	TC 4	Normalized pressure (L)	*	ns	**	ns	*
CF241	CP	Task 15	Normalized pressure (L)	*	ns	*	*	**
CF242	CP	Task 10	Pressure-time integrals of the reaction phase (L)	*	ns	*	*	ns
CF243	CP	Task 5	Normalized pressure (L)	*	ns	*	ns	ns
CF244	CP	Task 2	Time outside ideal pressure zone [s]	*	ns	*	ns	**
CF245	CP	Task 2	Normalized pressure (L)	*	ns	*	ns	ns
CF246	CP	Task 9	Time outside ideal pressure zone [s]	*	ns	*	ns	ns
CF247	CP	Task 16	Pressure-time integrals of the reaction phase (L)	*	ns	*	ns	**
CF248	CP	Task 5	Normalized pressure (R)	*	ns	*	ns	ns
CF249	CP	Task 13	Pressure-time integrals of the reaction phase (R)	*	ns	*	ns	ns
CF250	CP	Task 9	Pressure-time integrals of the reaction phase (L)	*	ns	ns	*	**
CF251	CP	TC 9	Time outside ideal pressure zone [s]	*	ns	ns	*	ns
CF252	CP	Task 15	Reaction time [s]	*	ns	ns	*	ns
CF253	CP	Task 3	Time outside ideal pressure zone [s]	*	ns	ns	**	ns
CF254	CP	Task 3	Pressure-time integrals of the execution phase (R)	*	ns	ns	**	ns
CF255	CP	TC 7	Reaction time [s]	*	ns	ns	ns	*
CF256	CP	Task 15	Pressure-time integrals of the reaction phase (L)	*	ns	ns	ns	*
CF257	CP	Task 1	Normalized pressure (L)	*	ns	ns	ns	ns
CF258	CP	Task 6	Normalized pressure (L)	*	ns	ns	ns	ns
CF259	CP	Task 11	Pressure differences between successive frames (R)	*	ns	ns	ns	ns
CF260	IJ	TC 6	Deviation from ideal pressure	****	****	****	ns	ns
CF261	IJ	TC 4	Deviation from ideal pressure	****	***	****	ns	ns
CF262	IJ	TC 4	Pressure differences between successive frames	****	***	****	ns	ns
CF263	IJ	TC 7	Deviation from ideal pressure	****	***	***	ns	ns
CF264	IJ	TC 6	Deviation from ideal pressure	***	***	**	ns	ns
CF265	IJ	Task 2	Deviation from ideal pressure	***	***	**	ns	ns
CF266	IJ	Task 2	Deviation from ideal pressure	***	***	*	ns	ns
CF267	IJ	TC 5	Mean pressure of execution phase	***	**	*	ns	ns
CF268	IJ	TC 7	Deviation from ideal pressure	***	*	***	ns	*
CF269	IJ	TC 6	Anticipation time [s]	***	*	***	ns	ns
CF270	IJ	Task 10	Attempt count (n)	**	***	*	ns	ns
CF271	IJ	Task 9	Pressure-time integrals	**	***	ns	*	*
CF272	IJ	TC 4	Execution time [s]	**	**	**	ns	**
CF273	IJ	TC 3	Anticipation time [s]	**	**	**	ns	ns
CF274	IJ	Task 4	Attempt count (n)	**	**	**	ns	ns
CF275	IJ	Task 4	Execution time [s]	**	**	*	ns	ns
CF276	IJ	Task 11	Execution time [s]	**	**	*	ns	ns
CF277	IJ	Task 9	Mean pressure of execution phase	**	**	ns	*	ns
CF278	IJ	TC 6	Pressure differences between successive frames	**	*	***	ns	ns
CF279	IJ	Task 1	Deviation from ideal pressure	**	*	**	ns	ns
CF280	IJ	Task 10	Pressure-time integrals	**	*	**	ns	ns
CF281	IJ	Task 13	Deviation from ideal pressure	**	*	**	ns	ns
CF282	IJ	Task 11	Attempt count (n)	**	*	*	*	*
CF283	IJ	Task 5	Pressure-time integrals	**	*	*	ns	*
CF284	IJ	TC 3	Deviation from ideal pressure	**	*	*	ns	ns
CF285	IJ	Task 11	Pressure-time integrals	**	*	*	ns	ns
CF286	IJ	Task 11	Pressure differences between successive frames	**	*	*	ns	ns
CF287	IJ	Task 6	Execution time [s]	**	*	ns	**	ns
CF288	IJ	Task 1	Pressure-time integrals	**	*	ns	ns	ns
CF289	IJ	TC 2	Pressure differences between successive frames	**	ns	**	ns	ns
CF290	IJ	Task 1	Pressure-time integrals	**	ns	*	*	ns
CF291	IJ	Task 16	Execution time [s]	*	**	ns	ns	*
CF292	IJ	Task 10	Mean pressure of execution phase	*	**	ns	ns	ns
CF293	IJ	TC 7	Deviation from ideal pressure	*	*	*	ns	*
CF294	IJ	Task 6	Pressure-time integrals	*	*	*	ns	ns
CF295	IJ	Task 16	Pressure-time integrals	*	*	*	ns	ns
CF296	IJ	Task 12	Anticipation time [s]	*	*	ns	ns	ns

CF297	IJ	Task 10	Deviation from ideal pressure	*	ns	**	ns	*
CF298	IJ	Task 6	Deviation from ideal pressure	*	ns	**	ns	ns
CF299	IJ	Task 14	Deviation from ideal pressure	*	ns	**	ns	ns
CF300	IJ	Task 15	Anticipation time [s]	*	ns	**	ns	ns
CF301	IJ	TC 3	Execution time [s]	*	ns	*	*	ns
CF302	IJ	Task 16	Deviation from ideal pressure	*	ns	*	ns	*
CF303	IJ	Task 6	Pressure differences between successive frames	*	ns	*	ns	ns
CF304	IJ	TC 2	Mean pressure of execution phase	*	ns	*	ns	ns
CF305	IJ	Task 1	Pressure differences between successive frames	*	ns	*	ns	ns
CF306	IJ	Task 2	Pressure-time integrals	*	ns	*	ns	ns
CF307	IJ	Task 5	Pressure differences between successive frames	*	ns	*	ns	ns
CF308	IJ	Task 14	Anticipation time [s]	*	ns	*	ns	ns
CF309	IJ	Task 15	Deviation from ideal pressure	*	ns	*	ns	ns
CF310	IJ	TC 7	Execution time [s]	*	ns	ns	*	*
CF311	IJ	TC 6	Pressure differences between successive frames	*	ns	ns	ns	ns
CF312	IJ	Task 9	Deviation from ideal pressure	*	ns	ns	ns	ns
CF313	IJ	Task 10	Execution time [s]	*	ns	ns	ns	ns
CF314	IJ	Task 11	Anticipation time [s]	*	ns	ns	ns	ns

*Supplementary Table 2. Results of intergroup difference tests of game features within cohort 2. Differences between groups were calculated using the Mann-Whitney U test, t-test, or chi-square test as appropriate. Significance levels: ns (p>0.05), * (p=0.01–0.05), ** (p=0.001–0.01), *** (p=0.0001–0.001), **** (p<0.0001). CF: candidate features; AC: Apple-Catch; BF: Balloon-Flying; CP: Cross-Pressure; IJ: Island-Jump; TC: task combination*

ID	Game	Task/TC	Feature Name	Signif	P Value	Statistic	Method	Normality
1	AC	Task 12	Reaction time [s]	***	0,00069	1896	Wilcoxon test	FALSE
2	AC	TC 8	Normalized pressure	**	0,00232	847	Wilcoxon test	FALSE
3	AC	Task 13	Normalized pressure	**	0,00656	918,5	Wilcoxon test	FALSE
4	AC	TC 10	Frequency outside catching area (n)	*	0,0138	980	Wilcoxon test	FALSE
5	AC	TC 9	Normalized pressure	*	0,01496	1752	Wilcoxon test	FALSE
6	AC	Task 13	Pressure gradients between successive frames	*	0,02454	1721,5	Wilcoxon test	FALSE
7	AC	Task 6	Pressure gradients between successive frames	*	0,02553	1719	Wilcoxon test	FALSE
8	AC	TC 4	Normalized pressure	*	0,02717	985	Wilcoxon test	FALSE
9	AC	TC 2	Anticipation time [s]	*	0,02838	-2,26	T-test	TRUE
10	AC	Task 8	Final virtual distance	*	0,03003	991,5	Wilcoxon test	FALSE
11	AC	Task 11	Anticipation time [s]	*	0,03766	1008,5	Wilcoxon test	FALSE
12	AC	TC 8	Reaction time [s]	*	0,03806	1689,5	Wilcoxon test	FALSE
13	AC	Task 4	Frequency outside catching area (n)	*	0,04291	1121	Wilcoxon test	FALSE
14	AC	Task 8	Pressure gradients between successive frames	*	0,04517	1681	Wilcoxon test	FALSE
15	AC	Task 13	Pressure gradients between successive frames	*	0,04577	2,06	T-test	TRUE
16	AC	Task 10	Normalized pressure	*	0,04725	1676	Wilcoxon test	FALSE
17	BF (L)	Task 7	Normalized pressure	*	0,03113	1706	Wilcoxon test	FALSE
18	BF (L)	Task 7	Normalized pressure	*	0,03178	1050	Wilcoxon test	FALSE
19	BF (L)	Task 6	Pressure differences between successive frames	*	0,03671	-2,15	T-test	TRUE
20	BF (L)	TC 4	Normalized pressure	*	0,03749	1020,5	Wilcoxon test	FALSE
21	BF (L)	TC 4	Minimal virtual distance smiley 3	*	0,04223	1016,5	Wilcoxon test	FALSE
22	BF (L)	TC 4	Virtual deviation of ideal flying route	*	0,04749	1022,5	Wilcoxon test	FALSE
23	BF (L)	Task 3	Minimal virtual distance smiley 2	*	0,04999	1673,5	Wilcoxon test	FALSE
24	BF (R)	Task 11	Pressure differences between successive frames	**	0,00407	875,5	Wilcoxon test	FALSE
25	BF (R)	Task 3	Virtual deviation of ideal flying route	*	0,02631	1717	Wilcoxon test	FALSE
26	BF (R)	TC 4	Pressure gradients between successive frames	*	0,04452	1682	Wilcoxon test	FALSE
27	BF (R)	Task 9	Pressure differences between successive frames	*	0,04677	1678,5	Wilcoxon test	FALSE
28	CP	TC 8	Pressure gradients between successive frames (R)	*	0,01139	932	Wilcoxon test	FALSE
29	CP	Task 4	Normalized pressure (R)	*	0,01169	933,5	Wilcoxon test	FALSE
30	CP	Task 10	Pressure-time integrals of the reaction phase (L)	*	0,01484	947,5	Wilcoxon test	FALSE
31	CP	Task 6	Time outside ideal pressure zone [s]	*	0,02079	1004,5	Wilcoxon test	FALSE
32	CP	Task 4	Anticipation time [s]	*	0,02118	1730,5	Wilcoxon test	FALSE
33	CP	Task 11	Time outside ideal pressure zone [s]	*	0,02297	1578	Wilcoxon test	FALSE
34	CP	TC 6	Time outside ideal pressure zone [s]	*	0,02369	977	Wilcoxon test	FALSE

35	CP	Task 6	Reaction time [s]	*	0,02415	977,5	Wilcoxon test	FALSE
36	CP	Task 7	Reaction time [s]	*	0,02592	982	Wilcoxon test	FALSE
37	CP	Task 4	Pressure-time integrals of the execution phase (R)	*	0,04319	-2,07	T-test	TRUE
38	CP	Task 11	Pressure gradients between successive frames (R)	*	0,04356	1683,5	Wilcoxon test	FALSE
39	CP	Task 9	Reaction time [s]	*	0,04546	1019,5	Wilcoxon test	FALSE
40	CP	Task 5	Normalized pressure (L)	*	0,04853	1024	Wilcoxon test	FALSE
41	CP	Task 8	Time outside ideal pressure zone [s]	*	0,04915	1054,5	Wilcoxon test	FALSE
42	IJ	Task 16	Deviation from ideal pressure	**	0,00548	899,5	Wilcoxon test	FALSE
43	IJ	TC 3	Execution time [s]	**	0,0065	900,5	Wilcoxon test	FALSE
44	IJ	TC 3	Anticipation time [s]	*	0,01421	945,5	Wilcoxon test	FALSE
45	IJ	Task 9	Execution time [s]	*	0,01434	1754,5	Wilcoxon test	FALSE
46	IJ	Task 9	Anticipation time [s]	*	0,01524	970	Wilcoxon test	FALSE
47	IJ	Task 3	Pressure differences between successive frames	*	0,01682	1695,5	Wilcoxon test	FALSE
48	IJ	Task 12	Anticipation time [s]	*	0,01898	962,5	Wilcoxon test	FALSE
49	IJ	TC 6	Deviation from ideal pressure	*	0,02128	969,5	Wilcoxon test	FALSE
50	IJ	Task 14	Anticipation time [s]	*	0,02323	992,5	Wilcoxon test	FALSE
51	IJ	Task 5	Pressure differences between successive frames	*	0,02507	1029,5	Wilcoxon test	FALSE
52	IJ	TC 4	Pressure differences between successive frames	*	0,02513	980	Wilcoxon test	FALSE
53	IJ	Task 2	Deviation from ideal pressure	*	0,02812	990,5	Wilcoxon test	FALSE
54	IJ	TC 6	Anticipation time [s]	*	0,03168	995	Wilcoxon test	FALSE
55	IJ	Task 2	Deviation from ideal pressure	*	0,03187	998	Wilcoxon test	FALSE
56	IJ	Task 6	Pressure differences between successive frames	*	0,03546	1002,5	Wilcoxon test	FALSE
57	IJ	Task 13	Deviation from ideal pressure	*	0,03997	1013	Wilcoxon test	FALSE
58	IJ	TC 5	Mean pressure of execution phase	*	0,04141	1013	Wilcoxon test	FALSE

*Supplementary Table 3. Results of intergroup difference tests of game features between normal and reduced/absent Aδ/C-fiber function groups in diabetes. Differences between groups were calculated using the Mann-Whitney U test, t-test, or chi-square test as appropriate. Significance levels: ns (p>0.05), * (p=0.01–0.05), ** (p=0.001–0.01), *** (p=0.0001–0.001), **** (p<0.0001). CF: candidate features; AC: Apple-Catch; BF: Balloon-Flying; CP: Cross-Pressure; IJ: Island-Jump; TC: task combination*

ID	Game	Task/TC	Feature Name	Signif	P.Value	Statistic	Method	Normality
1	AC	Task 13	Pressure gradients between successive frames	**	0,00381	2,99	T-test	TRUE
2	AC	TC 8	Final virtual distance	*	0,01287	669,5	Wilcoxon test	FALSE
3	AC	Task 12	Apple caught (yes/no)	*	0,01308	6,16	Chi-square test	FALSE
4	AC	TC 9	Pressure differences between successive frames	*	0,01829	1259	Wilcoxon test	FALSE
5	AC	Task 8	Time inside catching area [s]	*	0,02506	699,5	Wilcoxon test	FALSE
6	AC	TC 5	Normalized pressure	*	0,02817	705	Wilcoxon test	FALSE
7	AC	Task 12	Anticipation time [s]	*	0,03097	1233	Wilcoxon test	FALSE
8	AC	TC 12	Pressure differences between successive frames	*	0,03658	-2,12	T-test	TRUE
9	AC	TC 11	Frequency outside catching area (n)	*	0,04041	1188	Wilcoxon test	FALSE
10	AC	TC 10	Pressure differences between successive frames	*	0,04447	1216,5	Wilcoxon test	FALSE
11	AC	TC 2	Time inside catching area [s]	*	0,04698	-2,02	T-test	TRUE
12	BF (L)	Task 4	Virtual deviation of ideal flying route	*	0,01066	1282,5	Wilcoxon test	FALSE
13	BF (L)	Task 8	Pressure gradients between successive frames	*	0,01132	664	Wilcoxon test	FALSE
14	BF (L)	Task 6	Pressure-time integrals	*	0,01272	669	Wilcoxon test	FALSE
15	BF (L)	Task 11	Normalized pressure	*	0,01292	698,5	Wilcoxon test	FALSE
16	BF (L)	Task 6	Normalized pressure	*	0,01424	-2,51	T-test	TRUE
17	BF (L)	TC 1	Pressure gradients between successive frames	*	0,01494	676	Wilcoxon test	FALSE
18	BF (L)	TC 4	Minimal virtual distance smiley 2	*	0,01559	678	Wilcoxon test	FALSE
19	BF (L)	Task 12	Minimal virtual distance smiley 4	*	0,0156	1260	Wilcoxon test	FALSE
20	BF (L)	Task 12	Virtual deviation of ideal flying route	*	0,02064	690,5	Wilcoxon test	FALSE
21	BF (L)	Task 9	Pressure gradients between successive frames	*	0,0218	693	Wilcoxon test	FALSE
22	BF (L)	Task 9	Minimal virtual distance smiley 3	*	0,02411	700	Wilcoxon test	FALSE
23	BF (L)	Task 3	Virtual deviation of ideal flying route	*	0,02638	1242	Wilcoxon test	FALSE
24	BF (L)	Task 11	Pressure gradients between successive frames	*	0,03191	711	Wilcoxon test	FALSE
25	BF (L)	TC 2	Minimal virtual distance smiley 4	*	0,03325	713	Wilcoxon test	FALSE
26	BF (L)	Task 6	Pressure gradients between successive frames	*	0,04069	723	Wilcoxon test	FALSE
27	BF (L)	Task 5	Normalized pressure	*	0,04419	-2,05	T-test	TRUE
28	BF (L)	Task 5	Minimal virtual distance smiley 4	*	0,0452	772	Wilcoxon test	FALSE
29	BF (L)	Task 9	Virtual deviation of ideal flying route	*	0,04577	1215	Wilcoxon test	FALSE
30	BF (L)	Task 7	Minimal virtual distance smiley 4	*	0,04622	730	Wilcoxon test	FALSE
31	BF (R)	Task 3	Pressure-time integrals	***	0,00042	543	Wilcoxon test	FALSE
32	BF (R)	TC 2	Normalized pressure	***	0,00077	1381	Wilcoxon test	FALSE
33	BF (R)	Task 4	Normalized pressure	***	0,00095	1373,5	Wilcoxon test	FALSE
34	BF (R)	Task 3	Normalized pressure	**	0,00318	-3,05	T-test	TRUE

35	BF (R)	TC 2	Pressure differences between successive frames	**	0,00682	1301	Wilcoxon test	FALSE
36	BF (R)	TC 2	Pressure gradients between successive frames	**	0,00936	1288	Wilcoxon test	FALSE
37	BF (R)	Task 7	Pressure differences between successive frames	*	0,01186	666	Wilcoxon test	FALSE
38	BF (R)	TC 1	Pressure gradients between successive frames	*	0,01215	1277	Wilcoxon test	FALSE
39	BF (R)	Task 10	Normalized pressure	*	0,02231	-2,33	T-test	TRUE
40	BF (R)	TC 3	Pressure-time integrals	*	0,02277	1249	Wilcoxon test	FALSE
41	BF (R)	TC 4	Normalized pressure	*	0,02301	1248,5	Wilcoxon test	FALSE
42	BF (R)	TC 1	Normalized pressure	*	0,02748	2,26	T-test	TRUE
43	BF (R)	Task 9	Pressure differences between successive frames	*	0,03712	718,5	Wilcoxon test	FALSE
44	BF (R)	Task 9	Pressure differences between successive frames	*	0,03718	718,5	Wilcoxon test	FALSE
45	BF (R)	TC 3	Pressure differences between successive frames	*	0,04234	1219	Wilcoxon test	FALSE
46	BF (R)	Task 10	Pressure differences between successive frames	*	0,0494	2,01	T-test	TRUE
47	CP	TC 9	Pressure differences between successive frames (L)	**	0,00275	608	Wilcoxon test	FALSE
48	CP	Task 6	Normalized pressure (R)	**	0,00468	-2,91	T-test	TRUE
49	CP	TC 1	Pressure differences between successive frames (L)	**	0,00641	640,5	Wilcoxon test	FALSE
50	CP	Task 6	Normalized pressure (R)	*	0,0108	662	Wilcoxon test	FALSE
51	CP	TC 6	Pressure-time integrals of the execution phase (R)	*	0,01342	-2,54	T-test	TRUE
52	CP	TC 6	Pressure differences between successive frames (R)	*	0,01363	672	Wilcoxon test	FALSE
53	CP	Task 7	Normalized pressure (R)	*	0,01435	-2,53	T-test	TRUE
54	CP	Task 2	Pressure-time integrals of the reaction phase (L)	*	0,01851	689	Wilcoxon test	FALSE
55	CP	Task 7	Pressure differences between successive frames (R)	*	0,02156	692,5	Wilcoxon test	FALSE
56	CP	Task 6	Pressure-time integrals of the execution phase (L)	*	0,02495	-2,29	T-test	TRUE
57	CP	Task 12	Pressure-time integrals of the reaction phase (R)	*	0,02507	1244,5	Wilcoxon test	FALSE
58	CP	Task 6	Normalized pressure (R)	*	0,02534	700	Wilcoxon test	FALSE
59	CP	Task 2	Anticipation time [s]	*	0,02647	702,5	Wilcoxon test	FALSE
60	CP	Task 10	Pressure-time integrals of the reaction phase (L)	*	0,02758	1240	Wilcoxon test	FALSE
61	CP	TC 6	Pressure-time integrals of the execution phase (L)	*	0,02769	-2,25	T-test	TRUE
62	CP	Task 15	Normalized pressure (L)	*	0,03671	718	Wilcoxon test	FALSE
63	IJ	Task 16	Anticipation time [s]	**	0,00542	1283,5	Wilcoxon test	FALSE
64	IJ	Task 5	Pressure differences between successive frames	**	0,00568	1273	Wilcoxon test	FALSE
65	IJ	TC 6	Pressure differences between successive frames	*	0,01159	665	Wilcoxon test	FALSE
66	IJ	Task 12	Pressure differences between successive frames	*	0,02143	746,5	Wilcoxon test	FALSE
67	IJ	Task 8	Deviation from ideal pressure	*	0,03132	1231	Wilcoxon test	FALSE
68	IJ	Task 14	Pressure differences between successive frames	*	0,04149	724	Wilcoxon test	FALSE
69	IJ	Task 3	Anticipation time [s]	*	0,04613	742	Wilcoxon test	FALSE
70	IJ	Task 4	Pressure-time integrals	*	0,04808	1212,5	Wilcoxon test	FALSE

*Supplementary Table 4. Results of intergroup difference tests of game features between moderate and severe Aβ-fiber polyneuropathy groups in diabetes. Differences between groups were calculated using the Mann-Whitney U test, t-test, or chi-square test as appropriate. Significance levels: ns (p>0.05), * (p=0.01–0.05), ** (p=0.001–0.01), *** (p=0.0001–0.001), **** (p<0.0001). CF: candidate features; AC: Apple-Catch; BF: Balloon-Flying; CP: Cross-Pressure; IJ: Island-Jump; TC: task combination*

ID	Game	Task/TC	Feature Name	Signif	P.Value	Statistic	Method	Normality
1	AC	TC 12	Time outside catching area [s]	***	0,00022	966,5	Wilcoxon test	FALSE
2	AC	Task 2	Normalized pressure	***	0,00039	965	Wilcoxon test	FALSE
3	AC	TC 4	Final virtual distance	***	0,00081	946	Wilcoxon test	FALSE
4	AC	Task 8	Normalized pressure	**	0,0013	933	Wilcoxon test	FALSE
5	AC	TC 12	Frequency outside catching area (n)	**	0,00158	898,5	Wilcoxon test	FALSE
6	AC	TC 4	Anticipation time [s]	**	0,00288	331	Wilcoxon test	FALSE
7	AC	Task 7	Anticipation time [s]	**	0,00504	348,5	Wilcoxon test	FALSE
8	AC	Task 14	Normalized pressure	**	0,00654	2,96	T-test	TRUE
9	AC	Task 8	Reaction time [s]	**	0,00805	366	Wilcoxon test	FALSE
10	AC	Task 8	Anticipation time [s]	**	0,00828	364,5	Wilcoxon test	FALSE
11	AC	Task 2	Anticipation time [s]	*	0,01215	377	Wilcoxon test	FALSE
12	AC	Task 10	Normalized pressure	*	0,01242	2,68	T-test	TRUE
13	AC	TC 12	Normalized pressure	*	0,01392	381,5	Wilcoxon test	FALSE
14	AC	TC 9	Anticipation time [s]	*	0,01592	-2,6	T-test	TRUE
15	AC	TC 5	Anticipation time [s]	*	0,02298	-2,41	T-test	TRUE
16	AC	Task 6	Reaction time [s]	*	0,02752	410	Wilcoxon test	FALSE
17	AC	Task 10	Time outside catching area [s]	*	0,03225	748	Wilcoxon test	FALSE
18	AC	TC 4	Pressure differences between successive frames	*	0,03243	828,5	Wilcoxon test	FALSE
19	AC	TC 4	Pressure gradients between successive frames	*	0,03328	827,5	Wilcoxon test	FALSE
20	AC	Task 13	Pressure gradients between successive frames	*	0,03371	414	Wilcoxon test	FALSE
21	AC	TC 5	Pressure differences between successive frames	*	0,03639	417	Wilcoxon test	FALSE
22	AC	TC 6	Normalized pressure	*	0,03648	-2,21	T-test	TRUE
23	AC	Task 13	Normalized pressure	*	0,03914	421	Wilcoxon test	FALSE
24	AC	TC 8	Pressure differences between successive frames	*	0,03959	420,5	Wilcoxon test	FALSE
25	AC	TC 1	Time inside catching area [s]	*	0,03981	2,16	T-test	TRUE
26	AC	Task 6	Pressure gradients between successive frames	*	0,04125	422	Wilcoxon test	FALSE
27	AC	TC 3	Frequency outside catching area (n)	*	0,0425	443	Wilcoxon test	FALSE
28	AC	TC 10	Anticipation time [s]	*	0,04665	427	Wilcoxon test	FALSE
29	AC	TC 6	Anticipation time [s]	*	0,04788	-2,09	T-test	TRUE
30	BF (L)	TC 1	Pressure gradients between successive frames	**	0,00484	-2,96	T-test	TRUE
31	BF (L)	TC 4	Pressure differences between successive frames	**	0,00884	366	Wilcoxon test	FALSE
32	BF (L)	Task 4	Normalized pressure	*	0,01793	797	Wilcoxon test	FALSE
33	BF (L)	Task 10	Minimal virtual distance smiley 3	*	0,04103	422	Wilcoxon test	FALSE
34	BF (L)	Task 6	Normalized pressure	*	0,04136	765	Wilcoxon test	FALSE
35	BF (L)	TC 3	Minimal virtual distance smiley 4	*	0,04334	817	Wilcoxon test	FALSE
36	BF (R)	Task 7	Pressure differences between successive frames	**	0,00261	913	Wilcoxon test	FALSE

37	BF (R)	Task 1	Normalized pressure	**	0,00828	2,83	T-test	TRUE
38	BF (R)	Task 1	Normalized pressure	**	0,00875	860	Wilcoxon test	FALSE
39	BF (R)	Task 7	Normalized pressure	**	0,00904	367	Wilcoxon test	FALSE
40	BF (R)	TC 3	Normalized pressure	**	0,00939	368	Wilcoxon test	FALSE
41	BF (R)	TC 4	Pressure differences between successive frames	*	0,01875	392	Wilcoxon test	FALSE
42	BF (R)	Task 8	Pressure differences between successive frames	*	0,02908	-2,31	T-test	TRUE
43	BF (R)	TC 3	Virtual deviation of ideal flying route	*	0,03371	827	Wilcoxon test	FALSE
44	BF (R)	Task 1	Virtual deviation of ideal flying route	*	0,03638	417	Wilcoxon test	FALSE
45	BF (R)	TC 3	Pressure-time integrals	*	0,03639	417	Wilcoxon test	FALSE
46	BF (R)	Task 11	Minimal virtual distance smiley 1	*	0,04358	816,5	Wilcoxon test	FALSE
47	BF (R)	TC 1	Pressure differences between successive frames	*	0,04779	813	Wilcoxon test	FALSE
48	CP	Task 6	Normalized pressure (L)	**	0,0033	906	Wilcoxon test	FALSE
49	CP	TC 8	Pressure differences between successive frames (R)	**	0,00532	887	Wilcoxon test	FALSE
50	CP	Task 4	Time outside ideal pressure zone [s]	*	0,01137	844,5	Wilcoxon test	FALSE
51	CP	Task 4	Pressure differences between successive frames (R)	*	0,01205	376,5	Wilcoxon test	FALSE
52	CP	Task 6	Time outside ideal pressure zone [s]	*	0,01378	844,5	Wilcoxon test	FALSE
53	CP	TC 5	Normalized pressure (R)	*	0,02122	844,5	Wilcoxon test	FALSE
54	CP	Task 1	Pressure differences between successive frames (L)	*	0,02269	842	Wilcoxon test	FALSE
55	CP	Task 2	Time outside ideal pressure zone [s]	*	0,02596	830	Wilcoxon test	FALSE
56	CP	Task 7	Pressure-time integrals of the execution phase (L)	*	0,02702	405,5	Wilcoxon test	FALSE
57	CP	TC 4	Pressure-time integrals of the reaction phase (L)	*	0,03099	830	Wilcoxon test	FALSE
58	CP	Task 1	Normalized pressure (L)	*	0,04054	-2,16	T-test	TRUE
59	CP	Task 1	Pressure differences between successive frames (L)	*	0,04495	425,5	Wilcoxon test	FALSE
60	IJ	Task 4	Pressure differences between successive frames	**	0,00781	362	Wilcoxon test	FALSE
61	IJ	TC 6	Deviation from ideal pressure	*	0,0201	394,5	Wilcoxon test	FALSE
62	IJ	Task 4	Pressure-time integrals	*	0,02094	396	Wilcoxon test	FALSE
63	IJ	TC 2	Pressure gradients between successive frames	*	0,03371	414	Wilcoxon test	FALSE
64	IJ	Task 9	Deviation from ideal pressure	*	0,03423	415,5	Wilcoxon test	FALSE
65	IJ	Task 1	Pressure differences between successive frames	*	0,03593	416,5	Wilcoxon test	FALSE
66	IJ	Task 13	Deviation from ideal pressure	*	0,04244	425	Wilcoxon test	FALSE
67	IJ	TC 4	Pressure differences between successive frames	*	0,04334	424	Wilcoxon test	FALSE
68	IJ	TC 6	Pressure differences between successive frames	*	0,04442	425	Wilcoxon test	FALSE
69	IJ	Task 15	Anticipation time [s]	*	0,0472	427,5	Wilcoxon test	FALSE
70	IJ	Task 11	Mean pressure of execution phase	*	0,04869	439,5	Wilcoxon test	FALSE
71	IJ	Task 11	Execution time [s]	*	0,04896	812	Wilcoxon test	FALSE
72	IJ	TC 6	Deviation from ideal pressure	*	0,04956	429,5	Wilcoxon test	FALSE

*Supplementary Table 5. Results of intergroup difference tests of game features between normal and absent Achilles tendon reflex groups in diabetes. Differences between groups were calculated using the Mann-Whitney U test, t-test, or chi-square test as appropriate. Significance levels: ns (p>0.05), * (p=0.01–0.05), ** (p=0.001–0.01), *** (p=0.0001–0.001), **** (p<0.0001). CF: candidate features; AC: Apple-Catch; BF: Balloon-Flying; CP: Cross-Pressure; IJ: Island-Jump; TC: task combination*

ID	Game	Task/TC	Feature Name	Signif	P.Value	Statistic	Method	Normality
1	AC	Task 8	Normalized pressure	****	0,00001	471	Wilcoxon test	FALSE
2	AC	Task 10	Normalized pressure	***	0,00057	-3,58	T-test	TRUE
3	AC	TC 3	Time inside catching area [s]	**	0,00408	649,5	Wilcoxon test	FALSE
4	AC	TC 12	Time outside catching area [s]	**	0,00551	673,5	Wilcoxon test	FALSE
5	AC	Task 6	Time inside catching area [s]	**	0,00557	673	Wilcoxon test	FALSE
6	AC	Task 14	Normalized pressure	**	0,00673	-2,78	T-test	TRUE
7	AC	Task 6	Normalized pressure	**	0,00845	-2,69	T-test	TRUE
8	AC	TC 4	Normalized pressure	**	0,00941	683,5	Wilcoxon test	FALSE
9	AC	TC 1	Frequency outside catching area (n)	**	0,00998	1319	Wilcoxon test	FALSE
10	AC	TC 12	Pressure-time integrals	*	0,01174	2,57	T-test	TRUE
11	AC	TC 6	Normalized pressure	*	0,01735	713,5	Wilcoxon test	FALSE
12	AC	TC 8	Normalized pressure	*	0,0174	1298,5	Wilcoxon test	FALSE
13	AC	Task 10	Anticipation time [s]	*	0,01759	1298	Wilcoxon test	FALSE
14	AC	Task 10	Reaction time [s]	*	0,01921	1290,5	Wilcoxon test	FALSE
15	AC	TC 10	Anticipation time [s]	*	0,01998	1291	Wilcoxon test	FALSE
16	AC	TC 12	Final virtual distance	*	0,01998	718	Wilcoxon test	FALSE
17	AC	TC 9	Final virtual distance	*	0,02088	720	Wilcoxon test	FALSE
18	AC	Task 4	Normalized pressure	*	0,02509	-2,28	T-test	TRUE
19	AC	TC 8	Pressure gradients between successive frames	*	0,02812	733	Wilcoxon test	FALSE
20	AC	TC 12	Normalized pressure	*	0,03078	1271,5	Wilcoxon test	FALSE
21	AC	Task 14	Reaction time [s]	*	0,03275	1260,5	Wilcoxon test	FALSE
22	AC	Task 7	Anticipation time [s]	*	0,04079	1257	Wilcoxon test	FALSE
23	AC	TC 10	Normalized pressure	*	0,0469	-2,02	T-test	TRUE
24	AC	Task 8	Anticipation time [s]	*	0,04936	1247	Wilcoxon test	FALSE
25	BF (L)	TC 3	Normalized pressure	*	0,01323	2,53	T-test	TRUE
26	BF (L)	Task 1	Minimal virtual distance smiley 3	*	0,01689	709,5	Wilcoxon test	FALSE
27	BF (L)	TC 3	Normalized pressure	*	0,01793	1296	Wilcoxon test	FALSE
28	BF (L)	Task 1	Minimal virtual distance smiley 4	*	0,03572	1264	Wilcoxon test	FALSE
29	BF (L)	Task 8	Normalized pressure	*	0,04913	1185	Wilcoxon test	FALSE
30	BF (R)	Task 9	Minimal virtual distance smiley 4	**	0,00606	1338	Wilcoxon test	FALSE
31	BF (R)	TC 4	Pressure differences between successive frames	*	0,01287	1312	Wilcoxon test	FALSE
32	BF (R)	Task 4	Minimal virtual distance smiley 1	*	0,01414	1307	Wilcoxon test	FALSE
33	BF (R)	Task 1	Normalized pressure	*	0,03504	759,5	Wilcoxon test	FALSE
34	BF (R)	Task 10	Pressure differences between successive frames	*	0,04658	2,02	T-test	TRUE
35	CP	TC 5	Pressure differences between successive frames (R)	**	0,00382	1361	Wilcoxon test	FALSE
36	CP	Task 15	Normalized pressure (R)	*	0,01209	1313	Wilcoxon test	FALSE

37	CP	Task 14	Pressure differences between successive frames (L)	*	0,01941	2,39	T-test	TRUE
38	CP	TC 6	Pressure differences between successive frames (L)	*	0,02663	1278,5	Wilcoxon test	FALSE
39	CP	TC 6	Pressure differences between successive frames (R)	*	0,02923	1274	Wilcoxon test	FALSE
40	CP	Task 8	Pressure differences between successive frames (L)	*	0,03622	745,5	Wilcoxon test	FALSE
41	CP	Task 10	Reaction time [s]	*	0,04034	751	Wilcoxon test	FALSE
42	IJ	Task 9	Pressure-time integrals	**	0,0061	665,5	Wilcoxon test	FALSE
43	IJ	Task 9	Deviation from ideal pressure	*	0,01221	1312,5	Wilcoxon test	FALSE
44	IJ	Task 13	Pressure gradients between successive frames	*	0,01911	1293	Wilcoxon test	FALSE
45	IJ	Task 10	Mean pressure of execution phase	*	0,02143	722,5	Wilcoxon test	FALSE
46	IJ	Task 4	Anticipation time [s]	*	0,02885	1274	Wilcoxon test	FALSE
47	IJ	TC 5	Mean pressure of execution phase	*	0,03542	745	Wilcoxon test	FALSE
48	IJ	TC 6	Anticipation time [s]	*	0,03918	1259	Wilcoxon test	FALSE
49	IJ	Task 3	Pressure-time integrals	*	0,03918	750	Wilcoxon test	FALSE
50	IJ	TC 6	Anticipation time [s]	*	0,04852	1248,5	Wilcoxon test	FALSE

11.6. Introduction video and screenshots of the “Gamidiagnostics” application

The introduction video is available online:
https://1drv.ms/v/s!ApoW6w5vttZEgRsUqM92Hvgfc_oa?e=nI6ah9

The screenshots of the “Gamidiagnostics” App are presented here:

1. Insole Manager

2. Login page for study personal

3. Insole calibration (step 1 – 8)

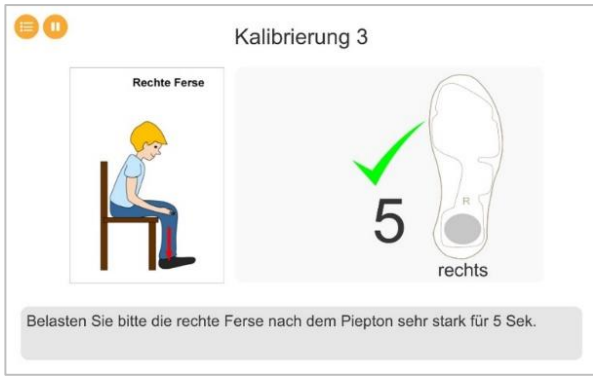

4. Apple-Catch game (task 1 – 14)

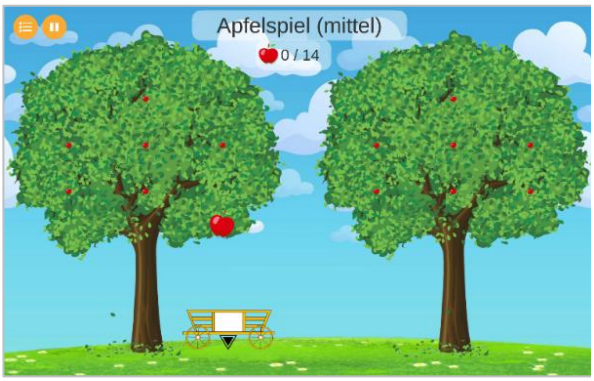

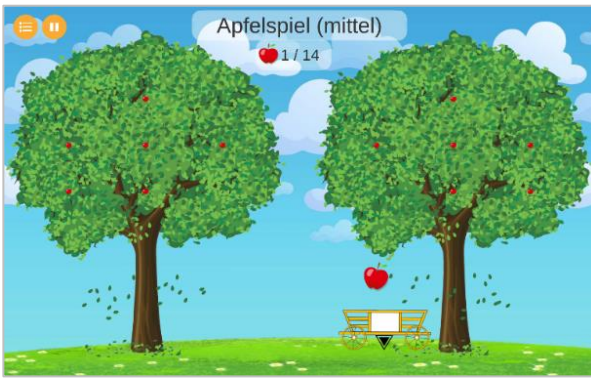

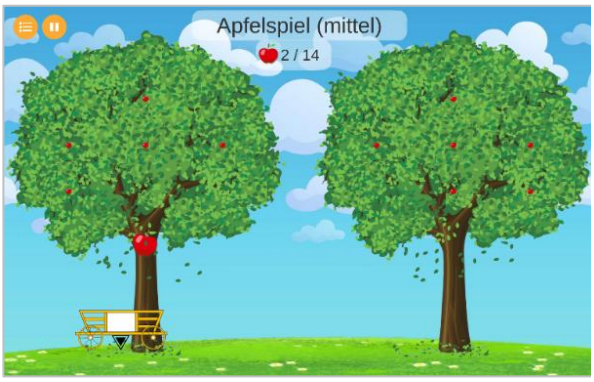

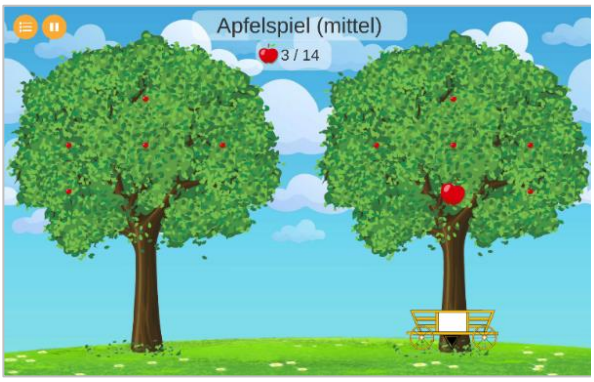

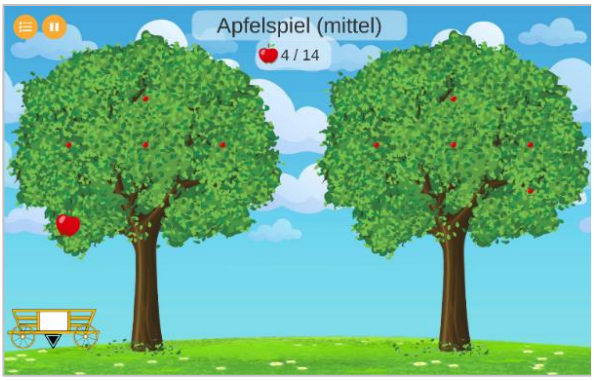
Apfelspiel (mittel)
4 / 14

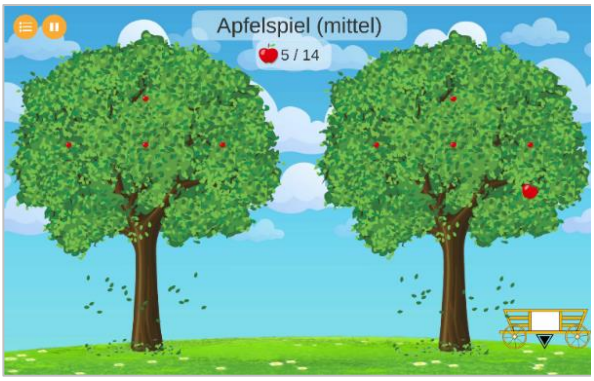
Apfelspiel (mittel)
5 / 14

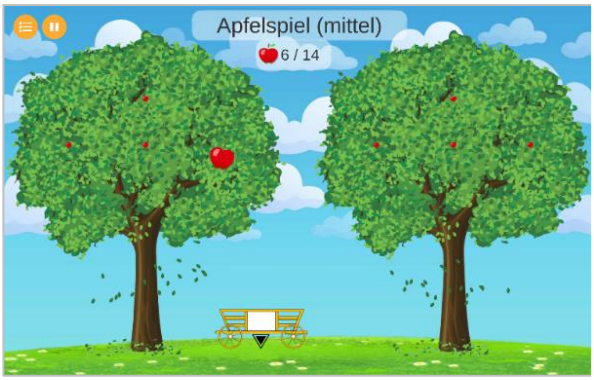
Apfelspiel (mittel)
6 / 14

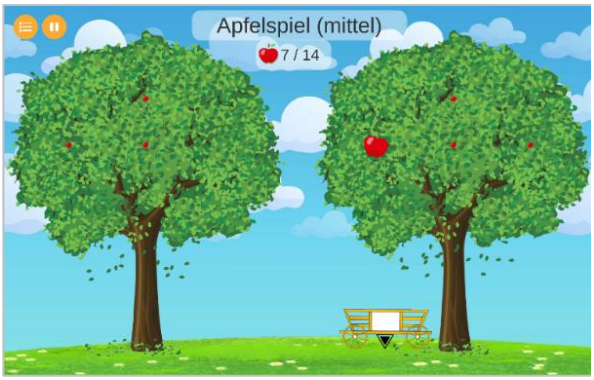
Apfelspiel (mittel)
7 / 14

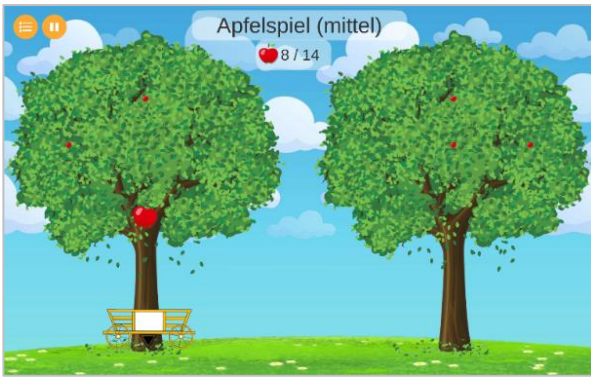
Apfelspiel (mittel)
8 / 14

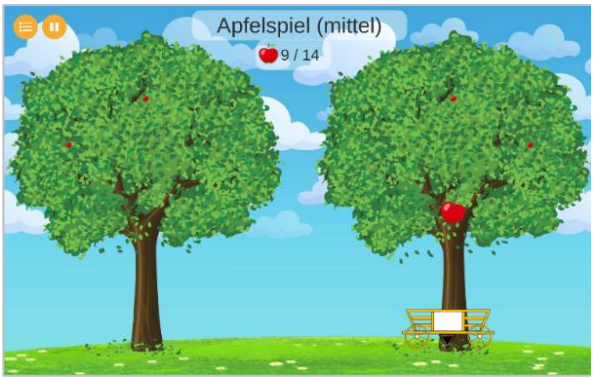
Apfelspiel (mittel)
9 / 14

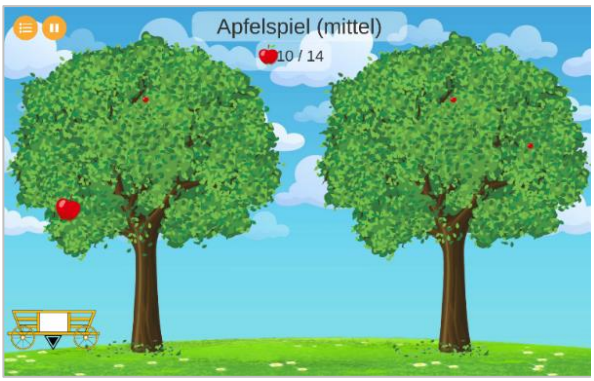
Apfelspiel (mittel)
10 / 14

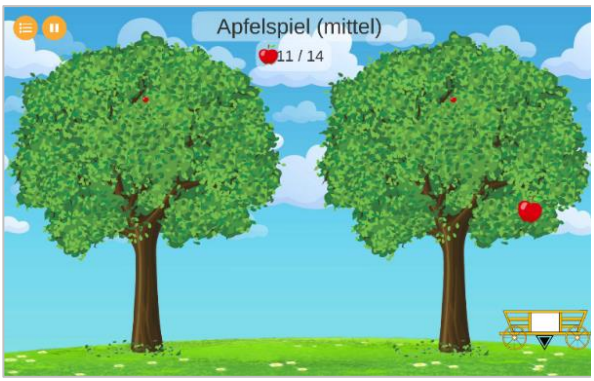
Apfelspiel (mittel)
11 / 14

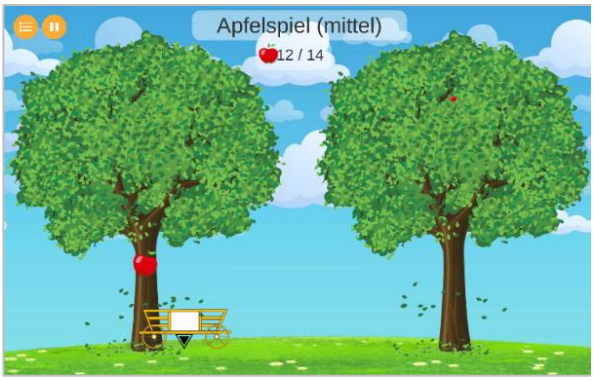

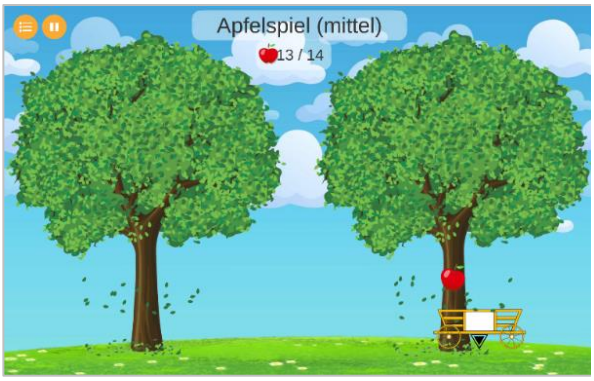

5. Balloon-Flying game (take off, task 1 – 12, and landing)

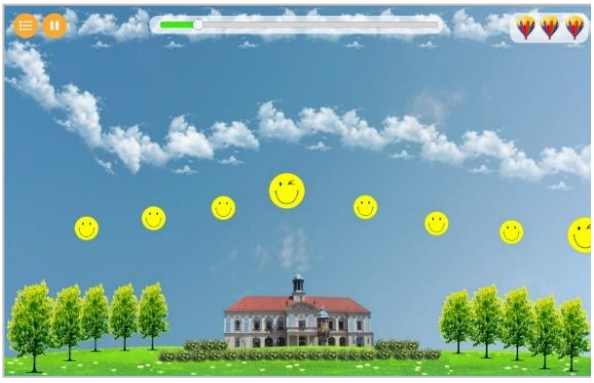

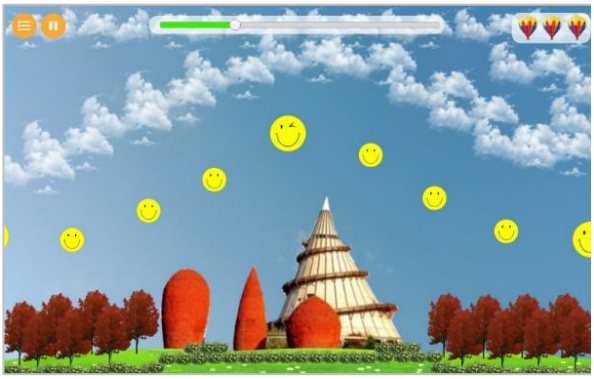

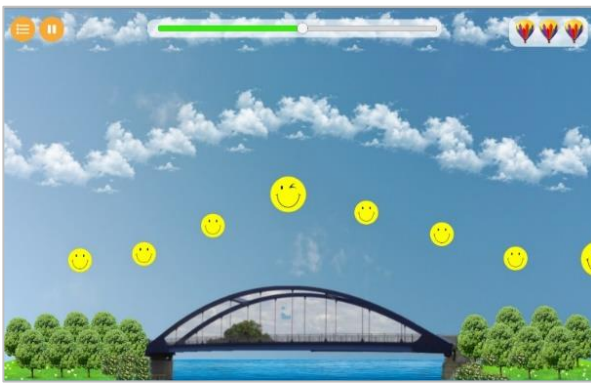

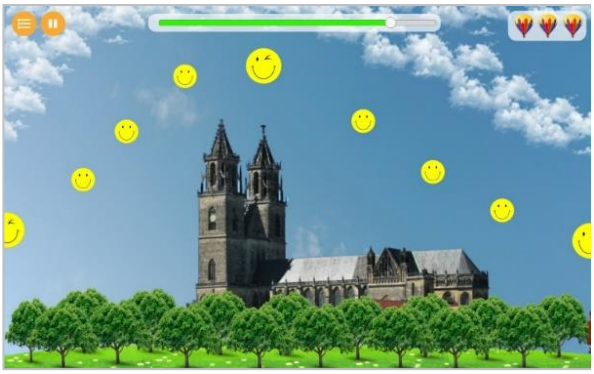

6. Cross-Pressure game (task 1 – 16)

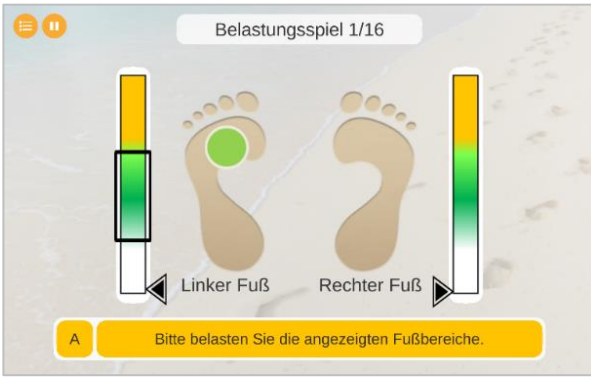

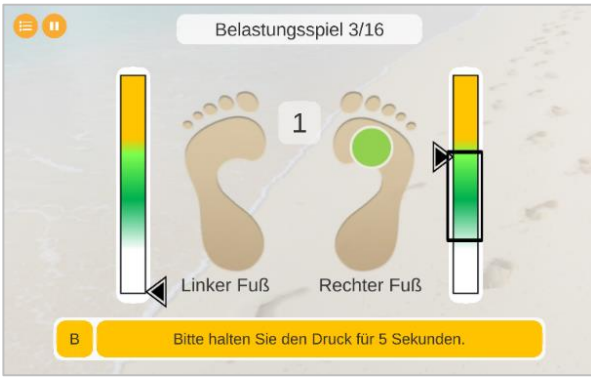

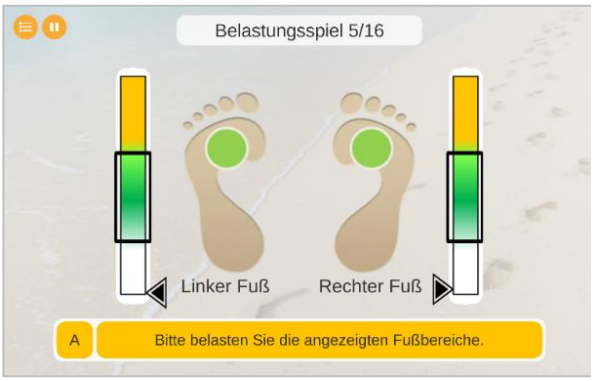

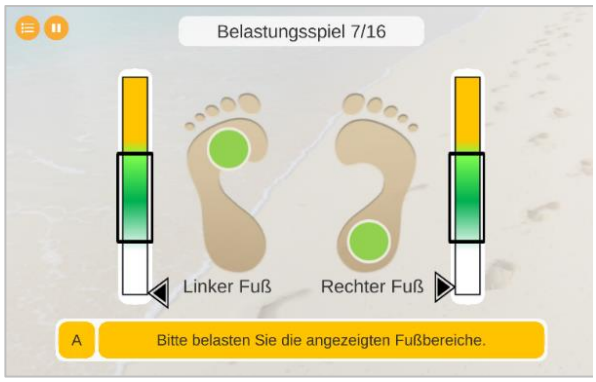
Belastungsspiel 7/16
Linker Fuß
Rechter Fuß
A
Bitte belasten Sie die angezeigten Fußbereiche.

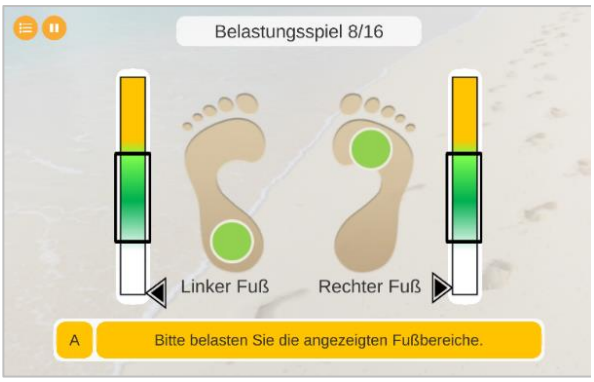
Belastungsspiel 8/16
Linker Fuß
Rechter Fuß
A
Bitte belasten Sie die angezeigten Fußbereiche.

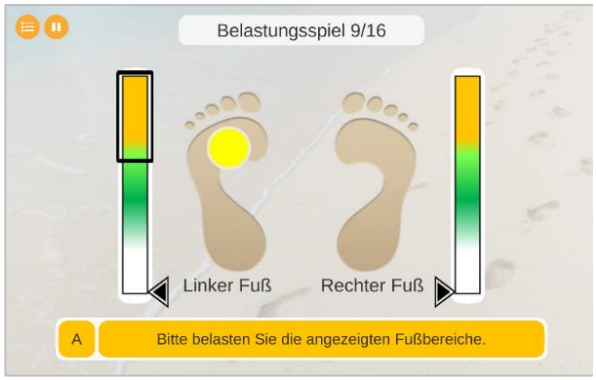
Belastungsspiel 9/16
Linker Fuß
Rechter Fuß
A
Bitte belasten Sie die angezeigten Fußbereiche.

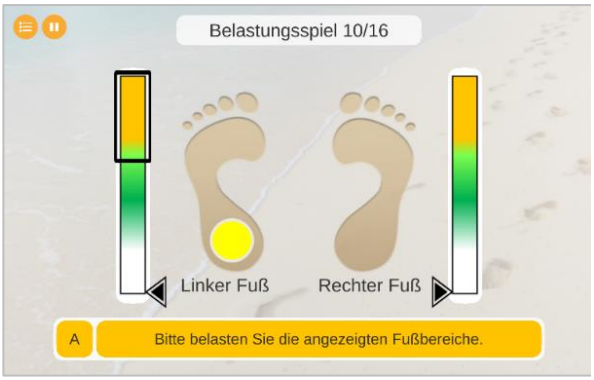
Belastungsspiel 10/16
Linker Fuß
Rechter Fuß
A
Bitte belasten Sie die angezeigten Fußbereiche.

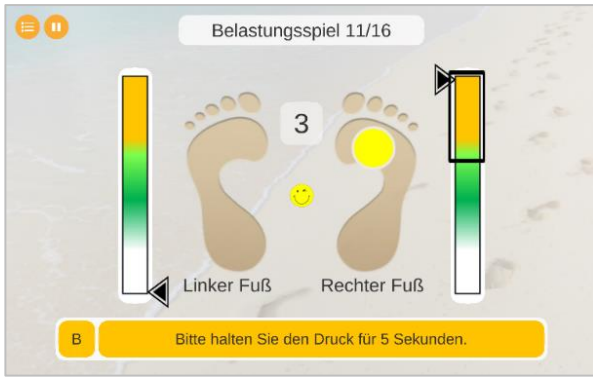
Belastungsspiel 11/16
3
Linker Fuß
Rechter Fuß
B
Bitte halten Sie den Druck für 5 Sekunden.

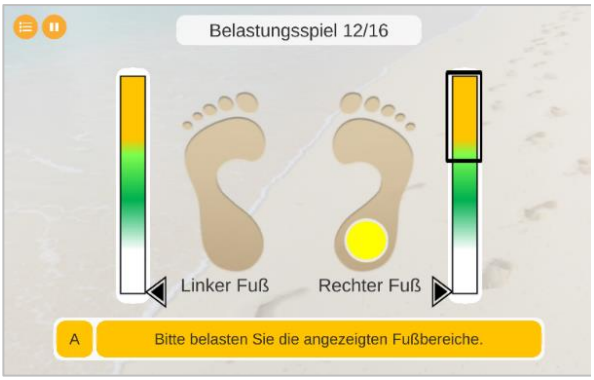
Belastungsspiel 12/16
Linker Fuß
Rechter Fuß
A
Bitte belasten Sie die angezeigten Fußbereiche.

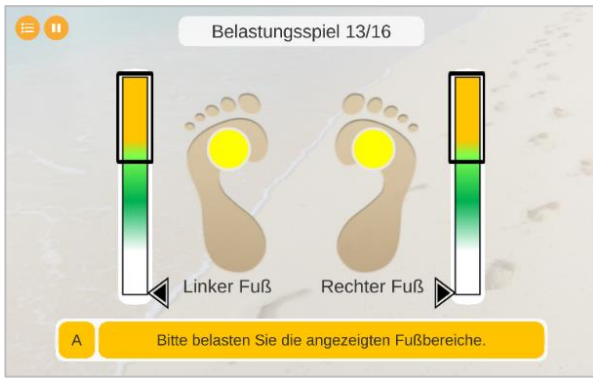
Belastungsspiel 13/16
Linker Fuß
Rechter Fuß
A
Bitte belasten Sie die angezeigten Fußbereiche.


Belastungsspiel 14/16
Linker Fuß
Rechter Fuß
A
Bitte belasten Sie die angezeigten Fußbereiche.

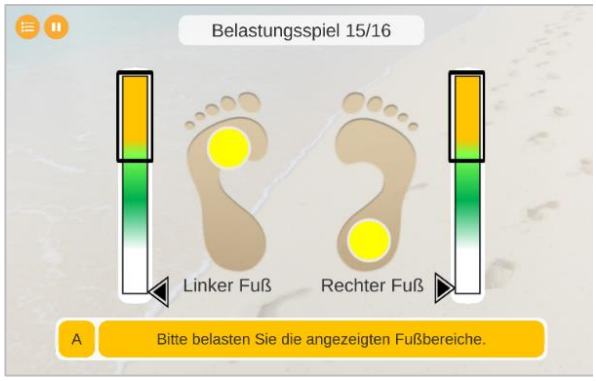

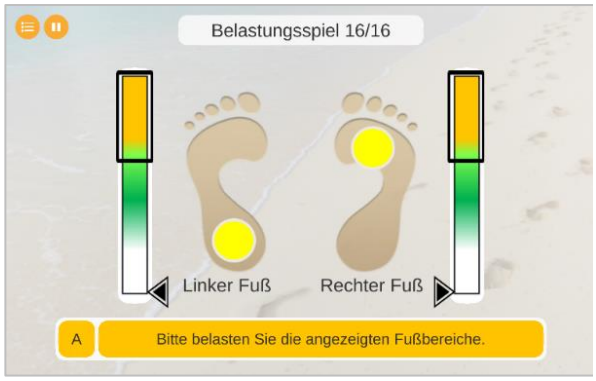

7. Island-Jump game (task 1 – 16)

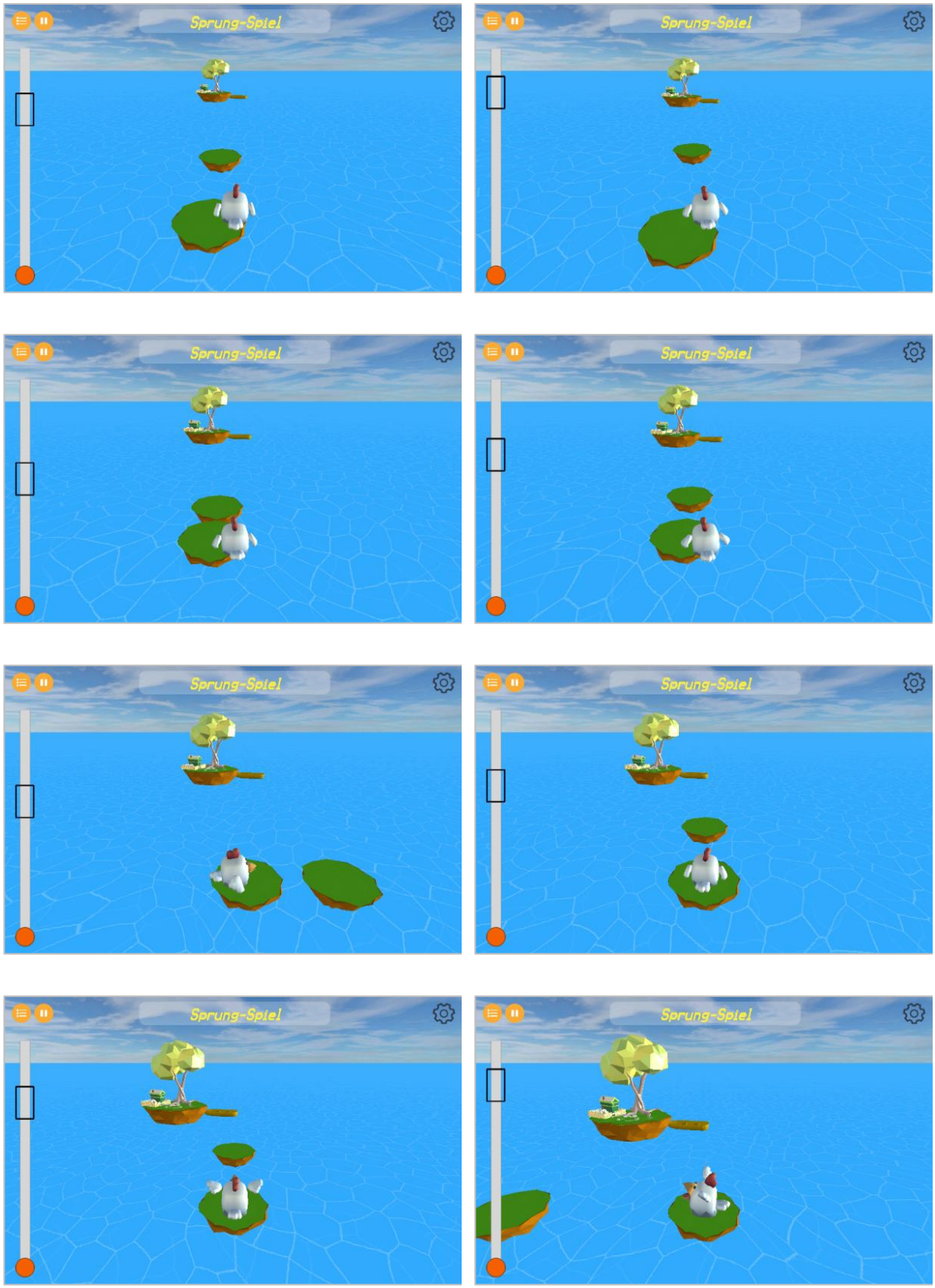
Sprung-Spiel
Sprung-Spiel
Sprung-Spiel
Sprung-Spiel
Sprung-Spiel
Sprung-Spiel
Sprung-Spiel
Sprung-Spiel

8. Assessment and feedback